Uncovering the molecular mechanism of flowering in a marine angiosperm, *Zostera marina*, and evaluating the effects of warming on flowering processes

Christine T. Nolan

A dissertation

submitted in partial fulfillment of the

requirements for the degree of

Doctor of Philosophy

University of Washington

2025

Reading Committee:

Takato Imaizumi, Chair

Jennifer L. Ruesink

Kerry A. Naish

Program Authorized to Offer Degree:

Department of Biology

University of Washington

Abstract

Uncovering the molecular mechanism of flowering in a marine angiosperm, *Zostera marina*, and evaluating the effects of warming on flowering processes

Christine T. Nolan

Chair of Supervisory Committee:

Takato Imaizumi

Department of Biology

Florigen and antiflorigen genes within the phosphatidylethanolamine-binding protein (PEBP) gene family regulate flowering in angiosperms. In eelgrass (*Zostera marina*), an estuarine foundation species, flowering and seed production are crucial for population resilience, especially in the face of rising seawater temperatures, more frequent extreme weather events, and anthropogenic disturbances. Yet, the molecular mechanism underpinning flowering remains unknown.

In Chapters 1 and 2, we investigate the role of florigen and antiflorigen genes in *Zostera marina* in the regulation and onset of flowering. We identified thirteen PEPB genes in *Z. marina* (*ZmaPEBP*); ten *FT* (florigen) homologs, two *TFL1* homologs, and one *MFT* homolog. Among these thirteen *ZmaPEBP* genes, when over-expressed in *Arabidopsis*, two genes (*ZmaFT2* and

ZmaFT4) caused an early flowering phenotype, and two genes (*ZmaFT9,* and *ZmaTFL1a*) caused a late flowering phenotype. To gain insight into the function of these four genes in eelgrass, we analyzed gene expression in different plant tissue from adult perennial shoots in either vegetative or flowering reproductive phases at three sites (Willapa Bay, WA USA). *ZmaFT2*, *ZmaFT4*, and *ZmaTFL1a* expression was higher in flowering rhizome and shoot tissues, while *ZmaFT9* was solely expressed in leaves of vegetative shoots. We also analyzed gene expression in annual eelgrass shoots over the growth season from three sites across two bays (Willapa Bay, WA and Yaquina Bay, OR USA). *ZmaFT2*, *ZmaFT4*, expression increased at the time of flowering and *ZmaTFL1a* expression increased after flowering onset occurred. *ZmaFT9* expression was high in leaves of early vegetative seedlings but decreased shortly before flowering onset. Our results suggest that *ZmaFT2* and *ZmaFT4* may promote flowering and *ZmaTFL1a* may be involved with flowering-related developmental processes, such as shoot architecture, while *ZmaFT9* may inhibit flowering in eelgrass.

In Chapter 3, using *Z. marina*, we applied a common garden approach to experimentally test how flowering and its underlying molecular mechanisms responded to elevated water temperature (+3°C). We focused on developmental and reproductive traits paired with *ZmaPEBP* gene expression to gain insight to the molecular mechanism underpinning differences in flowering responses. We compared annual shoots from two source populations (Willapa Bay and Padilla Bay, WA USA) to understand natural variation not only in morphological and reproductive traits, but also in *ZmaPEBP* gene expression governing flowering onset. At the individual and population levels, annual seedlings in the +3°C heated treatment produced more spathes and accelerated development of inflorescences so seeds dispersed sooner. Also, seedlings from Padilla Bay flowered at greater rates and earlier than Willapa Bay, and these differences

were exaggerated by the +3°C heated treatment. Two predicted floral activators, *ZmaFT2* and *ZmaFT4* had increasing expression throughout the summer regardless of population and showed no response to the temperature treatment. *ZmaFT9* expression, a predicted repressor of flowering onset, was expressed at lower levels in the shoots grown in the +3°C heated treatment, and even more so in the Padilla Bay population which flowered earlier than the Willapa Bay population. *ZmaTFL1a*, a gene predicted to be involved with downstream flowering processes, showed no significant response to the temperature treatment. These results highlight the contribution of *ZmaFT9* expression to the temperature-based response of timing of flowering onset. Elevated seawater temperature impacted flowering timing and spathe production, with potential consequences for seed yield and meadow resilience.

Combined, these studies support the key role of antiflorigen (*ZmaFT9*) in the molecular control of flowering in *Z. marina*, not only as the main determinant of flowering onset, but also as an integrator of temperature into the flowering response. Florigen genes that contribute to the activation of flowering (*ZmaFT2* and *ZmaFT4*) and genes that are responsible for flowering related developmental processes (*ZmaTFL1a*) are also important components of the flowering mechanism.

Table of Contents

Chapters 1 & 2

Florigen and antiflorigen gene expression correlates with reproductive state in a marine angiosperm, *Zostera marina*

Christine T. Nolan[1], Ian Campbell[1], Anna Farrell-Sherman[1,2], Bryan A. Briones Ortiz[3], Chansie Yang[1], Kerry A. Naish[3], Verónica S. Di Stilio[1], James E. Kaldy[4], Cinde Donoghue[5,6], Jennifer L. Ruesink[1], Takato Imaizumi[1,7,*]

[1]Department of Biology, University of Washington, Seattle, WA USA 98195
[2]Vaccine and Infectious Disease Division, Fred Hutch Cancer Center, Seattle, WA USA 98109
[3]School of Aquatic and Fishery Sciences, University of Washington, Seattle, WA USA 98195
[4]Pacific Ecological Systems Division, US EPA, Newport, OR USA 97365
[5]Washington Department of Natural Resources, Olympia, WA USA 98504
[6]Washington Department of Ecology, Lacey, WA USA 98503
[7]Lead Contact
*Correspondence: takato@uw.edu

Corresponding author: Takato Imaizumi, takato@uw.edu

SUMMARY

Florigen and antiflorigen genes within the phosphatidylethanolamine-binding protein (PEBP) family regulate flowering in angiosperms. In eelgrass (*Zostera marina*), an estuarine foundation species, flowering and seed production are crucial for population resilience. Yet, the molecular mechanism underpinning flowering remains unknown. Among thirteen *PEBP* genes in *Z. marina* (*ZmaPEBP*), we showed that four genes (*ZmaFT2, ZmaFT4, ZmaFT9,* and *ZmaTFL1a*) altered flowering time when overexpressed in *Arabidopsis*. We analyzed gene expression in different tissues and throughout the growth season from perennial and annual populations in Willapa Bay and Yaquina Bay, USA. Across six sites exhibiting different degrees of population genetic structure, *ZmaFT2* and *ZmaFT4* were expressed in leaves of vegetative and reproductive shoots and in rhizomes of reproductive shoots. *ZmaFT9* was solely expressed in leaves of vegetative shoots, while *ZmaTFL1a* levels increased after flowering shoots developed. Our results suggest that *ZmaFT2* and *ZmaFT4* may promote flowering, while *ZmaFT9* may inhibit flowering in eelgrass.

KEYWORDS

antiflorigen, florigen, flowering, foundation species, phosphatidylethanolamine-binding proteins (PEBP), seed production, *Zostera marina* (eelgrass)

INTRODUCTION

In angiosperms, flowering is induced by florigen genes, with *FLOWERING LOCUS T* (*FT*) as the main inducer of flowering processes. *FT* is a member of a larger family of genes that encode phosphatidylethanolamine-binding proteins (PEBP), which includes other genes relevant to flowering, all of which are highly conserved across flowering plants.[1,2] In *Arabidopsis thaliana*, there are six *FT*-like genes implicated in flowering processes. *FT* and *TWIN SISTER OF FT* (*TSF*) both activate flowering.[3–5] *TERMINAL FLOWER 1* (*TFL1*), *Arabidopsis thaliana CENTRORADIALIS homologue* (*ATC*), and *BROTHER OF FT AND TFL1* (*BFT*) all inhibit the onset of flowering.[6–8] *MOTHER OF FT AND TFL1* (*MFT*), while capable of activating flowering processes, plays a role in seed germination.[9,10] In *Arabidopsis*, *PEBP* genes involved with the photoperiodic flowering pathway show tissue-specific expression patterns. *FT* is expressed in leaf phloem companion cells, generating a long distance protein signal transported to the shoot

apical meristem.[5,11] *TFL1* expression occurs in meristem tissue in shoots and *FT* and *TFL1* antagonistically regulate shoot indeterminacy.[12–15] The *PEBP* gene family has undergone expansion in monocot lineages, specifically within the *FT* clade, with species like *Oryza sativa* and *Brachypodium distachyon* having 19 and 18 members of their *PEBP* gene families (13 and 12 within *FT* clades), respectively.[16–19] *PEBP* genes have multifaceted roles in development in plant species; *FT* and *TFL1* are both known to affect branching and shoot architecture in flowering plants including *Arabidopsis* and tomato.[20–22] *FT* homologs in potatoes and strawberries promote tuber and stolon formation, respectively.[23,24] *FT* expression is mainly controlled by photoperiod (daylength) and temperature, among other environmental conditions, which in turn regulates flowering time.[25–32]

FT function and the floral pathway have been extensively studied in various terrestrial plant species,[2] including eudicots such as *Beta vulgaris*[33] and *Chrysanthemum setiscupe*[34], and also monocot species such as *Allium cepa*[35] and *Oryza sativa.*[36] Characterization of *FT* function in aquatic species has only been recently explored in a fresh-water species, duckweed[37], and has not yet been investigated in marine species. Eelgrass (*Zostera marina*) is a seagrass native to both the Atlantic and Pacific Northern Hemisphere, one of about 60 species of marine angiosperms, and a member of the early-diverging monocot order *Alismatales*. Despite its small genome of 202.3 Mb[38], eelgrass is predicted to have at least thirteen *PEBP* genes[19] in line with the observed expansion in other monocot lineages.

Seagrasses are foundation species of coastal ecosystems and essential for nutrient cycling, sediment stabilization, and habitats for fish and invertebrates.[39,40] However, seagrasses are sensitive to natural and anthropogenic pressures such as eutrophication, direct bed disturbances, and experience higher mortality rates with higher water temperatures.[39,41] Flowering and seed production critically contribute to persistence and increasing genetic diversity within local *Z. marina* populations, and restoration efforts centered around seeds appear promising.[42–47] Annual and perennial populations exist and are largely regarded as distinct ecotypes. Annual ecotypes, where seeds germinate and shoots flower within one season, rely on flowering and seed production as a means of reproduction and continued persistence.[48,49] In perennial ecotypes, the predominant form, shoots persist for multiple seasons and use both vegetative propagation and sexual reproduction as means of growth and persistence.[43,50] Perennial populations produce fewer flowering shoots with large variation in flowering

frequency.[49] Overall, eelgrass shows large phenotypic variation in flowering timing and frequency across spatial scales and seasons.[49,51–53] Determining the causes for this variation is central to understanding the ecology, evolution, and restoration of the species.

In perennial *Z. marina* populations in Willapa Bay, USA, less than 25% of shoots typically flower each year,[49,51] and it is not currently possible to predict how many and which shoots will flower. Therefore, studying the molecular mechanism of flowering onset in perennial populations proves difficult. In the annual ecotypes, all shoots flower in the same year as germination, such that annual populations can exceed 70% flowering frequency.[49,54,55] Characterizing the mechanism underpinning sexual reproduction and its relationship to environmental stimuli in *Z. marina* is a key knowledge gap that if addressed, would improve our understanding of how seed production is affected by environmental factors. Identifying genetic markers of flowering would provide a method for predicting seed potential within a population. Such advances could allow for more strategic and efficient seed-based restoration efforts of eelgrass, through improved donor site selection and in the scaling-up of seed collection and planting efforts.[45,46,56] However, the relevant genes and mechanism by which *Z. marina* flowering onset is cued and regulated across populations remains unknown.

Here, we explored the mechanism of flowering in *Z. marina* and investigated the function of *FT/TFL1* homologs. We confirmed thirteen eelgrass florigen homologs (*ZmaPEBP*) and demonstrated that four likely have flowering function as activators and repressors. To elucidate *ZmaPEBP* function, we performed a heterologous functional assay in *Arabidopsis*. Overexpression of four *ZmaPEBP* genes, *ZmaFT2*, *ZmaFT4*, *ZmaFT9*, and *ZmaTFL1a,* resulted in either precocious or delayed flowering. We characterized expression patterns of these four genes in *Z. marina* shoots across three perennial and three annual sites to rule out patterns that are site- or life history-specific. Quantification of expression of these four genes across different tissue types and developmental stages suggests that *ZmaFT9* may inhibit floral transition and *ZmaFT2* and *ZmaFT4* contribute to flowering onset, while *ZmaTFL1a* likely functions in flowering shoot architecture.

RESULTS

Phylogenetic analysis revealed thirteen *PEBP* genes in *Z. marina*

We identified thirteen *Z. marina PEBP* homologous genes. Phylogenetic analysis incorporating other *PEBP* genes representing different plant lineages revealed these genes belong to three clades; *FT/TSF* (ten genes, named *ZmaFT1-10*), *TFL1/BFT* (two genes, *ZmaTFL1a* and *ZmaTFL1b*), and *MFT* (one gene, *ZmaMFT1*) (Figure 1). Monocot lineages harbor an expansion in *FT* genes (Figure S1), which have been reported to cluster into distinct clades, this finding was not reflected in our analysis.[18,19,57] It has been shown that the initial *FT* duplication within monocots occurred in *Alismatales*, the basal monocot lineage that includes *Z. marina* and the *Zosteraceae* family.[18] *Z. muelleri*, a sister species to *Z. marina*, has a similar gene duplication structure.

PEBP genes that induce flowering tend to cluster within the *FT* clade, while genes that repress flowering tend to cluster with the *TFL1* clade.[18,19,33] Our analysis showed *Z. marina* and *Z. muelleri* both have genes that cluster within the *FT* clade and *TFL1* clade, as well as one predicted *MFT* paralog each. While sequence similarity alone cannot predict gene function,[58] our analysis suggest that the *Z. marina* genome may have several representatives of the same floral pathway genes that are conserved across angiosperms.

Four *ZmaPEBP* genes affect flowering phenotype in overexpression assays

As a first step towards investigating the function of *ZmaPEBP* genes, we examined the deduced amino acid sequences. The predicted open reading frames for all *ZmaPEBP* genes encode proteins with high similarity to *Arabidopsis* FT and TFL1 and rice Hd3a (Figures 2A and S2). We also observe the conservation of key residues for FT function,[59,60] such as at position 85 where all genes show conservation relative to *Arabidopsis* FT and TFL (Y85 in FT, and H85 in TFL1).

To assess the conserved flowering function of each *ZmaPEBP* gene, we generated transgenic *Arabidopsis* overexpression lines. We validated all *ZmaPEBP* expression in the T_1 generation (Figure S3). Although the expression levels of each gene varied among T_1 plants, none of the constructs were silenced. Of the thirteen *ZmaPEBP* genes, four demonstrated a strong effect on flowering time. Overexpression of *ZmaFT2* and *ZmaFT4* resulted in early flowering in *Arabidopsis* under LD conditions, compared to a *35S:GFP* control (Figure 2B). Both genes are in the *FT/TSF* clade (Figure 1). Overexpression of *ZmaFT4* had a stronger effect on flowering time than *ZmaFT2* (Figures 2B, 2C, and S4A). *ZmaFT9* and *ZmaTFL1a* lines

showed a large delay in flowering time, with a stronger phenotype observed with *ZmaFT9* (Figures 2B and 2C). Unlike the striking late-flowering phenotypes of *ZmaFT9* and *ZmaTFL1a* overexpressors, several other *ZmaPEPB* genes (*ZmaFT3*, *ZmaFT5*, *ZmaFT6*, *ZmaFT10*, and *ZmaMFT1*) caused subtle late-flowering phenotypes (1-2 extra leaves on average than the control) in our assay. This indicates that they may have minor roles in flowering time regulation, although these small differences could also be caused by indirect effects of growth changes caused by the overexpression of these genes.

ZmaTFL1a is in the *TFL/BFT* clade with *Arabidopsis TFL1*, while *ZmaFT9* is found in the *FT/TSF* clade (Figure 1). We also observed a decrease in *LFY* and *API*, downstream targets of *FT*,[29,32] in *35S:ZmaFT9* and *35S:ZmaTFL1a* lines (Figure S4B). Flowers produced on T_1 plants showed morphological phenotypes similar to *TFL* overexpressors and to mutant *lfy* plants where leaf-like structures develop in place of floral organs (Figure S4C).[61,62] Together, these results suggest that *Z. marina* has two *PEBP* genes that promote flowering and two that strongly repress flowering, all of which do so through interaction with the conserved flowering pathway.

Genetic structure between annual and perennial ecotypes provides context for the potential roles of *ZmaPEBP* genes

To assess function of *ZmaFT2*, *ZmaFT4*, *ZmaFT9*, and *ZmaTFL1a* in eelgrass flowering in plants with varying genetic backgrounds, we analyzed expression in shoots across different populations. When eelgrass flowers, the vegetative shoot primarily produces a bolted flowering shoot, completely changing overall shoot architecture (Figures 3A-D). In our sample populations, perennial meadows experience both clonal and sexual reproduction, while in annual populations, sexual flowering is the predominant mode of reproduction (Figures 3E-G, Table S4).

The five populations sampled in Willapa Bay showed significant population structure, supporting our ability to look for common gene expression patterns associated with flowering despite genotypic variation. Based on 327 loci (single nucleotide polymorphisms; SNPs) across 224 individuals (Table S4), most genetic differentiation occurred between life history types (annual and perennial), while the western perennial population also differed from perennial populations in the east of the bay (Figures 3H and S5, Table S6). Small but significant genetic differentiation was also observed between the annual sites within Willapa Bay, and we expect

that Yaquina Bay annuals, 140 km to the south, were genetically distinct. Overall Fst's ranged from 0.013 to 0.142 (Figure 3H, Figure S5, Table S6). Similarly, DAPC analyses (Figure S5B) separated annual from perennial populations on the first axis (explaining 71.3% of the variation) and both north-south (annual sites) and east-west (perennial sites) geographic structure on the second axis (12.3% of the variation). Finally, tests for individual population assignment revealed two primary clusters ($K = 2$), explained primarily by the assignment of most individuals in the annual population one group, and those from perennial populations to the second group (Figure S5A). Overall, population structure across ecotypes and across small geographic distances within ecotypes, (less than 20km in a single bay) allowed us to test for common gene expression patterns associated with flowering. We also included annual samples from Yaquina Bay (Table S4), 140 km to the south, and likely genetically distinct,[63] in the expression analyses.

Expression of *ZmaPEBP* genes changes across development and tissue type

To gain insight into the roles of *ZmaFT2*, *ZmaFT4*, *ZmaFT9*, and *ZmaTFL1a* in eelgrass flowering, we analyzed gene expression in different tissues from both adult vegetative and flowering shoots from perennial populations (Figures 4A and 4B, Table S4). In *Z. marina*, the two flowering activators, *ZmaFT2* and *ZmaFT4* (Figures 2B and 2C), had higher expression in stem and rhizome of flowering compared to vegetative shoots, but expression in leaves was more similar between life stages (Figures 4B and S6, Table S7). Although *ZmaTFL1a* acted as a flowering repressor when overexpressed in *Arabidopsis* (Figures 2B and 2C), its expression decreased in flowering tissue relative to vegetative shoots, whereas expression in stem and rhizome tissue increased in flowering relative to vegetative shoots (Figures 4A and 4B). This result was surprising, since expression was observed in tissues beyond the shoot apical meristem (vegetative stem tissue), where *TFL1* expression is typically found.[12,13,64,65] Both *ZmaFT4* and *ZmaTFL1a* showed higher levels of expression in the tip of vegetative leaves compared to other sections of vegetative leaves (Figure S6, Table S8), similar to *FT* in *Arabidopsis*.[11] The expression levels of the other floral repressor, *ZmaFT9* (Figures 2B and 2C), were depleted in leaves from flowering shoots compared to vegetative shoots (Figures 4A, 4B, and S6, Table S3). Together, these results suggest that *ZmaFT9* expression correlates to the vegetative state in eelgrass.

Our results in *Z. marina* highlight the expression of floral activators in stem and rhizome tissue. *ZmaTFL1a*, contrary to its apparent function as a floral repressor in *Arabidopsis*, is upregulated in stem and rhizome flowering tissue. However, *TFL1* is known to play a role in shoot architecture and development in *Arabidopsis*,[6,66] which aligns with our observed expression in flowering stems. Overall, our results suggest that expression of *ZmaFT2*, *ZmaFT4*, *ZmaFT9*, and *ZmaTFL1a* genes are consistent with their predicted roles in eelgrass floral development based on the *Arabidopsis* heterologous assay and show tissue-specific expression patterns.

Expression of *ZmaPEBP* genes changes over the lifecycle of an annual ecotype

Due to the annual ecotype's predictability of flowering, annuals provide a system in which to study *PEBP* gene expression trends over the plant development throughout the growing season and their relationship to flowering onset. In the 2023 season in Willapa Bay, seedlings emerged in early April and differentiation to flowering occurred in late June (Figure 5A, Figure S7). The emergence of flowering shoots coincides with peak photoperiod (approximately 16 hours, Figure 5B).

In both *ZmaFT2* and *ZmaFT4*, we observed increasing expression over the season, with a more significant increase occurring when flowering shoots emerged (Figures 5C and S8, Table S9, Table S10). This trend was more apparent in root and rhizome tissue than in leaf tissue. A similar trend was observed in *ZmaTFL1a* expression (Figure S8). The peak in *ZmaFT2*, *ZmaFT4*, and *ZmaTFL1a* leaf expression also coincides with the maximum photoperiod (Figure 5B). *ZmaFT9*, unlike the other *ZmaPEBP* genes, is expressed at higher levels in leaves at earlier stages of vegetative development. Approximately one month before flowering shoots were observed, we saw a decrease in expression (Figure 5C). The average daily temperature rose 3°C (12°C to 15°C) and 1.9°C (14.9°C to 16.8°C) between 9 May 2023 (23129) and 18 May 2023 (23138) during this interval at ST-ANN and NP-ANN, respectively, with daily maxima ranging from 18°C to 29.5°C at ST-ANN and 17°C to 25.5°C at NP-ANN (Figures 5D and 5E). The large decline in *ZmaFT9* expression was followed by a slower decline in expression after flowering shoots emerged. These results align with tissue and developmental state-specific expression trends observed in perennial shoots (Figure 4B). We also analyzed expression levels of *ZmFT2*, *ZmFT4*, *ZmFT9*, and *ZmTFL1a* in annuals from Yaquina Bay (YQ-ANN). Trends in expression

of each gene align with expression patterns observed in ST-ANN and NP-ANN site (Figure S9). However, results from YQ-ANN were either not statistically significant or less significant, likely due to limited sample size and sampling of clonal branches rather than bolting portions (Tables S11 and S12).

To compare gene expression levels of all *ZmaPEBP* genes in annual and perennial life history types, we performed RNA sequencing in leaf tissue samples collected from annual shoots on 17 July 2023 (23198) and from perennial shoots on 15 Jul 2022 (22196) (Figure S10). Differential gene expression analysis largely aligned with qPCR results regarding expression of *ZmaFT2*, *ZmaFT4*, and *ZmaFT9*. The expression level of *ZmaFT9* in vegetative tissues was several folds higher than *ZmaFT2* and *ZmaFT4* levels. Expression of *ZmaTFL1a* was close to the detection limit. We also observed expression of *ZmaFT5*, *ZmaFT6*, and *ZmaMFT1* in perennial and annual leaf tissues.

Together, these results suggest that *ZmaFT2* and *ZmaFT4* are involved in the activation of flowering, potentially in the formation of floral meristems and inflorescences, with *ZmaTFL1a* involved in some shoot architecture function after the flowering shoot has bolted. Other *ZmaPEBP* genes expressed may also play a role in reproductive processes. *ZmaFT9* is seemingly involved with vegetative growth and appears to require a decrease in expression to allow flowering onset to occur.

DISCUSSION

In this study, we characterized florigen genes in eelgrass and their function in regulating the onset of flowering. The molecular controls for the flowering onset in *Z. marina* have not been previously investigated, despite the importance of sexual reproduction in improving population resiliency, a key goal for restoration efforts.[43] Identifying and characterizing flowering genes and their effect on flowering in eelgrass will inform how flowering is cued and how eelgrass is predicted to reproduce under climate change conditions.

Here, we provide evidence of eelgrass *FT/TFL1* homologs with both inducing and repressing function in flowering. We identify thirteen florigen homologous genes in eelgrass and demonstrate that at least four are functionally relevant to the flowering pathway. We show that *Z.*

marina, like other monocots, has an expanded *FT* clade within the *PEBP* gene family, which is also mirrored in *Z. marina*'s sister species, *Z. muelleri*. Using *Arabidopsis* to assess the function of *ZmaPEPB* genes, we demonstrate that overexpression of four *ZmaPEBP* genes results in precocious flowering (*ZmaFT2* and *ZmaFT4*) or strongly delayed flowering (*ZmaFT9* and *ZmTFL1a*). To the best of our knowledge, these results provide the first functional implication of florigen in marine angiosperms. Further, we observed tissue-specific expression of these *ZmaPEBP* genes that correlate to developmental state (flowering and vegetative) in both annual and perennial *Z. marina* shoots. We believe that the role of the four focal genes (*ZmaFT2*, *ZmaFT4*, *ZmaFT9*, and *ZmaTFL1a*) is conserved across annual and perennial ecotypes, and across geographically structured populations. Our findings add to the expanding body of knowledge on seasonal flowering through the balance of activators and repressors beyond terrestrial plants and model species.

Two *Z. marina FT* genes, *ZmaFT2* and *ZmaFT4,* likely contribute to flowering onset

In *Arabidopsis*, there are six *PEBP* genes (*FT*, *TSF*, *TFL1*, *ATC*, *BFT*, and *MFT*), with *FT* as the main inducer of flowering. Our phylogenetic analysis demonstrated an expansion in the *PEBP* gene family focused within the *FT* clade. Ten of *ZmaPEBP* genes identified fell within *FT/TSF* clade, consistent with phylogenetic analyses of *FT* genes described Liu et al.[19] Further annotation of the *Z. marina* genome may reveal other florigen genes as well as insights into other genes implicated in flowering processes. In eelgrass, the spatial and developmental expression patterns of *ZmaFT2* and *ZmaFT4* are similar and both likely contribute to the activation of flowering in a manner similar to *FT*. In wild populations, both *ZmaFT2* and *ZmaFT4* show increased expression in stem and rhizome tissue after the onset of flowering in both perennial and annual shoots. Given that rhizomes are modified stem structures,[67] these findings may indicate potential involvement of these genes in processes regarding shoot architecture and branching patterns, as seen in other terrestrial plant species.[10,20–23] Further, there is a slight increase in expression observed in leaf tissue before the emergence of flowering shoots. This peak in expression in annual populations approximately coincided with maximum photoperiod, indicating that photoperiod may be one influencing factor on the expression of these *ZmaFT* genes. This result aligns with previous literature, where temperature, salinity, and photoperiod

were found as environmental controls of flowering.[56,68,69] Collectively this mechanism likely influences the differential growth observed across local and seasonal eelgrass populations.

ZmaFT9 may be the main determinant of flowering through repression of flowering onset

Our results suggest that a repressor, *ZmaFT9*, may be a major determinant of flowering onset in *Z. marina*. Not only did overexpression of *ZmaFT9* have a significant delay in flowering time in *Arabidopsis*, but its expression was also restricted to vegetative leaves in both *Z. marina* annual and perennials. Moreover, *ZmaFT9* expression in leaves decreased sharply before flowering shoots emerge in the annual ecotype. Only after *ZmaFT9* expression decreases do we observe increased expression in *ZmaFT2* and *ZmaFT4*. Adult perennial shoots that remained vegetative express *ZmaFT9* at high levels, which was not seen in adult perennial flowering shoots. These results suggest the involvement of *ZmaFT9* in the repression of flowering. Given that *ZmaFT9* is found only in leaves, we hypothesize that *ZmaFT9* acts as an antiflorigen,[70] which prevents activation of flowering through repression of flower-activating gene expression. In *Arabidopsis*, flowering onset is proposed to be control by competition of binding to the same target transcription factor between florigen and antiflorigen.[71] If this is the case in eelgrasses, having higher expression levels of *ZmaFT9* than *ZmaFT2*/*ZmaFT4* in vegetative shoots may play an important role in repressing floral transition. In this framework, the presence of antiflorigen maintains the vegetative state in shoots, and when it is substantially reduced, the shoot experiences the onset of flowering.

Several *FT* homologs have been previously implicated to function antagonistically to canonical florigen. *BvFT1* in beets (*Beta vulgaris*) represses flowering through repression of *BvFT2*, the functionally conserved homolog of *Arabidopsis FT.*[33] Similarly, chrysanthemums (*Chrysanthemum seticuspe*) also contain an antiflorigenic FT/TFL1 family protein (CsAFT) that acts antagonistically to CsFTL3[72]. *ZmaFT9* is the first antiflorigen described in a marine angiosperm. Further study of *ZmaFT9* antiflorigen will reveal the mechanism of repression by which *Z. marina* regulates flowering in marine environments.

ZmaTFL1a may regulate flowering shoot architecture and other processes

While many genes within the *FT* or *TFL1* clade have previously described functions in regulating flowering, we know that several *PEBP* genes are implicated in developmental

processes other than flowering.[2] In strawberries (*Fragaria vesca*), three *FT* genes collectively impact plant architecture and *FveFT3* has an effect on fruit yield.[24] The *FT* homolog *StSP6A* induced tuberization in potato (*Solanum tuberosum*).[23] *TFL1* homologs are also plays a role in flowering shoot architecture, with *tfl1 Arabidopsis* plants having short stems with single terminal flowers.[6,66] Overexpression of *RCN1* and *RCN2*, the *TFL1* homologs in rice (*Oryza sativa*), prevents stem elongation and affects branching and panicle development in rice plants.[65] *ZmaTFL1a* is expressed at low levels in leaf tissue in vegetative shoots. In both ecotypes, *ZmaTFL1a* expression increases greatly in rhizome tissue once the floral transition has occurred (Figures 4, S7, and S10). Paired with the delayed flowering phenotype in *35S:ZmaTFL1a Arabidopsis* (Figure 2), we hypothesize that *ZmaTFL1a* may contribute to shoot architecture. Further study of *ZmaTFL1a* function and regulation within *Z. marina* populations may yield new insights into increasing seed potential in a population, a key component of increasing population genetic diversity[43] and a strategy currently being used in restoration practices in the eastern United States.[42,44,45]

Our study focused primarily on flowering onset and therefore did not pursue inquiry in other developmental functions. However, we used RNA sequencing to capture expression of all thirteen *PEBP* genes we identified in our phylogenetic analyses. In addition to *ZmaFT2*, *ZmaFT4*, *ZmaFT9*, and *ZmaTFL1a*, we observed expression of *ZmaFT5*, *ZmaFT6*, and *ZmaMFT1* at consistent levels across vegetative and flowering perennials and annuals (Figure S10). *ZmaFT5*, *ZmaFT6*, and *ZmaMFT1* had weak but statistically significant effects on flowering time in heterologous functional assays in *Arabidopsis* (Figure 2), and detectable expression of these genes may indicate some minor role in flowering or reproductive processes. Among tissues examined, we did not see clear difference in *ZmaPEPB* expression between perennials and annual flowering shoots, indicating that the transcriptional regulation of *ZmaPEPB* genes in these tissues is similar between two life history types.

It is also possible *ZmaPEBP* genes may have also experienced subfunctionalization or neofunctionalization regarding processes attributed to *FT*. For example, *FT* is involved in regulation of stomata opening,[73] but *ZmaPEBP* genes would lack this role since eelgrass lack stomata and genes responsible for stomata differentiation.[38] Given the wide array of effects expression of these genes has on various developmental processes in other plants, we expect that future studies will elucidate other roles of *PEBP* genes in eelgrass that were not brought to light

due to experimental limitations and lack of gene-editing tools. Our methodology described here may also facilitate the study of *PEBP* genes in other marine angiosperms. Further, we expect that study of activating and repressing florigens in the context of eelgrass populations on a larger scale will provide more insights to how these genes are influenced by local environmental factors. Continued research into function of *ZmaPEBP* genes in flowering will impact reproduction- and restoration-focused research and allow for more strategic and efficient seed-based restoration efforts of eelgrass.

Conclusion

Our study begins to address the long-standing question of why certain eelgrass shoots flower and why flowering frequency varies across spatial scales and seasonally. There is a breadth of work exploring this question from the population level, often comparing local environmental factors,[49,52,55,69,74] but no studies to date approaching this question from a molecular and mechanistic perspective. Rising atmospheric and water temperatures and increasing frequency of extreme climate events predicted as a result of climate change will likely increase the thermal stress on marine and aquatic ecosystems and have impacts on eelgrass population health.[75–77] With global loss of seagrass populations estimated at 7% annually and rising[39,78] and given the importance of seeds in promoting resiliency in eelgrass populations,[43] a key gap has been understanding how climate change and warming events will impact eelgrass reproduction and persistence. Characterization of the interacting genetic by environmental controls of flowering will lead to a better understanding of factors affecting seed production and to improved seed-based restoration strategies to inform their restoration and management.

Limitations of study

Because there are no molecular genetic tools in eelgrass, we were able to use heterologous function assays in *Arabidopsis* to evaluate gene function. Heterologous assays, while useful and commonly used to assess the function of *PEBP* homologs, provide only information about genes that result in strong and obvious phenotypes when expressed. Because eelgrass morphology and development are different from *Arabidopsis*, heterologous assays alone may not capture the multifaceted role of *ZmaPEBP* genes in eelgrass. Although the florigen function is thought to be conserved in angiosperms, at the molecular level, potential

compatibility differences of each eelgrass PEBP protein with specific *Arabidopsis* flowering signal molecules may interfere the outcome of the flowering function assay. In addition, without loss- and gain-of-function analyses, we were only able to determine correlations between expression patterns in *Z. marina* and reproductive and developmental state in our samples, rather than causal relations. Future studies will be needed to further elucidate the exact function, mechanism, and roles in processes beyond flowering onset of *ZmaPEBP* genes in eelgrass.

ACKNOWLEDGEMENTS

We thank A. K. Hempton, W. Albers, C. Nguyen, K. Kranzler, and A. Keely for technical support. This research was funded by Washington State Department of Natural Resources Interagency Agreements (93-102930 to J. L. R. and T. I.., and 93-106455 to T. I.), U.S. Geological Survey Northwest Climate Adaptation Science Center award G17AC00218 to C. T. N., the University of Washington Biology Department (W. T. Edmonson Award, Lawrence Giles Botanical Field Research Award, and the Kruckeberg-Walker Award to C. T. N., and the Frye-Hotson Rigg Award to I. C.), and in part by the National Institute of Health (R01GM079712 to T.I.). The views expressed in this article are those of the authors and do not necessarily represent the views or policies of the U.S. Environmental Protection Agency.

COMPETING INTERESTS

The authors declare no competing interest.

AUTHOR CONTRIBUTIONS

C. T. N, C. D., J. L. R., and T. I. designed the research. C. T. N., I. C., A. F.-S., and B. A. B. O. performed research. C. T. N., I. C., A. F.-S., B. A. B. O., C. Y., K. A. N., V. S. D. S., J.E.K., and J. L. R. analyzed, collected, and/or interpreted data. C. T. N, I. C., J. L. R., and T. I. obtained funding. C. T. N., B. A. B. O., K. A. N., J. L. R., and T. I. wrote the manuscript, together with all authors' contribution.

RESOURCE AVAILABILITY

Lead contact: Further information and requests for resources and reagents should be directed to and will be fulfilled by the lead contact, Takato Imaizumi (takato@uw.edu).

Material Availability: All data required to support the claims of this paper are included in the main and supplemental information. All reagents generated in this study are available on request from the lead contact.

Data and code availability: All sequencing data were deposited to the National Center for Biotechnology Information (NCBI) Sequence Read Archive (SRA) under BioProject number PRJNA1251697. All alignments, scripts, population metadata, and genotypes (filtered and unfiltered) are available on Dryad at the following link: https://doi.org/10.5061/dryad.sbcc2frh0

SUPPLEMENTAL INFORMATION

Figure S1: Phylogenetic tree of *FT* ortholog genes from species represented in Figure 1.

Figure S2: Amino acid sequence alignment of ZmaFT, ZmaTFL1, and ZmaMFT proteins with *Arabidopsis* FT and TFL1 and *Oryza sativa* Hd3a (FT ortholog).

Figure S3: Expression levels of *ZmaPEBP* genes in T_1 overexpression lines under a *35S* promoter.

Figure S4: Characterization of *ZmaFT2, ZmaFT4, ZmaFT9* and *ZmaTFL1a Arabidopsis* overexpressor.

Figure S5: Population structure and genetic relationships of eelgrass populations used in our study.

Figure S6: Relative expression levels of *ZmaFT2*, *ZmaFT4*, *ZmaFT9*, and *ZmaTFL1a* across different leaf tissues.

Figure S7: Representative *Z. marina* annual shoots from Stackpole Annual in April, May, June, and July timepoints.

Figure S8: Expression of *ZmaFT4* and *ZmaTFL1A* genes in leaf and rhizome tissue across the 2023 growing season at ST-ANN and NP-ANN sites.

Figure S9: Expression of *ZmaFT2*, *ZmaFT4*, *ZmaFT9* and *ZmaTFL1A* genes in leaf and rhizome tissue across the 2023 growing season at YQ-ANN site.

Figure S10: Normalized counts of *ZmaPEBP* genes from RNA sequencing.

Table S1: Accession and GenBank numbers for DNA sequences used in phylogenic analysis.

Table S2: qPCR primers used in this study.

Table S3: Primers used for pENTR-cloning in this study.

Table S4: GPS coordinates and tidal elevation of study sites within Willapa Bay.

Table S5: Filtering steps applied to the sequenced reads.

Table S6: Pairwise genetic divergence of populations sites in our study.

Table S7: Three-way ANOVA results of linear model testing gene expression in relation to three factors (Site, Life stage, Tissue Type)

Table S8: Two-way ANOVA results of linear model testing gene expression in relation to two factors (Site, Leaf tissue)

Table S9: Two-way ANOVA results gene expression in relation to time in time-series at Stackpole Annual (ST-ANN) and Nahcotta Port Annual (NP-ANN) sites.

Table S10: Statistically significant groupings of time-points at Stackpole Annual (ST-ANN) and Nahcotta Port Annual (NP-ANN) site based on post-hoc Tukey tests.

Table S11: One-way ANOVA results gene expression in relation to time in time-series at Yaquina Bay Annual (YQ-ANN) site.

Table S12: Statistically significant groupings of time-points at Yaquina Bay Annual (ST-ANN) and Nahcotta Port Annual (NP-ANN) site based on post-hoc Tukey tests.

Table S13: Differential gene expression of *ZmaPEBP* genes, calculated as logFold Change from RNA sequencing of Stackpole leaf tissue samples.

Supplemental References

REFERENCES:

1. Pin, P.A., and Nilsson, O. (2012). The multifaceted roles of FLOWERING LOCUS T in plant development. Plant Cell Environ. *35*, 1742–1755. https://doi.org/10.1111/j.1365-3040.2012.02558.x.

2. Wickland, D.P., and Hanzawa, Y. (2015). The *FLOWERING LOCUS T/TERMINAL FLOWER 1* gene family: functional evolution and molecular mechanisms. Mol. Plant *8*, 983–997. https://doi.org/10.1016/j.molp.2015.01.007.

3. Kardailsky, I., Shukla, V.K., Ahn, J.H., Dagenais, N., Christensen, S.K., Nguyen, J.T., Chory, J., Harrison, M.J., and Weigel, D. (1999). Activation tagging of the floral inducer *FT*. Science *286*, 1962–1965. https://doi.org/10.1126/science.286.5446.1962.

4. Yamaguchi, A., Kobayashi, Y., Goto, K., Abe, M., and Araki, T. (2005). *TWIN SISTER OF FT (TSF)* acts as a floral pathway integrator redundantly with *FT*. Plant Cell Physiol. *46*, 1175–1189. https://doi.org/10.1093/pcp/pci151.

5. Corbesier, L., Vincent, C., Jang, S., Fornara, F., Fan, Q., Searle, I., Giakountis, A., Farrona, S., Gissot, L., Turnbull, C., et al. (2007). FT protein movement contributes to long-distance signaling in floral induction of *Arabidopsis*. Science *316*, 1030–1033. https://doi.org/10.1126/science.1141752.

6. Kobayashi, Y., Kaya, H., Goto, K., Iwabuchi, M., and Araki, T. (1999). A pair of related genes with antagonistic roles in mediating flowering signals. Science *286*, 1960–1962. https://doi.org/10.1126/science.286.5446.1960.

7. Mimida, N., Goto, K., Kobayashi, Y., Araki, T., Ahn, J.H., Weigel, D., Murata, M., Motoyoshi, F., and Sakamoto, W. (2001). Functional divergence of the *TFL1*-like gene family in *Arabidopsis* revealed by characterization of a novel homologue. Genes Cells *6*, 327–336. https://doi.org/10.1046/j.1365-2443.2001.00425.x.

8. Yoo, S.J., Chung, K.S., Jung, S.H., Yoo, S.Y., Lee, J.S., and Ahn, J.H. (2010). *BROTHER OF FT AND TFL1 (BFT)* has *TFL1*-like activity and functions redundantly with *TFL1* in inflorescence meristem development in Arabidopsis. Plant J. *63*, 241–253. https://doi.org/10.1111/j.1365-313X.2010.04234.x.

9. Yoo, S.Y., Kardailsky, I., Lee, J.S., Weigel, D., and Ahn, J.H. (2004). Acceleration of flowering by overexpression of *MFT* (*MOTHER OF FT AND TFL1*). Mol. Cells *17*, 95–101. https://doi.org/10.1016/S1016-8478(23)13012-3.

10. Xi, W., Liu, C., Hou, X., and Yu, H. (2010). *MOTHER OF FT AND TFL1* regulates seed germination through a negative feedback loop modulating ABA signaling in *Arabidopsis*. Plant Cell *22*, 1733–1748. https://doi.org/10.1105/tpc.109.073072.

11. Takada, S., and Goto, K. (2003). TERMINAL FLOWER2, an Arabidopsis homolog of HETEROCHROMATIN PROTEIN1, counteracts the activation of *FLOWERING LOCUS T*

by CONSTANS in the vascular tissues of leaves to regulate flowering time. Plant Cell *15*, 2856–2865. https://doi.org/10.1105/tpc.016345.

12. Ratcliffe, O.J., Bradley, D.J., and Coen, E.S. (1999). Separation of shoot and floral identity in *Arabidopsis*. Development *126*, 1109–1120. https://doi.org/10.1242/dev.126.6.1109.

13. Bradley, D., Ratcliffe, O., Vincent, C., Carpenter, R., and Coen, E. (1997). Inflorescence commitment and architecture in *Arabidopsis*. Science *275*, 80–83. https://doi.org/10.1126/science.275.5296.80.

14. Baumann, K., Venail, J., Berbel, A., Domenech, M.J., Money, T., Conti, L., Hanzawa, Y., Madueno, F., and Bradley, D. (2015). Changing the spatial pattern of *TFL1* expression reveals its key role in the shoot meristem in controlling *Arabidopsis* flowering architecture. J. Exp. Bot. *66*, 4769–4780. https://doi.org/10.1093/jxb/erv247.

15. Liu, T.-S., Wu, K.-F., Jiang, H.-W., Chen, K.-W., Nien, T.-S., Bryant, D.A., and Ho, M.-Y. (2023). Identification of a far-red light-inducible promoter that exhibits light intensity dependency and reversibility in a cyanobacterium. ACS Synth. Biol. *12*, 1320–1330. https://doi.org/10.1021/acssynbio.3c00066.

16. Itoh, H., Nonoue, Y., Yano, M., and Izawa, T. (2010). A pair of floral regulators sets critical day length for *Hd3a* florigen expression in rice. Nat. Genet. *42*, 635–638. https://doi.org/10.1038/ng.606.

17. Wu, L., Liu, D., Wu, J., Zhang, R., Qin, Z., Liu, D., Li, A., Fu, D., Zhai, W., and Mao, L. (2013). Regulation of *FLOWERING LOCUS T* by a microRNA in *Brachypodium distachyon*. Plant Cell *25*, 4363–4377. https://doi.org/10.1105/tpc.113.118620.

18. Bennett, T., and Dixon, L.E. (2021). Asymmetric expansions of FT and TFL1 lineages characterize differential evolution of the EuPEBP family in the major angiosperm lineages. BMC Biol. *19*, 181. https://doi.org/10.1186/s12915-021-01128-8.

19. Liu, H., Liu, X., Chang, X., Chen, F., Lin, Z., and Zhang, L. (2023). Large-scale analyses of angiosperm *Flowering Locus T* genes reveal duplication and functional divergence in monocots. Front. Plant Sci. *13*, 1039500. https://doi.org/10.3389/fpls.2022.1039500.

20. Niwa, M., Daimon, Y., Kurotani, K., Higo, A., Pruneda-Paz, J.L., Breton, G., Mitsuda, N., Kay, S.A., Ohme-Takagi, M., Endo, M., et al. (2013). BRANCHED1 interacts with FLOWERING LOCUS T to repress the floral transition of the axillary meristems in *Arabidopsis*. Plant Cell *25*, 1228–1242. https://doi.org/10.1105/tpc.112.109090.

21. Weng, L., Bai, X., Zhao, F., Li, R., and Xiao, H. (2016). Manipulation of flowering time and branching by overexpression of the tomato transcription factor *SlZFP2*. Plant Biotechnol. J. *14*, 2310–2321. https://doi.org/10.1111/pbi.12584.

22. Lifschitz, E., Ayre, B.G., and Eshed, Y. (2014). Florigen and anti-florigen – a systemic mechanism for coordinating growth and termination in flowering plants. Front. Plant Sci. *5*, 465. https://doi.org/10.3389/fpls.2014.00465.

23. Navarro, C., Abelenda, J.A., Cruz-Oró, E., Cuéllar, C.A., Tamaki, S., Silva, J., Shimamoto, K., and Prat, S. (2011). Control of flowering and storage organ formation in potato by FLOWERING LOCUS T. Nature *478*, 119–122. https://doi.org/10.1038/nature10431.

24. Gaston, A., Potier, A., Alonso, M., Sabbadini, S., Delmas, F., Tenreira, T., Cochetel, N., Labadie, M., Prévost, P., Folta, K.M., et al. (2021). The FveFT2 florigen/FveTFL1 antiflorigen balance is critical for the control of seasonal flowering in strawberry while FveFT3 modulates axillary meristem fate and yield. New Phytol. *232*, 372–387. https://doi.org/10.1111/nph.17557.

25. Blázquez, M.A., Ahn, J.H., and Weigel, D. (2003). A thermosensory pathway controlling flowering time in *Arabidopsis thaliana*. Nat. Genet. *33*, 168–171. https://doi.org/10.1038/ng1085.

26. Balasubramanian, S., Sureshkumar, S., Lempe, J., and Weigel, D. (2006). Potent induction of *Arabidopsis thaliana* flowering by elevated growth temperature. PLOS Genet. *2*, e106. https://doi.org/10.1371/journal.pgen.0020106.

27. Lee, J.H., Yoo, S.J., Park, S.H., Hwang, I., Lee, J.S., and Ahn, J.H. (2007). Role of *SVP* in the control of flowering time by ambient temperature in *Arabidopsis*. Genes Dev. *21*, 397–402. https://doi.org/10.1101/gad.1518407.

28. de Montaigu, A., Tóth, R., and Coupland, G. (2010). Plant development goes like clockwork. Trends Genet. *26*, 296–306. https://doi.org/10.1016/j.tig.2010.04.003.

29. Song, Y.H., Ito, S., and Imaizumi, T. (2013). Flowering time regulation: photoperiod- and temperature-sensing in leaves. Trends Plant Sci. *18*, 575–583. https://doi.org/10.1016/j.tplants.2013.05.003.

30. Kinmonth-Schultz, H.A., Tong, X., Lee, J., Song, Y.H., Ito, S., Kim, S.-H., and Imaizumi, T. (2016). Cool night-time temperatures induce the expression of *CONSTANS* and *FLOWERING LOCUS T* to regulate flowering in *Arabidopsis*. New Phytol. *211*, 208–224. https://doi.org/10.1111/nph.13883.

31. Susila, H., Nasim, Z., and Ahn, J. (2018). Ambient temperature-responsive mechanisms coordinate regulation of flowering time. Int. J. Mol. Sci. *19*, 3196. https://doi.org/10.3390/ijms19103196.

32. Takagi, H., Hempton, A.K., and Imaizumi, T. (2023). Photoperiodic flowering in *Arabidopsis*: Multilayered regulatory mechanisms of *CONSTANS* and the florigen *FLOWERING LOCUS T*. Plant Commun. *4*, 100552. https://doi.org/10.1016/j.xplc.2023.100552.

33. Pin, P.A., Benlloch, R., Bonnet, D., Wremerth-Weich, E., Kraft, T., Gielen, J.J.L., and Nilsson, O. (2010). An antagonistic pair of FT homologs mediates the control of flowering time in sugar beet. Science *330*, 1397–1400. https://doi.org/10.1126/science.1197004.

34. Oda, A., Narumi, T., Li, T., Kando, T., Higuchi, Y., Sumitomo, K., Fukai, S., and Hisamatsu, T. (2012). *CsFTL3*, a chrysanthemum *FLOWERING LOCUS T*-like gene, is a key regulator of photoperiodic flowering in chrysanthemums. J. Exp. Bot. *63*, 1461–1477. https://doi.org/10.1093/jxb/err387.

35. Lee, R., Baldwin, S., Kenel, F., McCallum, J., and Macknight, R. (2013). *FLOWERING LOCUS T* genes control onion bulb formation and flowering. Nat. Commun. *4*, 2884. https://doi.org/10.1038/ncomms3884.

36. Kojima, S., Takahashi, Y., Kobayashi, Y., Monna, L., Sasaki, T., Araki, T., and Yano, M. (2002). *Hd3a*, a rice ortholog of the *Arabidopsis FT* gene, promotes transition to flowering downstream of *Hd1* under short-day conditions. Plant Cell Physiol. *43*, 1096–1105. https://doi.org/10.1093/pcp/pcf156.

37. Yoshida, A., Taoka, K., Hosaka, A., Tanaka, K., Kobayashi, H., Muranaka, T., Toyooka, K., Oyama, T., and Tsuji, H. (2021). Characterization of frond and flower development and identification of FT and FD genes from duckweed *Lemna aequinoctialis* Nd. Front. Plant Sci. *12*, 697206. https://doi.org/10.3389/fpls.2021.697206.

38. Olsen, J.L., Rouzé, P., Verhelst, B., Lin, Y.-C., Bayer, T., Collen, J., Dattolo, E., De Paoli, E., Dittami, S., Maumus, F., et al. (2016). The genome of the seagrass *Zostera marina* reveals angiosperm adaptation to the sea. Nature *530*, 331–335. https://doi.org/10.1038/nature16548.

39. Orth, R.J., Carruthers, T.J.B., Dennison, W.C., Duarte, C.M., Fourqurean, J.W., Heck, K.L., Hughes, A.R., Kendrick, G.A., Kenworthy, W.J., Olyarnik, S., et al. (2006). A global crisis for seagrass ecosystems. BioScience *56*, 987–996. https://doi.org/10.1641/0006-3568(2006)56[987:AGCFSE]2.0.CO;2.

40. Hays, C.G., Hanley, T.C., Hughes, A.R., Truskey, S.B., Zerebecki, R.A., and Sotka, E.E. (2021). Local adaptation in marine foundation species at microgeographic scales. Biol. Bull. *241*, 16–29. https://doi.org/10.1086/714821.

41. Nejrup, L.B., and Pedersen, M.F. (2008). Effects of salinity and water temperature on the ecological performance of *Zostera marina*. Aquat. Bot. *88*, 239–246. https://doi.org/10.1016/j.aquabot.2007.10.006.

42. Marion, S.R., and Orth, R.J. (2010). Innovative techniques for large-scale seagrass restoration using *Zostera marina* (eelgrass) seeds. Restor. Ecol. *18*, 514–526. https://doi.org/10.1111/j.1526-100X.2010.00692.x.

43. Kendrick, G.A., Waycott, M., Carruthers, T.J.B., Cambridge, M.L., Hovey, R., Krauss, S.L., Lavery, P.S., Les, D.H., Lowe, R.J., Vidal, O.M. i, et al. (2012). The central role of dispersal in the maintenance and persistence of seagrass populations. BioScience *62*, 56–65. https://doi.org/10.1525/bio.2012.62.1.10.

44. Orth, R.J., Moore, K.A., Marion, S.R., Wilcox, D.J., and Parrish, D.B. (2012). Seed addition facilitates eelgrass recovery in a coastal bay system. Mar. Ecol. Prog. Ser. *448*, 177–195. https://doi.org/10.3354/meps09522.

45. Orth, R.J., Lefcheck, J.S., McGlathery, K.S., Aoki, L., Luckenbach, M.W., Moore, K.A., Oreska, M.P.J., Snyder, R., Wilcox, D.J., and Lusk, B. (2020). Restoration of seagrass habitat leads to rapid recovery of coastal ecosystem services. Sci. Adv. *6*, eabc6434. https://doi.org/10.1126/sciadv.abc6434.

46. van Katwijk, M.M., Thorhaug, A., Marbà, N., Orth, R.J., Duarte, C.M., Kendrick, G.A., Althuizen, I.H.J., Balestri, E., Bernard, G., Cambridge, M.L., et al. (2016). Global analysis of seagrass restoration: the importance of large-scale planting. J. Appl. Ecol. *53*, 567–578. https://doi.org/10.1111/1365-2664.12562.

47. Cronau, R.J.T., de Fouw, J., van Katwijk, M.M., Bouma, T.J., Heusinkveld, J.H.T., Hoeijmakers, D., Lamers, L.P.M., and van der Heide, T. (2023). Seed- versus transplant-based eelgrass (*Zostera marina L.*) restoration success in a temperate marine lake. Restor. Ecol. *31*, e13786. https://doi.org/10.1111/rec.13786.

48. Robertson, A.I., and Mann, K.H. (1984). Disturbance by ice and life-history adaptations of the seagrass *Zostera marina*. Mar. Biol. *80*, 131–141. https://doi.org/10.1007/BF02180180.

49. Ruesink, J.L., Ortiz, B.A.B., Mawson, C.H., and Boardman, F.C. (2022). Tradeoffs in life history investment of eelgrass *Zostera marina* across estuarine intertidal conditions. Mar. Ecol. Prog. Ser. *686*, 61–70. https://doi.org/10.3354/meps14000.

50. Qin, L.-Z., Li, W.-T., Zhang, X.-M., Nie, M., and Li, Y. (2014). Sexual reproduction and seed dispersal pattern of annual and perennial *Zostera marina* in a heterogeneous habitat. Wetl. Ecol. Manag. *22*, 671–682. https://doi.org/10.1007/s11273-014-9363-5.

51. Thom, R.M., Borde, A.B., Rumrill, S., Woodruff, D.L., Williams, G.D., Southard, J.A., and Sargeant, S.L. (2003). Factors influencing spatial and annual variability in eelgrass (*Zostera marina* L.) meadows in Willapa Bay, Washington, and Coos Bay, Oregon, estuaries. Estuaries *26*, 1117–1129. https://doi.org/10.1007/BF02803368.

52. Yang, S., Wheat, E.E., Horwith, M.J., and Ruesink, J.L. (2013). Relative impacts of natural stressors on life history traits underlying resilience of intertidal eelgrass (*Zostera marina L.*). Estuaries Coasts *36*, 1006–1013. https://doi.org/10.1007/s12237-013-9609-0.

53. Qin, L.-Z., Kim, S.H., Song, H.-J., Suonan, Z., Kim, H., Kwon, O., and Lee, K.-S. (2020). Influence of regional water temperature variability on the flowering phenology and sexual reproduction of the seagrass *Zostera marina* in Korean coastal waters. Estuaries Coasts *43*, 449–462. https://doi.org/10.1007/s12237-019-00569-3.

54. Keddy, C.J. (1987). Reproduction of annual eelgrass: Variation among habitats and comparison with perennial eelgrass (*Zostera marina* L.). Aquat. Bot. *27*, 243–256. https://doi.org/10.1016/0304-3770(87)90044-1.

55. Phillips, R.C., Stewart Grant, W., and Peter McRoy, C. (1983). Reproductive strategies of eelgrass (*Zostera marina* L.). Aquat. Bot. *16*, 1–20. https://doi.org/10.1016/0304-3770(83)90047-5.

56. Harwell, M.C., and Rhode, J.M. (2007). Effects of edge/interior and patch structure on reproduction in *Zostera marina* L. in Chesapeake Bay, USA. Aquat. Bot. *87*, 147–154. https://doi.org/10.1016/j.aquabot.2007.04.007.

57. Zheng, R., Meng, X., Hu, Q., Yang, B., Cui, G., Li, Y., Zhang, S., Zhang, Y., Ma, X., Song, X., et al. (2023). OsFTL12, a member of FT-like family, modulates the heading date and plant architecture by florigen repression complex in rice. Plant Biotechnol. J. *21*, 1343–1360. https://doi.org/10.1111/pbi.14020.

58. Delaux, P.-M., Hetherington, A.J., Coudert, Y., Delwiche, C., Dunand, C., Gould, S., Kenrick, P., Li, F.-W., Philippe, H., Rensing, S.A., et al. (2019). Reconstructing trait evolution in plant evo–devo studies. Curr. Biol. *29*, R1110–R1118. https://doi.org/10.1016/j.cub.2019.09.044.

59. Ho, W.W.H., and Weigel, D. (2014). Structural features determining flower-promoting activity of *Arabidopsis* FLOWERING LOCUS T. Plant Cell *26*, 552–564. https://doi.org/10.1105/tpc.113.115220.

60. Hanzawa, Y., Money, T., and Bradley, D. (2005). A single amino acid converts a repressor to an activator of flowering. Proc. Natl. Acad. Sci. *102*, 7748–7753. https://doi.org/10.1073/pnas.0500932102.

61. Huala, E., and Sussex, I.M. (1992). LEAFY interacts with floral homeotic genes to regulate Arabidopsis floral development. Plant Cell *4*, 901–913. https://doi.org/10.1105/tpc.4.8.901.

62. Hanano, S., and Goto, K. (2011). *Arabidopsis* TERMINAL FLOWER1 is involved in the regulation of flowering time and inflorescence development through transcriptional repression. Plant Cell *23*, 3172–3184. https://doi.org/10.1105/tpc.111.088641.

63. Yu, L., Khachaturyan, M., Matschiner, M., Healey, A., Bauer, D., Cameron, B., Cusson, M., Emmett Duffy, J., Joel Fodrie, F., Gill, D., et al. (2023). Ocean current patterns drive the worldwide colonization of eelgrass (Zostera marina). Nat. Plants *9*, 1207–1220. https://doi.org/10.1038/s41477-023-01464-3.

64. MacAlister, C.A., Park, S.J., Jiang, K., Marcel, F., Bendahmane, A., Izkovich, Y., Eshed, Y., and Lippman, Z.B. (2012). Synchronization of the flowering transition by the tomato *TERMINATING FLOWER* gene. Nat. Genet. *44*, 1393–1398. https://doi.org/10.1038/ng.2465.

65. Nakagawa, M., Shimamoto, K., and Kyozuka, J. (2002). Overexpression of *RCN1* and *RCN2*, rice *TERMINAL FLOWER 1/CENTRORADIALIS* homologs, confers delay of phase transition and altered panicle morphology in rice. Plant J. *29*, 743–750. https://doi.org/10.1046/j.1365-313X.2002.01255.x.

66. Shannon, S., and Meeks-Wagner, D.R. (1991). A mutation in the arabidopsis *TFL1* gene affects inflorescence meristem development. Plant Cell *3*, 877–892. https://doi.org/10.1105/tpc.3.9.877.

67. Holm, Theo. (1929). The application of the term “rhizome.” Rhodora *31*, 6–17.

68. McMillan, C. (1976). Experimental studies on flowering and reproduction in seagrasses. Aquat. Bot. *2*, 87–92. https://doi.org/10.1016/0304-3770(76)90011-5.

69. Blok, S.E., Olesen, B., and Krause-Jensen, D. (2018). Life history events of eelgrass *Zostera marina L.* populations across gradients of latitude and temperature. Mar. Ecol. Prog. Ser. *590*, 79–93. https://doi.org/10.3354/meps12479.

70. Higuchi, Y. (2018). Florigen and anti-florigen: flowering regulation in horticultural crops. Breed. Sci. *68*, 109–118. https://doi.org/10.1270/jsbbs.17084.

71. Jaeger, K.E., Pullen, N., Lamzin, S., Morris, R.J., and Wigge, P.A. (2013). Interlocking feedback loops govern the dynamic behavior of the floral transition in *Arabidopsis*. Plant Cell *25*, 820–833. https://doi.org/10.1105/tpc.113.109355.

72. Higuchi, Y., Narumi, T., Oda, A., Nakano, Y., Sumitomo, K., Fukai, S., and Hisamatsu, T. (2013). The gated induction system of a systemic floral inhibitor, antiflorigen, determines obligate short-day flowering in chrysanthemums. Proc. Natl. Acad. Sci. *110*, 17137–17142. https://doi.org/10.1073/pnas.1307617110.

73. Kinoshita, T., Ono, N., Hayashi, Y., Morimoto, S., Nakamura, S., Soda, M., Kato, Y., Ohnishi, M., Nakano, T., Inoue, S., et al. (2011). Flowering locus t regulates stomatal opening. Curr. Biol. *21*, 1232–1238. https://doi.org/10.1016/j.cub.2011.06.025.

74. von Staats, D.A., Hanley, T.C., Hays, C.G., Madden, S.R., Sotka, E.E., and Hughes, A.R. (2021). Intra-meadow variation in seagrass flowering phenology across depths. Estuaries Coasts *44*, 325–338. https://doi.org/10.1007/s12237-020-00814-0.

75. Jager, H.I., King, A.W., Gangrade, S., Haines, A., DeRolph, C., Naz, B.S., and Ashfaq, M. (2018). Will future climate change increase the risk of violating minimum flow and maximum temperature thresholds below dams in the Pacific Northwest? Clim. Risk Manag. *21*, 69–84. https://doi.org/10.1016/j.crm.2018.07.001.

76. Kendrick, G.A., Nowicki, R.J., Olsen, Y.S., Strydom, S., Fraser, M.W., Sinclair, E.A., Statton, J., Hovey, R.K., Thomson, J.A., Burkholder, D.A., et al. (2019). A systematic review of how multiple stressors from an extreme event drove ecosystem-wide loss of resilience in an iconic seagrass community. Front. Mar. Sci. *6*, 455.

77. Hobday, A.J., Oliver, E.C.J., Gupta, A.S., Benthuysen, J.A., Burrows, M.T., Donat, M.G., Holbrook, N.J., Moore, P.J., Thomsen, M.S., Wernberg, T., et al. (2018). Categorizing and naming marine heatwaves. Oceanography *31*, 162–173.

78. Waycott, M., Duarte, C.M., Carruthers, T.J.B., Orth, R.J., Dennison, W.C., Olyarnik, S., Calladine, A., Fourqurean, J.W., Heck, K.L., Hughes, A.R., et al. (2009). Accelerating loss of seagrasses across the globe threatens coastal ecosystems. Proc. Natl. Acad. Sci. *106*, 12377–12381. https://doi.org/10.1073/pnas.0905620106.

79. Ransbotyn, V., and Reusch, T.B.H. (2006). Housekeeping gene selection for quantitative real-time PCR assays in the seagrass *Zostera marina* subjected to heat stress. Limnol. Oceanogr. Methods *4*, 367–373. https://doi.org/10.4319/lom.2006.4.367.

80. Song, Y.H., Kubota, A., Kwon, M.S., Covington, M.F., Lee, N., Taagen, E.R., Laboy Cintrón, D., Hwang, D.Y., Akiyama, R., Hodge, S.K., et al. (2018). Molecular basis of flowering under natural long-day conditions in *Arabidopsis*. Nat. Plants *4*, 824–835. https://doi.org/10.1038/s41477-018-0253-3.

81. Takagi, H., Lee, N., Hempton, A.K., Purushwani, S., Notaguchi, M., Yamauchi, K., Shirai, K., Kawakatsu, Y., Uehara, S., Albers, W.G., et al. (2025). Florigen-producing cells express FPF1-LIKE PROTEIN 1 to accelerate flowering and stem growth in Arabidopsis. Dev. Cell *0*. https://doi.org/10.1016/j.devcel.2025.02.003.

82. Altschul, S.F., Gish, W., Miller, W., Myers, E.W., and Lipman, D.J. (1990). Basic local alignment search tool. J. Mol. Biol. *215*, 403–410. https://doi.org/10.1016/S0022-2836(05)80360-2.

83. Madeira, F., Madhusoodanan, N., Lee, J., Eusebi, A., Niewielska, A., Tivey, A.R.N., Lopez, R., and Butcher, S. (2024). The EMBL-EBI Job Dispatcher sequence analysis tools framework in 2024. Nucleic Acids Res. *52*, W521–W525. https://doi.org/10.1093/nar/gkae241.

84. Nguyen, L.T., Schmidt, H.A., von Haeseler, A., and Bui, M.Q. (2014). IQ-TREE: a fast and effective stochastic algorithm for estimating maximum-likelihood phylogenies. *32*, 268–274.

85. Kalyaanamoorthy, S., Minh, B.Q., Wong, T.K.F., von Haeseler, A., and Jermiin, L.S. (2017). ModelFinder: fast model selection for accurate phylogenetic estimates. Nat. Methods *14*, 587–589. https://doi.org/10.1038/nmeth.4285.

86. Hoang, D.T., Chernomor, O., von Haeseler, A., Minh, B.Q., and Vinh, L.S. (2018). Ufboot2: improving the ultrafast bootstrap approximation. Mol. Biol. Evol. *35*, 518–522. https://doi.org/10.1093/molbev/msx281.

87. Maddison, W.P., and Maddison, D.R. (2023). Mesquite: a modular system for evolutionary analysis. Version Version 3.81.

88. Katoh, K., Misawa, K., Kuma, K., and Miyata, T. (2002). MAFFT: a novel method for rapid multiple sequence alignment based on fast Fourier transform. Nucleic Acids Res. *30*, 3059–3066.

89. Patro, R., Duggal, G., Love, M.I., Irizarry, R.A., and Kingsford, C. (2017). Salmon provides fast and bias-aware quantification of transcript expression. Nat. Methods *14*, 417–419. https://doi.org/10.1038/nmeth.4197.

90. Love, M.I., Huber, W., and Anders, S. (2014). Moderated estimation of fold change and dispersion for RNA-seq data with DESeq2. Genome Biol. *15*, 550. https://doi.org/10.1186/s13059-014-0550-8.

91. Chen, S., Zhou, Y., Chen, Y., and Gu, J. (2018). fastp: an ultra-fast all-in-one FASTQ preprocessor. Bioinformatics *34*, i884–i890. https://doi.org/10.1093/bioinformatics/bty560.

92. Bates, D., Mächler, M., Bolker, B., and Walker, S. (2015). Fitting linear mixed-effects models using lme4. J. Stat. Softw. *67*, 1–48. https://doi.org/10.18637/jss.v067.i01.

93. Searle, S.R., Speed, F.M., and Milliken, G.A. (1980). Population marginal means in the linear model: an alternative to least squares means. Am. Stat.

94. Catchen, J., Hohenlohe, P.A., Bassham, S., Amores, A., and Cresko, W.A. (2013). Stacks: an analysis tool set for population genomics. Mol. Ecol. *22*, 3124–3140. https://doi.org/10.1111/mec.12354.

95. DeRaad, D.A. (2022). snpfiltr: An R package for interactive and reproducible SNP filtering. Mol. Ecol. Resouces *22*, 2443–2453. https://doi.org/10.1111/1755-0998.13618.

96. Chang, C.C., Chow, C.C., Tellier, L.C., Vattikuti, S., Purcell, S.M., and Lee, J.J. (2015). Second-generation PLINK: rising to the challenge of larger and richer datasets. Gigascience *4*, 7. https://doi.org/10.1186/s13742-015-0047-8.

97. de Meeûs, T., and Goudet, J. (2007). A step-by-step tutorial to use HierFstat to analyse populations hierarchically structured at multiple levels. Infect. Genet. Evol. *7*, 731–735. https://doi.org/10.1016/j.meegid.2007.07.005.

98. Pritchard, J.K., Stephens, M., and Donnelly, P. (2000). Inference of population structure using multilocus genotype data. Genetics *155*, 945–959. https://doi.org/10.1093/genetics/155.2.945.

99. Jombart, T., and Ahmed, I. (2011). adegenet 1.3-1: new tools for the analysis of genome-wide SNP data. Bioinformatics *27*, 3070–3071. https://doi.org/10.1093/bioinformatics/btr521.

100. Hickey, B.M., and Banas, N.S. (2003). Oceanography of the U.S. Pacific Northwest Coastal Ocean and estuaries with application to coastal ecology. Estuaries *26*, 1010–1031. https://doi.org/10.1007/BF02803360.

101. Ruesink, J.L., Feist, B.E., Harvey, C.J., Hong, J.S., Trimble, A.C., and Wisehart, L.M. (2006). Changes in productivity associated with four introduced species: ecosystem transformation of a ‘pristine’ estuary. Mar. Ecol. Prog. Ser. *311*, 203–215. https://doi.org/10.3354/meps311203.

102. Duffy, J.E., Stachowicz, J.J., Reynolds, P.L., Hovel, K.A., Jahnke, M., Sotka, E.E., Boström, C., Boyer, K.E., Cusson, M., Eklöf, J., et al. (2022). A Pleistocene legacy structures variation in modern seagrass ecosystems. Proc. Natl. Acad. Sci. *119*, e2121425119. https://doi.org/10.1073/pnas.2121425119.

103. Briones Ortiz, B.A., Boardman, F.C., Ruesink, J.L., and Naish, K.A. (2025). Adaptive genetic differentiation between spatially proximate annual and perennial life history types of a marine foundation species. Mol. Ecol. *n/a*, e17730. https://doi.org/10.1111/mec.17730.

104. Astronomical Applications Department, U. S. Naval Observatory (2023). Duration of daylight/darkness table for one year. https://aa.usno.navy.mil/calculated/durdaydark?year=2023&task=0&lat=46.013&lon=124.034&label=&tz=0.00&tz_sign=-1&submit=Get+Data.

105. Lee, H., Golicz, A.A., Bayer, P.E., Jiao, Y., Tang, H., Paterson, A.H., Sablok, G., Krishnaraj, R.R., Chan, C.-K.K., Batley, J., et al. (2016). The genome of a southern hemisphere seagrass species (*Zostera muelleri*). Plant Physiol. *172*, 272–283. https://doi.org/10.1104/pp.16.00868.

106. Dutt, M., Dhekney, S.A., Soriano, L., Kandel, R., and Grosser, J.W. (2014). Temporal and spatial control of gene expression in horticultural crops. Hortic. Res. *1*, 14047. https://doi.org/10.1038/hortres.2014.47.

107. Karimi, M., Inzé, D., and Depicker, A. (2002). GATEWAY^{TM} vectors for *Agrobacterium*-mediated plant transformation. Trends Plant Sci. *7*, 193–195. https://doi.org/10.1016/S1360-1385(02)02251-3.

108. Weigel, D., and Glazebrook, J. (2002). Weigel, D. and Glazebrook, J. (2002) Arabidopsis: a laboratory manual. Cold Spring Harbor Laboratory Press, New York. (Cold Spring Harbor Laboratory Press).

109. Ali, O.A., O'Rourke, S.M., Amish, S.J., Meek, M.H., Luikart, G., Jeffres, C., and Miller, M.R. (2016). RAD Capture (Rapture): Flexible and efficient sequence-based genotyping. Genetics *202*, 389–400. https://doi.org/10.1534/genetics.115.183665.

110. Ma, X., Olsen, J.L., Reusch, T.B.H., Procaccini, G., Kudrna, D., Williams, M., Grimwood, J., Rajasekar, S., Jenkins, J., Schmutz, J., et al. (2021). Improved chromosome-level genome assembly and annotation of the seagrass, *Zostera marina* (eelgrass). F1000Res. *10*, 289. https://doi.org/10.12688/f1000research.38156.1.

111. Li, H. (2013). Aligning sequence reads, clone sequences and assembly contigs with BWA-MEM. ArXiv Q-BioGN.

112. Rochette, N.C., and Catchen, J.M. (2017). Deriving genotypes from RAD-seq short-read data using Stacks. Nat. Protoc. *12*, 2640–2659. https://doi.org/10.1038/nprot.2017.123.

113. Weir, B.S., and Cockerham, C.C. (1984). Estimating F-Statistics for the analysis of population structure. Evolution *38*, 1358–1370. https://doi.org/10.2307/2408641.

114. Goudet, J. (2005). hierfstat, a package for r to compute and test hierarchical F-statistics. Mol. Ecol. Notes *5*, 184–186. https://doi.org/10.1111/j.1471-8286.2004.00828.x.

115. Evanno, G., Regnaut, S., and Goudet, J. (2005). Detecting the number of clusters of individuals using the software structure: a simulation study. Mol. Ecol. *14*, 2611–2620. https://doi.org/10.1111/j.1365-294X.2005.02553.x.

116. Lee, N., Ozaki, Y., Hempton, A.K., Takagi, H., Purusuwashi, S., Song, Y.H., Endo, M., Kubota, A., and Imaizumi, T. (2023). The FLOWERING LOCUS T gene expression is controlled by high-irradiance response and external coincidence mechanism in long days in Arabidopsis. New Phytol. *239*, 208–221. https://doi.org/10.1111/nph.18932.

117. Chen, A., Li, C., Hu, W., Lau, M.Y., Lin, H., Rockwell, N.C., Martin, S.S., Jernstedt, J.A., Lagarias, J.C., and Dubcovsky, J. (2014). PHYTOCHROME C plays a major role in the acceleration of wheat flowering under long-day photoperiod. Proc. Natl. Acad. Sci. *111*, 10037–10044. https://doi.org/10.1073/pnas.1409795111.

118. R Core Team (2024). A language and environment for statistical computing_. (R Foundation for Statistical Computing).

STAR METHODS

KEY RESOURCES TABLE

REAGENT or RESOURCE	SOURCE	IDENTIFIER
Bacterial and virus strains		
Escherichia coli strain DH10B	ThermoFisher	Cat# EC0113
Escherichia coli strain DH5α	ThermoFisher	Cat# EC0112
Agrobacterium tumefaciens strain GV3101	GoldBio	Cat# CC-207-5x50
Biological samples		
Z. marina perennial tissue collected from Willapa Bay, USA	This paper	N/A
Z. marina annual tissue collected from Willapa Bay, USA	This paper	N/A
Z. marina annual tissue collected from Yaquina Bay, USA	This paper	N/A
Chemicals, peptides, and recombinant proteins		
Tris	Fisher Scientific	Cat# BP152
EDTA	ThermoFisher	Cat# 17892
Bacto™Tryptone	Gibco	Cat# 211705
Bacto™ Yeast Extract	Gibco	Cat# 212750
NaCl	Fisher Scientific	Cat# 271-3
Linsmaier-Skoog	PhytoTech Labs	Cat# L689
Spectinomycin	PhytoTech Labs	Cat# S742
Ampicillin	PhytoTech Labs	Cat# A116
Basta (DL-Phosphinithricin)	PhytoTech Labs	Cat# P679
Ticarcillin (Timentin)	PhytoTech Labs	Cat# T869
Sucrose	ThermoFisher	Cat# S512
Silwet L-77 (Bioworld)	Fisher Scientific	Cat# NC1915706
Dynabeads M-280 Streptavidin	Invitrogen	Cat# 11205D
Critical commercial assays		
RNeasy Plant Kit	Qiagen	Cat# 74904
iScript complementary DNA synthesis kit	BioRad	Cat# 1708891
Sso Advance Universal SYPGR Green Supermix	BioRad	Cat# 1725275
DNeasy Plant Pro Kit	Qiagen	Cat# 69204
Agencourt Ampure Beads	Beckman Coulter	Cat# A63880
NEBNext Ultra II DNA Library Prep Kit	NEB	Cat# E7645S/L
T4 DNA Ligase & Buffer	NEB	Cat# M0202M
Sbf1-HF restriction enzyme	NEB	R3642S
Gateway™ LR Clonase™ II Enzyme Mix	ThermoFisher	Cat# 11791020
GeneJET Plasmid Mini Prep Kit	ThermoFisher	FERK0503
Phusion High-Fidelity Polymerase	ThermoFisher	F531S
Deposited data		
RNA-seq	This paper	PRJNA1251697
RAD-seq data and code	This paper	DOI: 10.5061/dryad.sbcc2frh0
Phylogenetic alignment	This paper	DOI: 10.5061/dryad.sbcc2frh0

Experimental models: Organisms/strains		
Arabidopsis thaliana ecotype Columbia-0	ABRC	CS70000
Arabidopsis: 35S:GFP	This paper	N/A
Arabidopsis: 35S:ZmaFT1	This paper	N/A
Arabidopsis: 35S:ZmaFT2	This paper	N/A
Arabidopsis: 35S:ZmaFT3	This paper	N/A
Arabidopsis: 35S:ZmaFT4	This paper	N/A
Arabidopsis: 35S:ZmaFT5	This paper	N/A
Arabidopsis: 35S:ZmaFT6	This paper	N/A
Arabidopsis: 35S:ZmaFT7	This paper	N/A
Arabidopsis: 35S:ZmaFT8	This paper	N/A
Arabidopsis: 35S:ZmaFT9	This paper	N/A
Arabidopsis: 35S:ZmaFT10	This paper	N/A
Arabidopsis: 35S:ZmaTFL1a	This paper	N/A
Arabidopsis: 35S:ZmaTFL1b	This paper	N/A
Arabidopsis: 35S:ZmaMFT1	This paper	N/A
Oligonucleotides		
ZmaPEBP coding sequences	Twist BioSciences (Table S1)	See Table S1
RT-qPCR primers	This paper; Ransbotyn and Reusch[79]; Song et al.,[80]; Takagi et al.,[81] (Table S2)	N/A
pENTR Cloning primers	This paper (Table S3)	N/A
Recombinant DNA		
pENTR/D-TOPO	Invitrogen	RRID:Cat# K240020SP
pB7WG2	Karimi et al.,[61]	N/A
Software and algorithms		
CFX Manager (ver 3.1.1517.0823)	Bio-Rad	N/A
BLAST	Altschul et al.,[82]	N/A
EMBI-EBI Portal	Madeira et al.,[83]	https://www.ebi.ac.uk/
IQ-TREE	Nguyen et al.,[84]	http://www.iqtree.org/
ModelFinder	Kalyaanamoorthy et al.,[85]	N/A
UFBoot	Hoang et al.,[86]	N/A
Mesquite Version 3.70	Maddison and Maddison[87]	https://www.mesquiteproject.org/
MAFFT	Katoh et al.,[88]	https://mafft.cbrc.jp/
Salmon	Patro et al.,[89]	https://combine-lab.github.io/salmon/
DDSeq2	Love et al.,[90]	https://bioconductor.org/packages/release/bioc/html/DESeq2.html
fastp	Chen et al.,[91]	https://github.com/OpenGene/fastp

lme4	Bates et al.,[92]	https://cran.r-project.org/web/packages/lme4/index.html
emmeans	Searle et al.,[93]	https://cran.r-project.org/web/packages/emmeans/index.html
STACKS	Catchen et al.,[94]	https://catchenlab.life.illinois.edu/stacks/
BWA-MEM	Li et al.,[111]	https://github.com/lh3/bwa
SNPFILTR	DeRaad et al.,[95]	https://devonderaad.github.io/SNPfiltR/
PLINK	Chang et al.,[96]	https://www.cog-genomics.org/plink/
HIERFSTAT	Goudet[97], deMeeûs and Goudet[97]6/12/25 5:43:00 PM	https://cran.r-project.org/web/packages/hierfstat/index.html
STRUCTURE v2.1.1.5	Pritchard et al.,[98]	https://web.stanford.edu/group/pritchardlab/structure.html
ADEGENET	Jombart and Ahmed[99]	https://adegenet.r-forge.r-project.org/

EXPERIMENTAL MODEL DETAILS

All *Arabidopsis* lines were grown in long-day (LD) conditions (16 h light, 8 h dark, 100 μmol/m^2s, 22 °C, 70% relative humidity) on either selection media [1xLinsmaier-Skoog (PhytoTech Labs, Lenexa KS) media, 2% sucrose (wt/vol), 100 mg/L ticarcillin, 16 μg/mL Basta], 1X LS media [1xLinsmaier-Skoog], or a soil mixture (Sunshine #4, Sun Gro Horticulture, Agawam MA) as described in Song et al.[29] with supplemented slow-release fertilizer (Osmocote 14-14-14, Scotts Miracle-Gro, Marysville OH) and pesticide (Systemic Granules, Bonide, Oriskany NY). All seeds were sterilized and once sown, were kept at 4°C for 2-5 days for stratification. Plants grown on media were at 22°C in incubators (Percival Scientific, Perry IA) under white fluorescent or LED light with a fluence rate of 90-110μmol m^{-2} sec^{-1}. Plants grown on soil were in the same conditions but grown in PGC Flex reach-in models equipped with broad-spectrum white light (Conviron, Controlled Environments, Pembina ND). Number of rosette and cauline leaves in flowering assays were counted in soil-grown plants when the bolted flowering stem had reached approximately 1cm in height. We collected

seedlings (T_1 and T_3) for gene expression analysis at ZT16 (zeitgeber time 16) and stored samples at -80°C.

Field studies on *Z. marina* flowering occurred in two shallow bays of the U.S. Pacific coast: Willapa Bay, Washington (240 km^2 at mean tide[100] with 34 km^2 of eelgrass meadows[101]) and Yaquina Bay, Oregon (13 km^2)[100] (Table S4). Both bays contain perennial and annual ecotypes. For samples used for restriction-site associated DNA sequencing, 50 shoots were collected from Bay Center and Long Island in April 2023, with 1-2 m spacing between each individual to reduce the probability of collecting clones.[102] The meristem region (3-5 cm) was stored at -80ºC.[103] Samples from Stackpole, Stackpole Annual, and Nahcotta Port Annual sites were collected in 2019 as described in Briones Ortiz et al.[103] For gene expression analysis, *Z. marina* tissues (including rhizome and roots, vegetative mature leaves, inflorescence, and spathes) were collected from perennial population sites in Willapa Bay (Figure 3, Table S4) in a three-consecutive-day period in July (13-15 Jul 2022). We collected tissue from at least 15 adult plants at each site, with 1-2m spacing between each individual. Samples from two annual populations in Willapa Bay (ST-ANN and NP-ANN)[49] and one from Yaquina Bay (YQ-ANN) were collected in a similar manner at two-week intervals from April and August 2023. Samples were placed at -80°C for long-term storage. Photoperiod data was obtained from the US Naval Astronomical Applications Department.[104] Temperature data was collected at the sediment surface using iButtons (Dallas Semiconductor, Dallas TX) in 2-hour increments at Willapa Bay annual sites.

METHOD DETAILS

Phylogenetic analysis and identifying *ZmaPEBP* genes

To identify *PEBP* family genes in *Z. marina*, we performed a BLAST search[82] using *Arabidopsis* FT (AT1G65480) amino acid sequence against the *Z. marina* genome.[38] Sequences of other *PEBP* family genes were obtained from the literature (Table S1), or from the genomes of the order *Alismatales* via a BLAST search with the *Arabidopsis FT* and *ZmaPEBP* sequence as queries. To assess the evolution and expansion of the *PEBP* gene family within *Zostera* species, we included *Zostera muelleri.*[105] *Z. muelleri PEBP* genes were identified via local BLAST search in its genome using *Arabidopsis FT* sequences as query.

To create a phylogenetic tree, all full-length *Alismatales* sequences were aligned with previously described *PEBP* family sequences from *A. thaliana*, *O. sativa, A. coerulea, C. seticuspe,* and *B. distrachyon* by Multiple Sequence Comparison by Log-Expectation (MUSCLE) on the EMBL-EBI portal.[83] The alignment was fine-tuned by hand in Mesquite v 3.70 with the Multiple Sequence Alignment module.[87] We used IQ-TREE[84] to build a maximum-likelihood phylogenetic tree with 1000 bootstraps using ModelFinder[85] to predict the best substitution matrix and UFBoot[86] to compute ultra-fast bootstrap values. Mesquite Version 3.70 was used to build the consensus tree out of 400 base trees including sequences from *Z. marina, Z. muelleri, A. thaliana, B. distachyon, A. coerulea, Lemna aequinoctialis, Symplocarpus renifolius, Spirodela polyrhiza, C. seticuspe, O. sativa*, and *Allium cepa*.

Amino acid residues important in canonical FT and TFL1 structure and function[59,60] were analyzed using a multiple sequence alignment (MAFFT)[88] of amino acid sequences of *Z. marina*, *Arabidopsis* FT and TFL1, and *O. sativa* Hd3a to have a monocot FT sequence as comparison.

Generating *ZmaPEBP* overexpression lines and quantifying flowering time in *Arabidopsis*

To investigate conserved flowering function of *ZmaPEBP* genes, we overexpressed each in the *Arabidopsis* wild-type Col-0 accession. To generate *35S:ZmaPEBP* lines,[106] the coding sequences for each *ZmaPEBP* gene from the *Z. marina* reference genome[38] were synthesized (Twist Bioscience, South San Francisco CA), amplified using Phusion polymerase (ThermoFisher, Bothell WA) with gene-specific primers (Table S2, S3), and cloned into the pENTR D-TOPO plasmid (Invitrogen, Waltham MA). Once verified by sequencing (Azenta Life Sciences, South Plainfield, NJ USA), the *ZmaPEBP* inserts were transferred to the overexpression binary vector, pB7WG2.[107] We transformed *Agrobacterium tumefaciens* strain GV3101 harboring each plasmid via electroporation. According to conventional floral-infiltration methods,[108] cells were grown overnight at 30°C in LB medium [10g/L tryptone, 5g/L yeast extract, 10g/L NaCl] supplemented with Spectinomycin [100µg/mL], and 50mL of culture were used to inoculate 600mL of LB medium, which was then incubated at 30°C for 6 hours. Cells were pelleted and resuspended in the infiltration buffer [50% sucrose, 0.04% Silwet]. Whole flowering stems of *Arabidopsis* plants were submerged in the infiltration buffer for 60 seconds (now T_0). The *35S:GFP* line was generated in a similar manner as a control. Expression levels of *ZmaPEBP* inserts were verified in T_1 and T_3 lines using RT-qPCR.

To screen for altered flowering phenotypes in *35S:ZmaPEBP* lines, we used T_1 generation plants in the initial flowering time assay with all *35S:ZmaPEBP* and *35S:GFP* lines. In the T_1 flowering time assay, sterilized seeds were germinated on selection media and 14-day-old seedlings in were transferred to soil. Flowering assays in the T_1 generation included at least 16 individuals per construct. We recorded rosette leaf number at time of flowering.

Candidate genes that altered flowering time were assayed using homozygous T_3 *35S:ZmaPEBP* plants with a single T-DNA insertion. In the T_3 flowering assays, sterilized seeds were sown directly into soil under LD conditions. We quantified flowering time in a similar manner in T_1 and T_3 lines with at least 10 individuals per line.

Analyses of population genetic structure

Three perennial and two annual populations in Willapa Bay were evaluated for population-level genetic structure was determined using reduced representation sequencing across five sites (RAD-seq; Figure 3G, Table S4).[109]

High-molecular-weight genomic DNA was extracted using DNeasy Plant Pro Kit (Qiagen, Hilden, Germany). Genomic libraries were constructed for restriction-site associated DNA sequencing (RAD-seq)[109] with the restriction enzyme *Sbf1* sequenced using the Illumina NovaSeq 6000 SP platform using 150 bp paired-end reads (University of Oregon, Genomics and Cell Characterization Core Facility). Pooled-library reads were demultiplexed using the *process_radtags* program with *–best-rad* settings and trimmed to 137 bp in STACKS[94]. The single-end reads were aligned to the published genome of *Z. marina*[38,110], using BWA-MEM[111], with minimum alignment and mapping Phred quality scores of 30.

Genotyping of polymorphic loci was conducted using the *ref_map* pipeline in STACKS[112]. Subsequent filtering was performed using the R-package SNPFILTR[95] (steps described in Table S5). Identical multilocus genotypes (MLGs, >95% shared alleles between individuals), a result of clonal reproduction, were identified using PLINK (function –genome)[96]. Only one representative sample of each clonal genotype was retained for further processing. Samples in the Stackpole perennial and both annual sites were initially collected as seedlings resulting from sexual reproduction, and no clones were found.

Population structure was examined using measures of population genetic differentiation (F_{ST})[113] using the R-package HIERFSTAT[97,114]. Population structure was also inferred using a

test of population assignment of individuals, implemented in STRUCTURE v2.1.1.5[98]. The number of clusters (*K*) tested ranged from 1 to 10, and the most likely ancestral groups were evaluated using the mean log probability of the data, $L(K)$[98] and the ΔK statistic[115]. Genetic relationships among individual samples were visualized using a discriminant analysis of principal components (DAPC) plot, implemented in the R package ADEGENET[99].

Collection of plant material, RNA extraction and quantitative RT-PCR

We performed quantitative RT-PCR (RT-qPCR) to analyze gene expression in three instances: *A. thaliana* T_1 and T_3 lines, and *Z. marina* in field collections. For gene expression analysis in T_1 lines, sterilized seeds were germinated selection media in LD conditions to isolate transformants. Two-week-old transformants were transferred to 1xLS media and antibiotics. After one week, transformants (21-day-old) were harvested at ZT16. For gene expression analysis in T_3 lines, plants were grown on 1xLS media for 14 days in LD conditions and collected at ZT16. To account for possible diurnal expression trends of *FT* homologous genes in fields, we collected all *Z. marina* plant material between ZT3-5 to capture peak expression, which occurs in the morning (ZT4) in many long-day plants.[80,116,117] All plant tissue collected was stored in RNAlater stabilization solution (ThermoFisher).

Total RNA was isolated using RNeasy Plant Mini Kit (Qiagen), including an on-column DNA digestion procedure. Complementary DNA (cDNA) was generated with iScript cDNA synthesis kit (Bio-Rad). The qPCR reaction was performed using SSoAdvance SYBR Super Mix (Bio-Rad) with specific primers (Table S2).

We used two reference genes to normalize expression in transgenic *Arabidopsis*, *ISOPENTENYL PYROPHOSPHATE / DIMETHYLALYLL PYROPHOSPHATE ISOMOERASE* (*IPP2*) and *SERINE/THREONINE PROTEIN PHOSPHOTASE 2A* (*PP2A*).[80] We used three reference genes for expression analysis in *Z. marina,*[79] *CYCLOPHILIN 2* (*CYP2*), *EUKARYOTIC INITIATION FACTOR4A* (*ELF4A*), and *RIBOSOME STRUCTURAL PROTEIN L28* (*RPL28*). Samples with no detectable expression were treated as having a cycle threshold (C_T) value as C_T=40. A baseline threshold of relative fluorescence units (RFU) was set for consistency across primers to compare between plates, and resulting C_T values were analyzed using a delta C_T method. The average C_T values of all reference genes were used for calculation.

RNA sequencing sample preparation

To compare expression of all *ZmaPEBP* genes in different reproductive states and across life history types, we performed RNA sequencing on our isolated RNA samples from comparable leaf tissue types from the Stackpole sites ST and ST-ANN (Perennial Vegetative Leaf Tip, collected 15 Jul 2022; Perennial Flowering Leaf, collected 15 Jul 2022; and Annual Flowering Leaf, collected 17 Jul 2023). Samples were processed at GENEWIZ (Azenta Life Sciences) for next-generation sequencing.

QUANTIFICATION AND STATISTICAL ANALYSES

RNA sequencing gene expression analysis

Resulting fasta files of 150 bp paired-end reads were processed and filtered using fastp v0.24.0[91] with the default parameters. To perform alignment and quantification, the fastp outputs of forward and reverse reads were processed with Salmon quant[89] (Galaxy Version 1.10.1+galaxy2) with default settings except for the use of the --gcBias flag. The reference transcriptome and genome were obtained from Olsen et al. 2016[38] (JGI Data portal) under *Zostera marina* v3.1 draft assembly. Quantification is performed on the transcriptome. The genome is supplied to allow for building a decoy aware index. The output files from salmon were processed with tximport v1.34.0. To obtain normalized counts, the DESeqDataSetFromTximport() function from DESeq2 v1.46.0[90] was used to create a DESeq object. Then, the functions estimateSizeFactors() and counts(dds, normalized=TRUE) were used to obtain normalized counts.

Statistical analysis of *Z. marina* qPCR gene expression data

We performed statistical analyses on the *Z. marina* expression data to compare tissue-specific expression in flowering and vegetative life stages across three sites (Jul 2022), and to examine the time series of expression in annual eelgrass (Apr-Aug 2023). Expression of candidate genes (*ZmaFT2*, *ZmaFT4*, *ZmaFT9*, and *ZmaTFL1a*) were analyzed separately. In the first comparison, linear models (analysis of variance, ANOVA) were constructed with relative expression values (delta C_T) as response variable and with site, tissue, and life stage, as well as tissue x life stage interaction included as fixed factors. To be comparable between vegetative and

flowering life stages, the included tissue types were rhizome, stem, and leaf middle (middle 10 cm of leaf blade, Figure 3).

In the second comparison, each of the eight collection timepoints was considered a separate level of a categorical factor. Using a linear model framework, delta C_T was the response variable and fixed effects were timepoint, site, and the timepoint x site interaction which would account for different phenology between sites. Expression values required log-transformation to generate a Gaussian distribution in all analyses. Significant factors or interactions were followed up by post-hoc tests to determine significant differences between groups based on Tukey HSD significance levels. Statistical models were built in R[118] using the package lme4[92], with post-hoc tests from emmeans.[93]

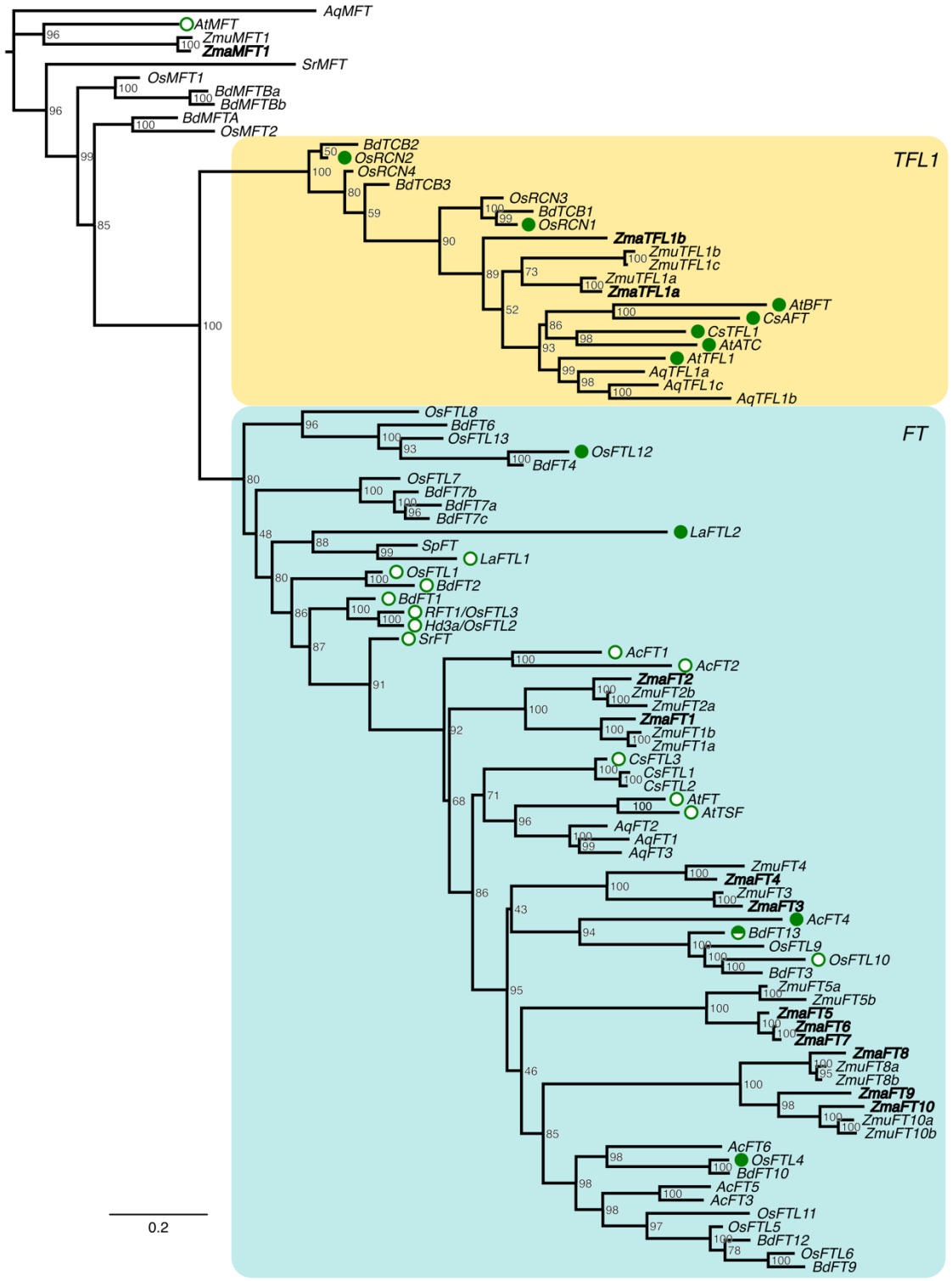

Figure 1: Phylogenetic tree of phosphatidylethanolamine binding protein (PEBP) genes in angiosperms. See Table S1 for sequence accession numbers. Nucleotide-level maximum likelihood analysis with 100 bootstraps, values shown at nodes. Species were chosen to represent the different angiosperm lineages having *PEBP* gene family members, with over-representation of monocotyledoneous and *Alismatales* taxa (monocotyledons: *B. distachyon, O. sativa*, *A. cepa*;

Alismatales: *L. aequinoctialis, S. polyrhiza, S. renifolius, Z. marina, Z. muelleri;* other: *A. thaliana, A. coerulea, C. seticuspe*). *Z. marina* characterized here is shown in bold, and the tree includes its sister species *Z. muelleri* (*Zmu*). *PEBP* genes fall into two clades: *FT* (*FLOWERING LOCUS T,* blue) and *TFL1* (*TERMINAL FLOWER 1*, yellow). Open circles denote previously described activators of flowering, closed circles denote repressors, and half-filled circle denotes activator (under short-day conditions) and repressor (under long-day conditions).

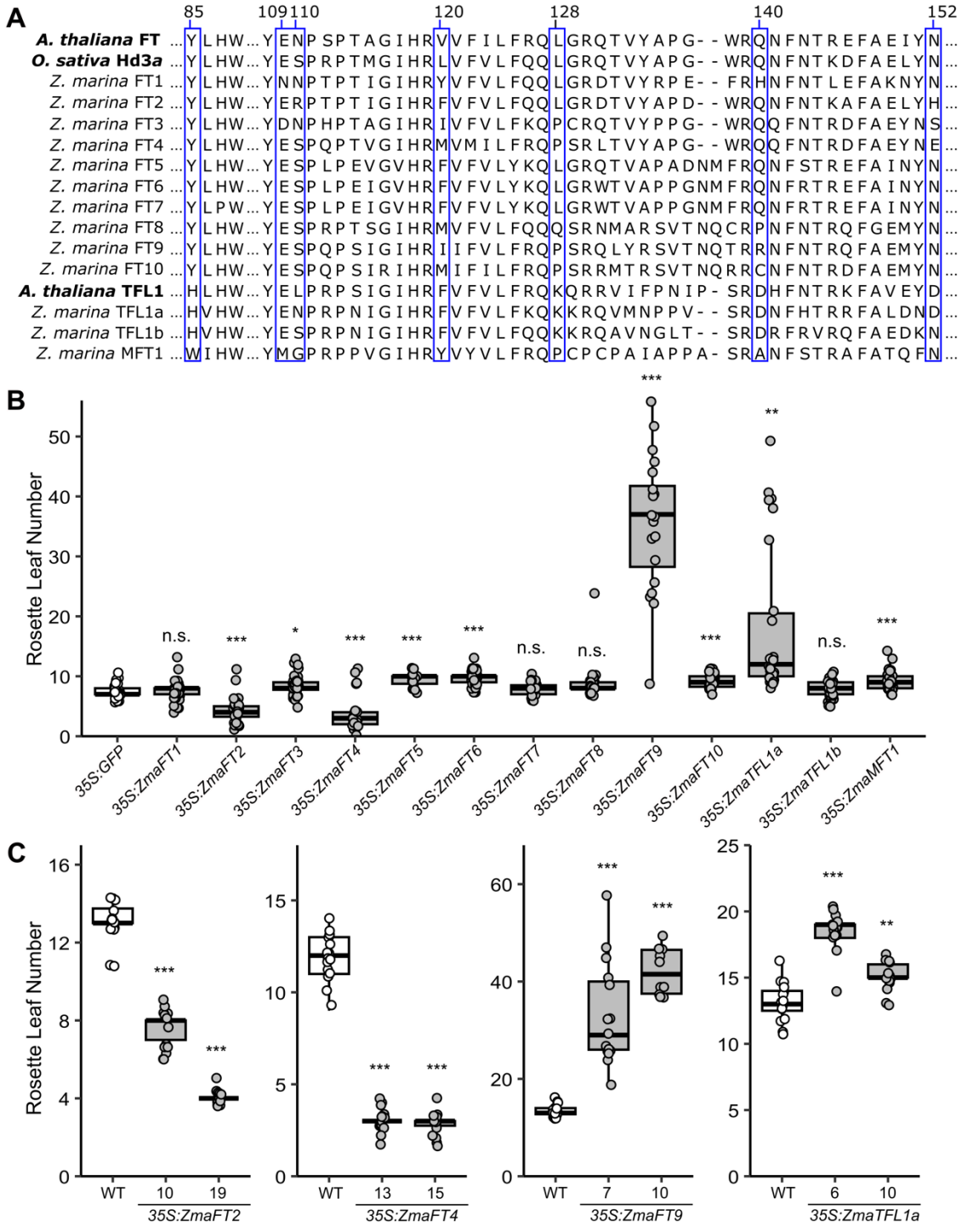

Figure 2: *ZmaFT* and *ZmaTFL1* genes alter flowering phenotype when overexpressed in *Arabidopsis thaliana.* **(A)** Amino acid sequence alignment of ZmaFT and ZmaTFL1 with *Arabidopsis thaliana* FT and TFL1 and *Oryza sativa* Hd3a (an FT ortholog). Blue boxes highlight residues important for FT function as a flowering promoter (blue). **(B)** Overexpression of thirteen *ZmaPEBP* orthologs under the control of the *35S* promoter highlighted four candidates that altered flowering time. *ZmaFT2* and *ZmaFT4* cause precocious flowering, while

ZmaFT9 and *ZmaTFL1A* caused delayed flowering in the T_1 generation under long-day conditions. Asterisks indicate significance based on t-test against the control (*35:GFP*), with Bonferroni correction defining $p=\alpha/n$ (n=number of comparisons) (n.s.: non-significant, *: $p < 0.0038$, **: $p < 0.00077$, ***: $p < 0.000077$). **C)** Altered flowering time phenotype was confirmed in homozygous individuals (T_3 generation). Number labels on x-axis represent homozygous lines. Asterisks indicate significance based on t-test comparing to wild type (WT) with Bonferroni correction ($p=\alpha/n$; **: $p < 0.005$, ***: $p < 0.0005$).
All individuals are shown as data points (n≥16), with median indicated by center line in box, upper and lower quartile by box boundaries, and highest and lowest value within two interquartile ranges by whiskers.

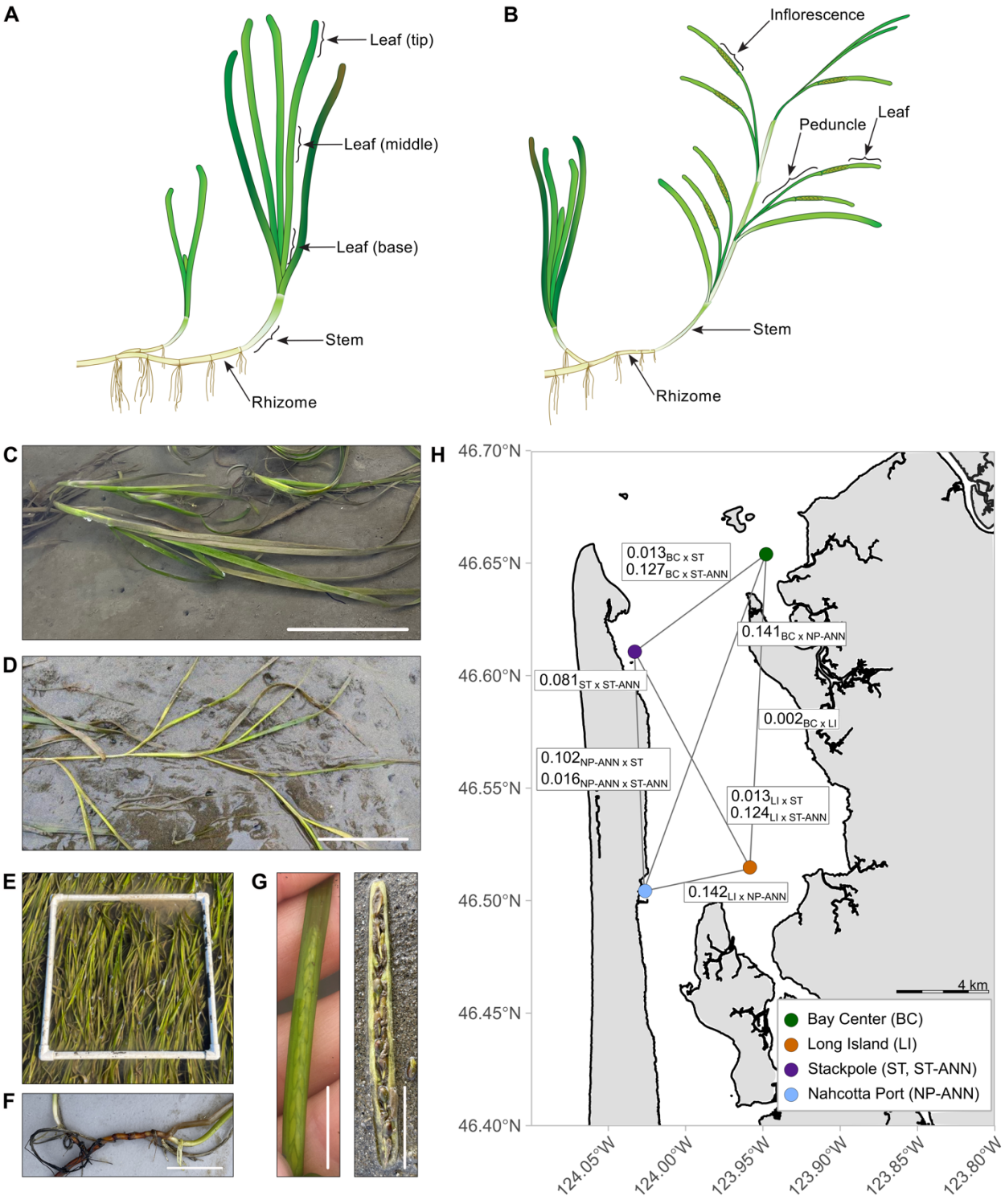

Figure 3: Description of *Zostera marina* (eelgrass) sampling approaches, life stages, and sites used in this study. Tissue isolated from **(A)** vegetative and **(B)** flowering shoots. Eelgrass **(C)** vegetative and **(D)** flowering shoots. Scale bar approximately 10 cm. **(E)** Eelgrass meadows form through **(F)** clonal reproduction via rhizome extension or **(G)** from the formation of inflorescences and seeds within spathes**.** Scale bar approximately 1 cm. **(H)** Geographic location of study sites in Willapa Bay, WA USA: Bay Center (BC), Long Island (LI), Stackpole (ST),

Stackpole Annual (ST-ANN) (ST and ST-ANN represented by sample point on map due to proximity), and Nahcotta Port Annual (NP-ANN) (Table S4). Pairwise genetic distance, F_{ST}, estimated through estimated RAD-Seq analysis shown in white boxes (n=48 per population). Subscript of F_{ST} indicates which sites included in the pair-wise comparison. Scale bar approximately 4 km. Photographs of annual plants are in Supplemental Figure S7.

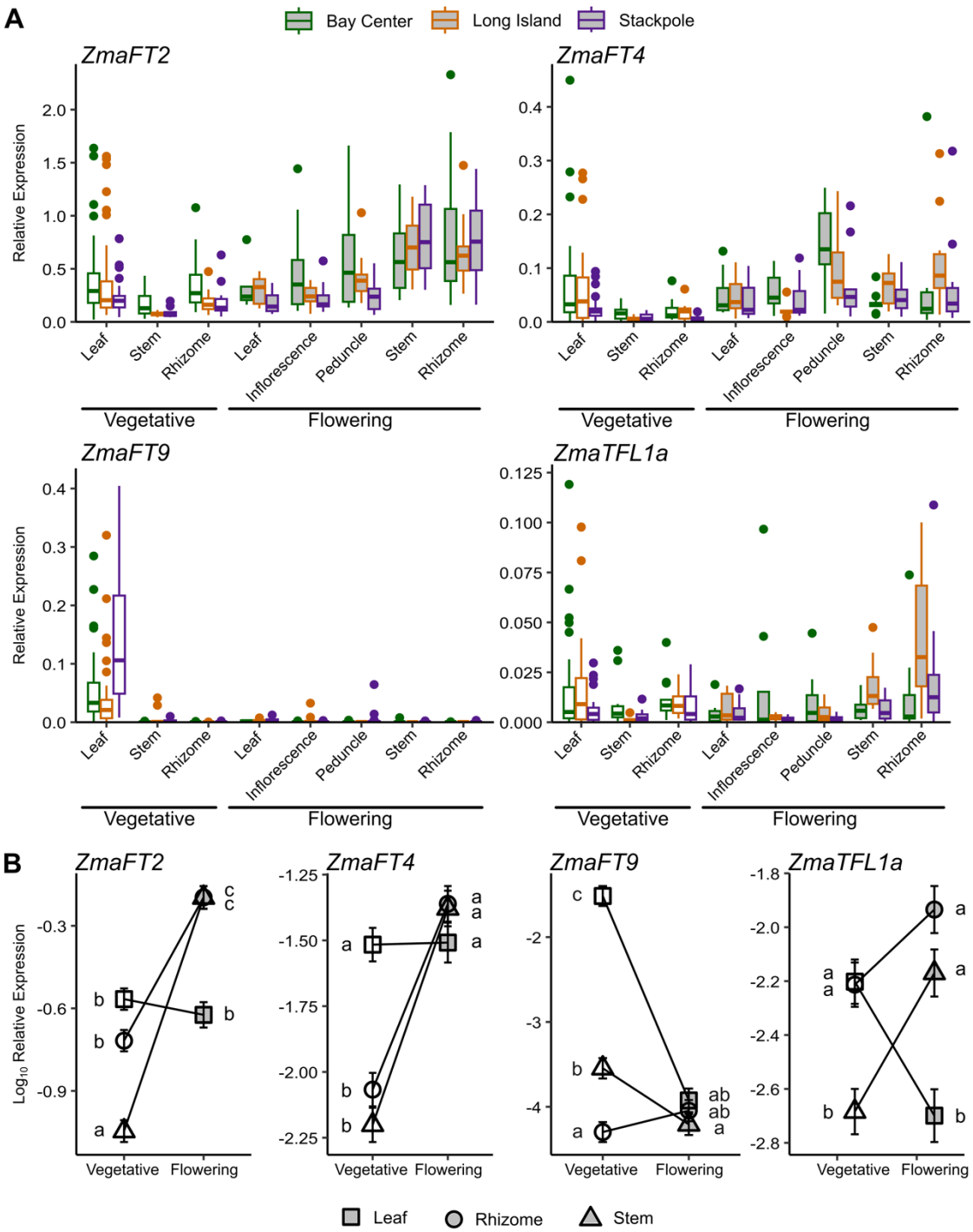

Figure 4: Expression of florigen genes in different *Z. marina* tissues. **(A)** Relative expression levels of *ZmaFT2*, *ZmaFT4*, *ZmaFT9*, and *ZmaTFL1a* across different tissue types in different developmental stages, vegetative (white) and flowering (grey). Expression in tissues was measured in samples (n≥10) from 3 sites shown in Figure 3H. All expression values are relative to 3 reference genes (*CYP2*, *ELF4A*, and *RPL28*). Median is indicated by center line in box, upper and lower quartiles by box boundaries, and highest and lowest values within two interquartile ranges by whiskers. **(B)** Comparing means between tissue types across reveals different trends of expression changes within tissue types across vegetative (white) and flowering

(grey) developmental stages. Mean expression was calculated using $\log_{10}$ transformed expression values. Error bars are standard errors of means. Different letters indicate statistically significantly different groups determined by one-way ANOVA test with post-hoc Tukey HSD of $\log_{10}$ transformed values.

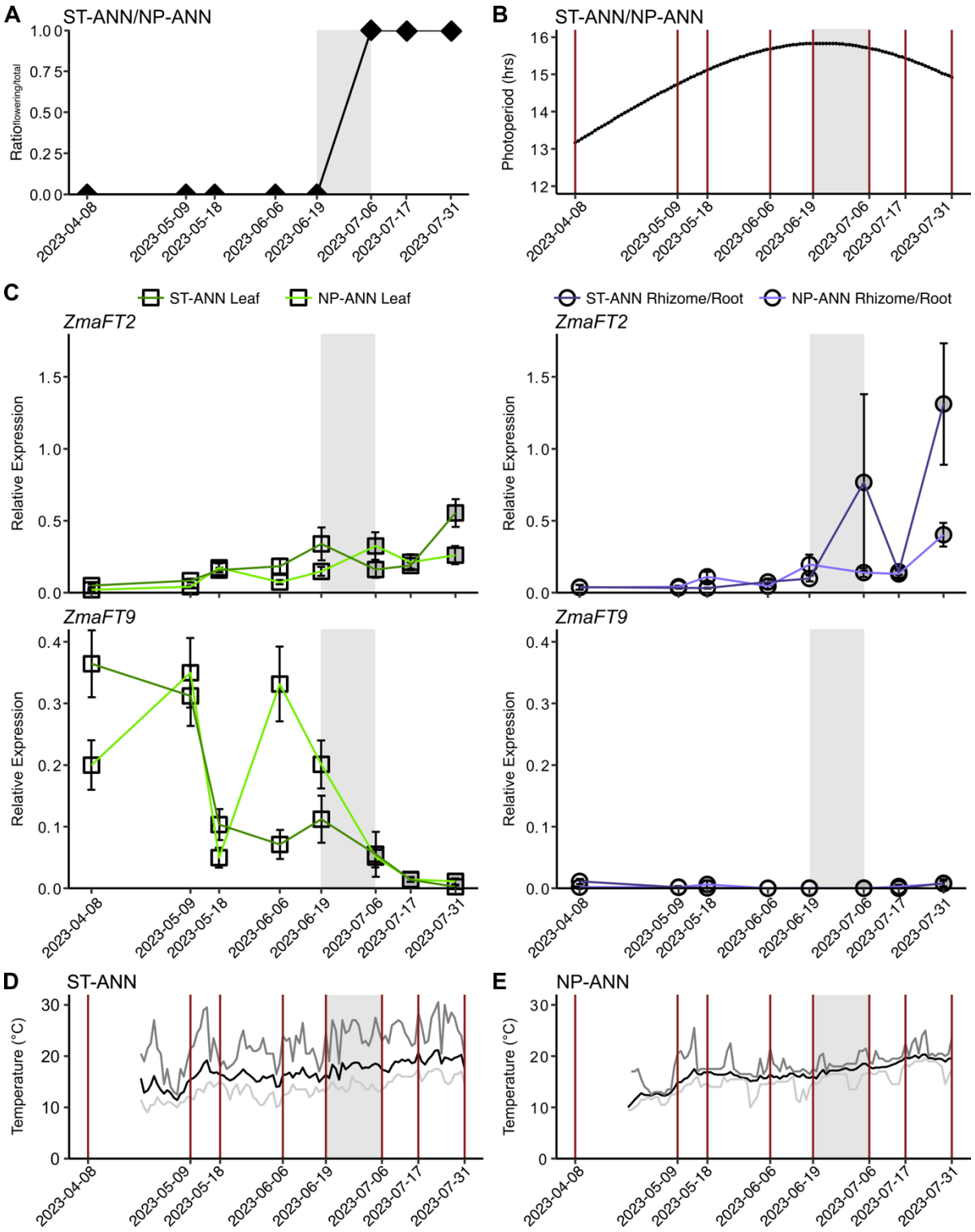

Figure 5: Expression of *ZmaFT2* and *ZmaFT9* genes in leaf and rhizome tissue across the 2023 growing season at ST-ANN and NP-ANN sites (Figure 3H, Table S4). **(A)** Ratio of flowering shoots to total shoots collected at each time point for both ST-ANN populations and NP-ANN population, n≥10. Grey shaded region in each panel indicates when flowering shoots emerged. **(B)** Photoperiod regime over growing season in Willapa Bay. Data obtained from the US Naval

Astronomical Applications Department. Red lines indicate days samples were collected for gene expression analysis. **(C)** Relative expression levels of *ZmaFT2* and *ZmaFT9* across leaf (square) and rhizome and root (circle) throughout the growing season (April-July). Lighter green and purple lines indicate NP-ANN site, while darker green and purple lines indicate ST-ANN site. Time points where shoots are vegetative shown in white and time points where shoots had flowered are filled grey. All expression values are relative to 3 reference genes (*CYP2*, *ELF4A*, and *RPL28*). Plot point represents mean, and error bars are standard error. Statistically significant groupings based on post-hoc Tukey HSD of $\log_{10}$ transformed values are listed in Table S10. **(D, E)** Daily average temperature (black), daily minimum temperature (light grey), and daily maximum temperature (dark grey) at ST-ANN site **(D)** and NP-ANN site **(E)** throughout the growing season. Temperatures were collected at the sediment surface using iButtons (Dallas Semiconductor) every 2 hours. Red lines indicate days samples were collected for gene expression analysis. Temperature from 2023-04-08 to 2023-04-23 was not recorded.

Supporting Information

Figure S1: Phylogenetic tree of *FT* ortholog genes from species represented in Figure 1.
Figure S2: Amino acid sequence alignment of ZmaFT, ZmaTFL1, and ZmaMFT proteins with *Arabidopsis* FT and TFL1 and *Oryza sativa* Hd3a (FT ortholog).
Figure S3: Expression levels of *ZmaPEBP* genes in T_1 overexpression lines under a *35S* promoter.
Figure S4: Characterization of *ZmaFT2, ZmaFT4, ZmaFT9* and *ZmaTFL1a Arabidopsis* overexpressor.
Figure S5: Population structure and genetic relationships of eelgrass populations used in our study.
Figure S6: Relative expression levels of *ZmaFT2*, *ZmaFT4*, *ZmaFT9*, and *ZmaTFL1a* across different leaf tissues.
Figure S7: Representative *Z. marina* annual shoots from Stackpole Annual in April, May, June, and July timepoints.
Figure S8: Expression of *ZmaFT4* and *ZmaTFL1A* genes in leaf and rhizome tissue across the 2023 growing season at ST-ANN and NP-ANN sites.
Figure S9: Expression of *ZmaFT2*, *ZmaFT4*, *ZmaFT9* and *ZmaTFL1A* genes in leaf and rhizome tissue across the 2023 growing season at YQ-ANN site.
Figure S10: Normalized counts of *ZmaPEBP* genes from RNA sequencing.
Table S1: Accession and GenBank numbers for DNA sequences used in phylogenic analysis.
Table S2: qPCR primers used in this study.
Table S3: Primers used for pENTR-cloning in this study.
Table S4: GPS coordinates and tidal elevation of study sites within Willapa Bay.
Table S5: Filtering steps applied to the sequenced reads.
Table S6: Pairwise genetic divergence of populations sites in our study.
Table S7: Three-way ANOVA results of linear model testing gene expression in relation to three factors (Site, Life stage, Tissue Type)
Table S8: Two-way ANOVA results of linear model testing gene expression in relation to two factors (Site, Leaf tissue)
Table S9: Two-way ANOVA results gene expression in relation to time in time-series at Stackpole Annual (ST-ANN) and Nahcotta Port Annual (NP-ANN) sites.
Table S10: Statistically significant groupings of time-points at Stackpole Annual (ST-ANN) and Nahcotta Port Annual (NP-ANN) site based on post-hoc Tukey tests.
Table S11: One-way ANOVA results gene expression in relation to time in time-series at Yaquina Bay Annual (YQ-ANN) site.
Table S12: Statistically significant groupings of time-points at Yaquina Bay Annual (ST-ANN) and Nahcotta Port Annual (NP-ANN) site based on post-hoc Tukey tests.
Table S13: Differential gene expression of *ZmaPEBP* genes, calculated as logFold Change from RNA sequencing of Stackpole leaf tissue samples.
Supplemental References

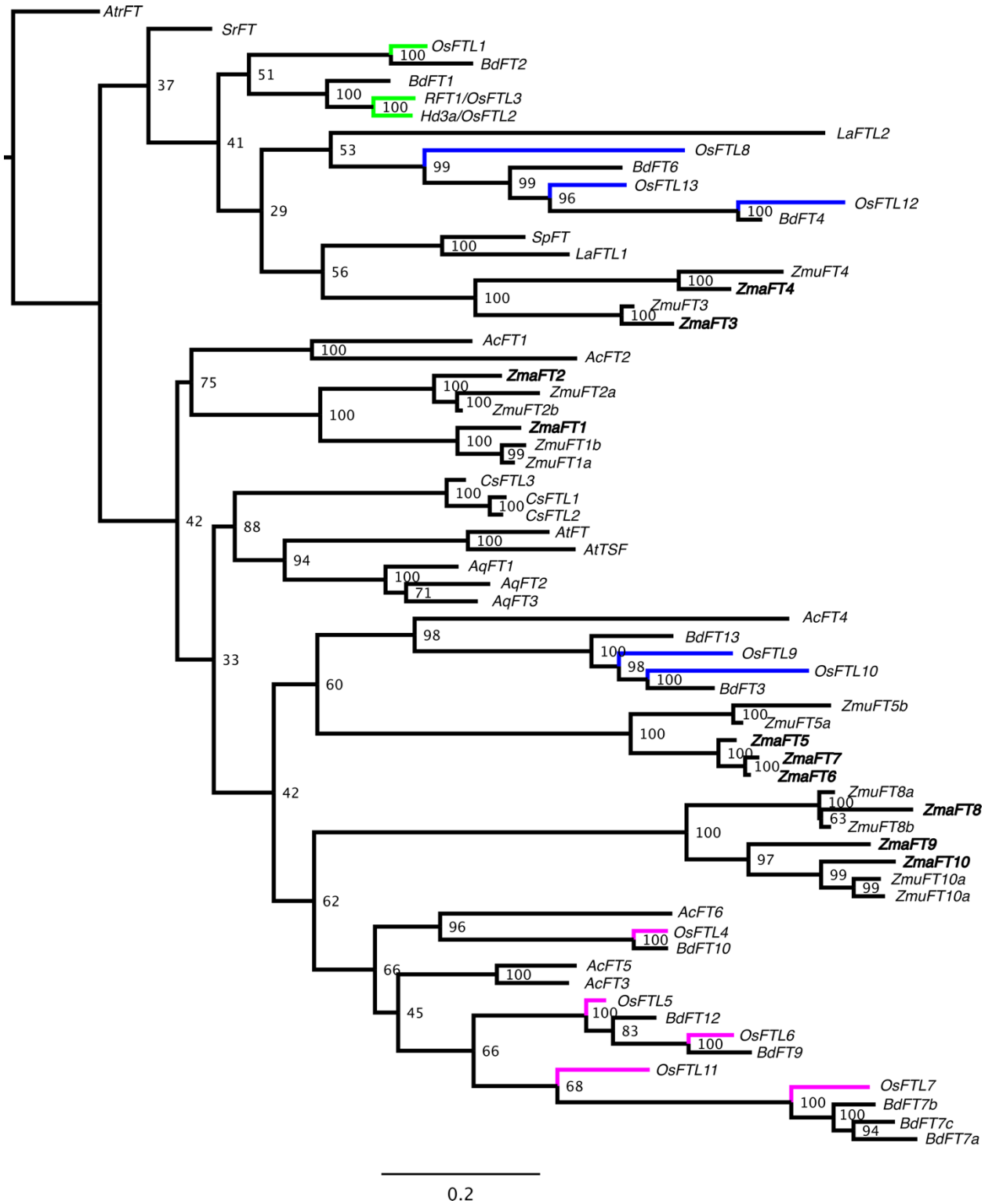

Figure S1: Phylogenetic tree of *FT* ortholog genes from species represented in Figure 1 (monocots: *B. distachyon, O. sativa*, *A. cepa*; *Alismatales*: *L. aequinoctialis, S. polyrhiza, S. renifolius, Z. marina, Z. muelleri;* eudicots: *A. thaliana, A. coerulea, C. seticuspe*). Basal angiosperm *Amborella trichopoda FT* (*AtrFT*) was chosen as an outgroup. See Table S1 for sequence accession numbers. Nucleotide-level maximum likelihood analysis with 100 bootstraps, values shown at nodes. Colors of branches correspond

to clade-designation of *OsFT-like* genes described in Liu et al. 2023;[1] clade I (green), clade II (blue), and clade III (pink). *Z. marina* characterized in study is shown in bold.

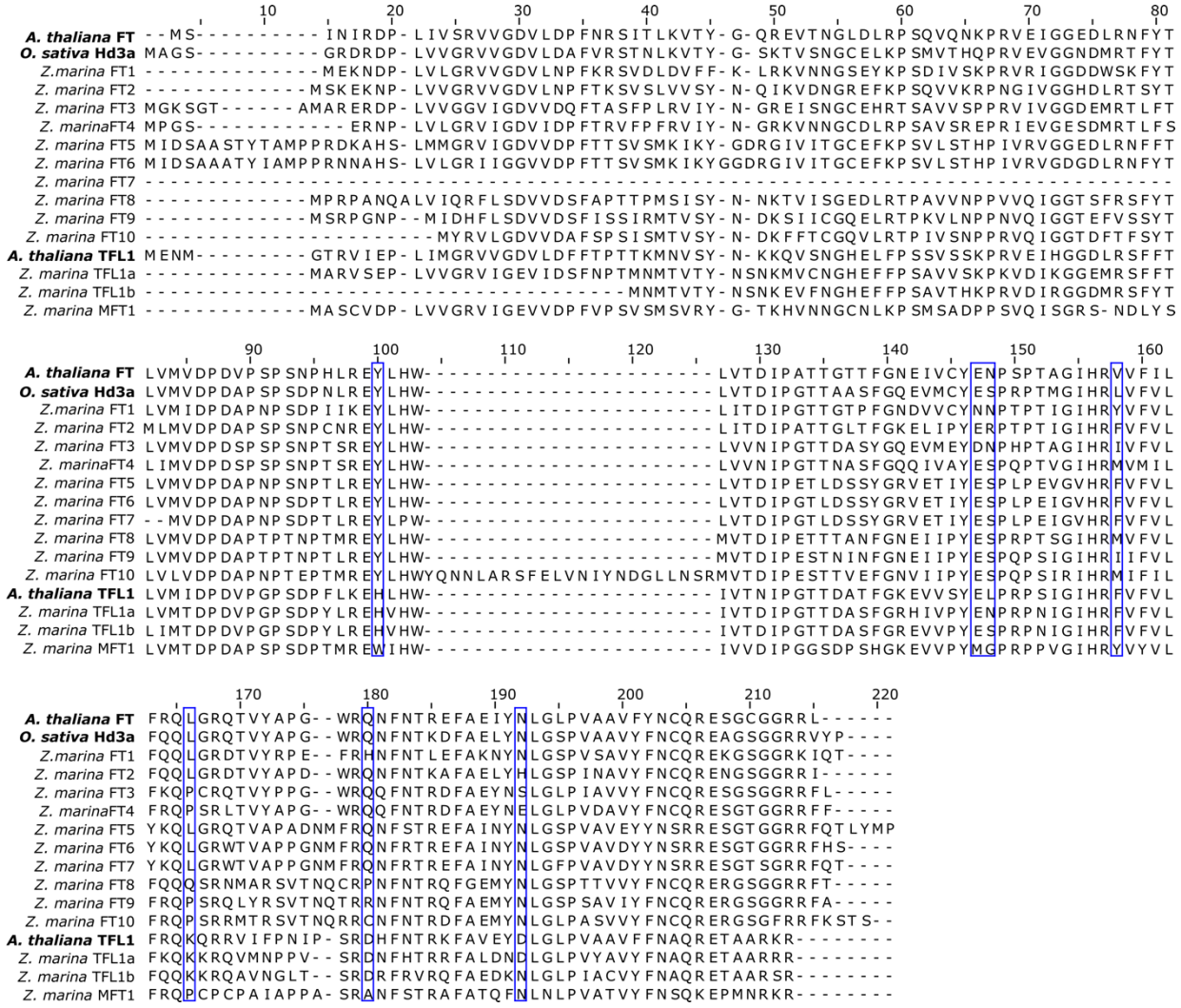

Figure S2: Amino acid sequence alignment of ZmaFT, ZmaTFL1, and ZmaMFT proteins with *Arabidopsis* FT and TFL1 and *Oryza sativa* Hd3a (FT ortholog). Blue boxes highlight residues important for function of *Arabidopsis* FT as flowering activator (Y85, E109, N110, V120, L128, Q140, and N152).

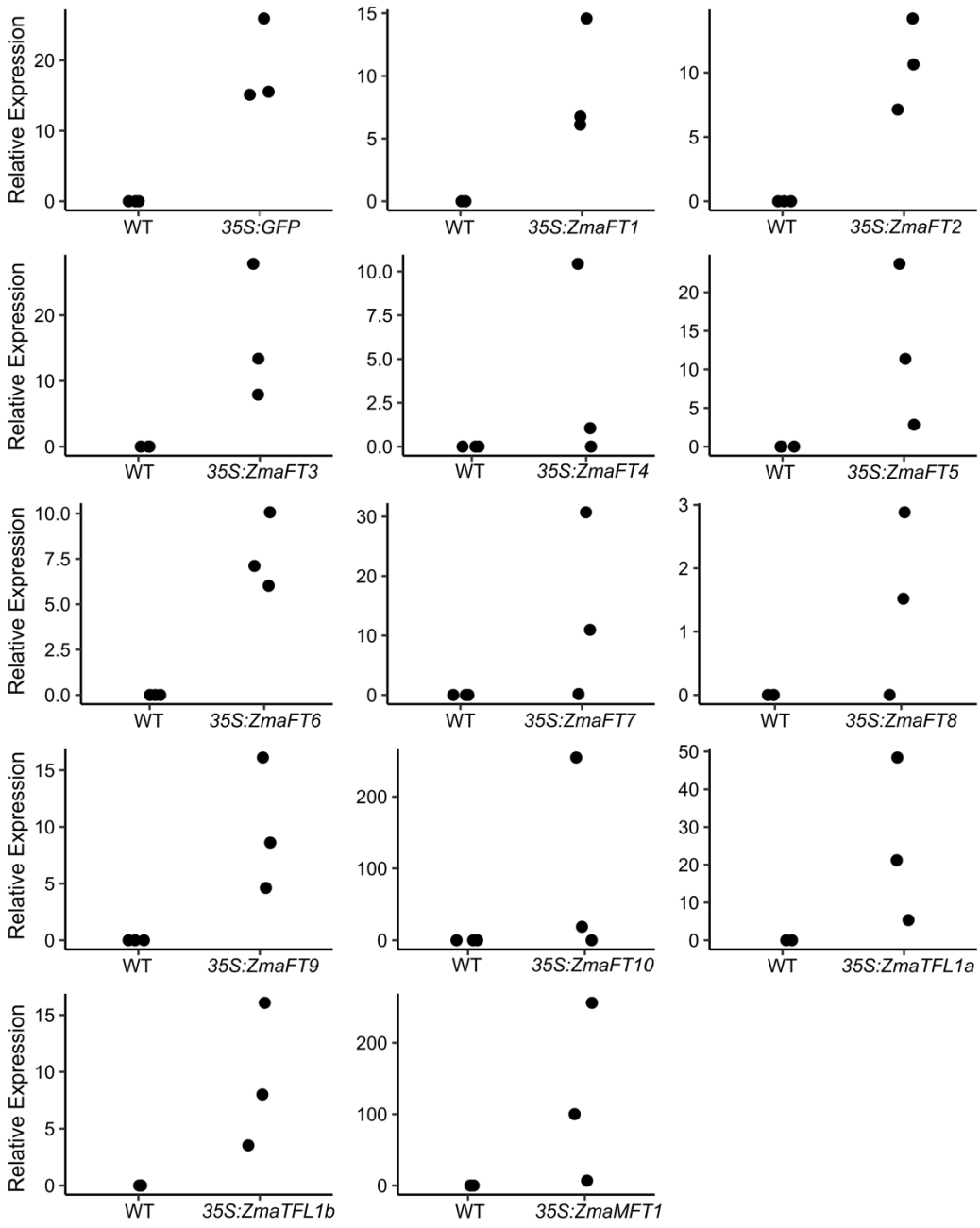

Figure S3: Expression levels of *ZmaPEBP* genes in T_1 overexpression lines under a *35S* promoter. All lines are in Col-0 background. Each point represents a biological replicate of 4-6 individual T_1 plants pooled per sample.

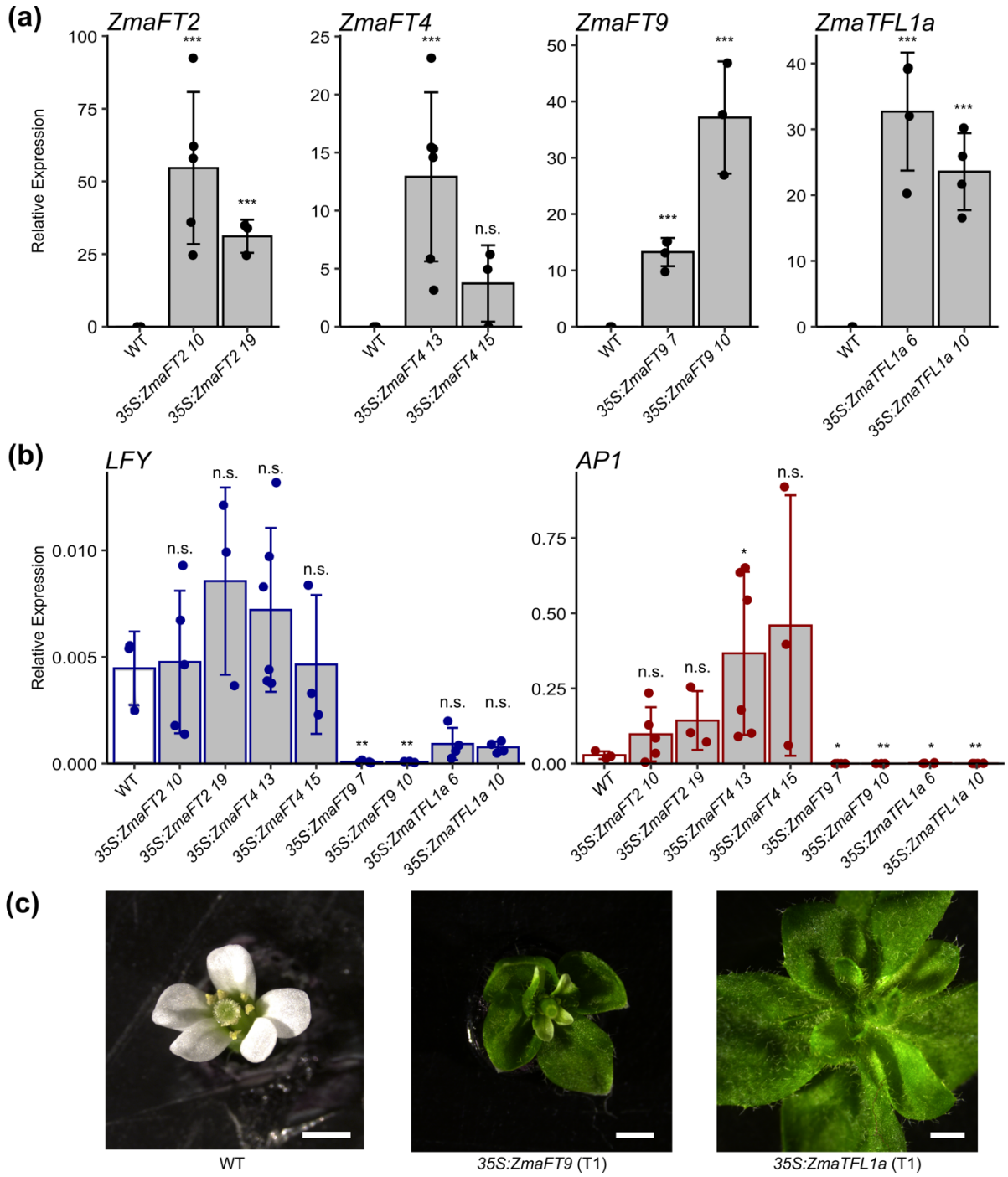

Figure S4: Characterization of *ZmaFT2, ZmaFT4, ZmaFT9* and *ZmaTFL1a Arabidopsis* overexpressor. **(A)** Expression of *ZmaFT2, ZmaFT4, ZmaFT9* and *ZmaTFL1a* genes in homozygous T_3 overexpression lines under the *35S* promoter. All lines are in Col-0 background. Numbers on x-axis represent different inbred lines. Asterisks indicate significance based on t-test comparing to wild type (WT) with Bonferroni correction with $\log_{10}$ transformed values ($p=\alpha/n$; n.s.: not significant, ***: $p < 0.0005$). **(B)** Expression of *LFY* and *AP1* in homozygous T_3 overexpression lines. Asterisks indicate significance based on t-test comparing to wild type (WT) with Bonferroni correction with $\log_{10}$ transformed values ($p=\alpha/n$; n.s.: not significant, *: $p < 0.006$, **: $p < 0.001$). **(C)** We observed altered flower morphology in lines

overexpressing *35S:ZmaFT9* and *35S:ZmaTFL1* compared to WT (Col-0) in T_1 generation. Scale bar 1mm.

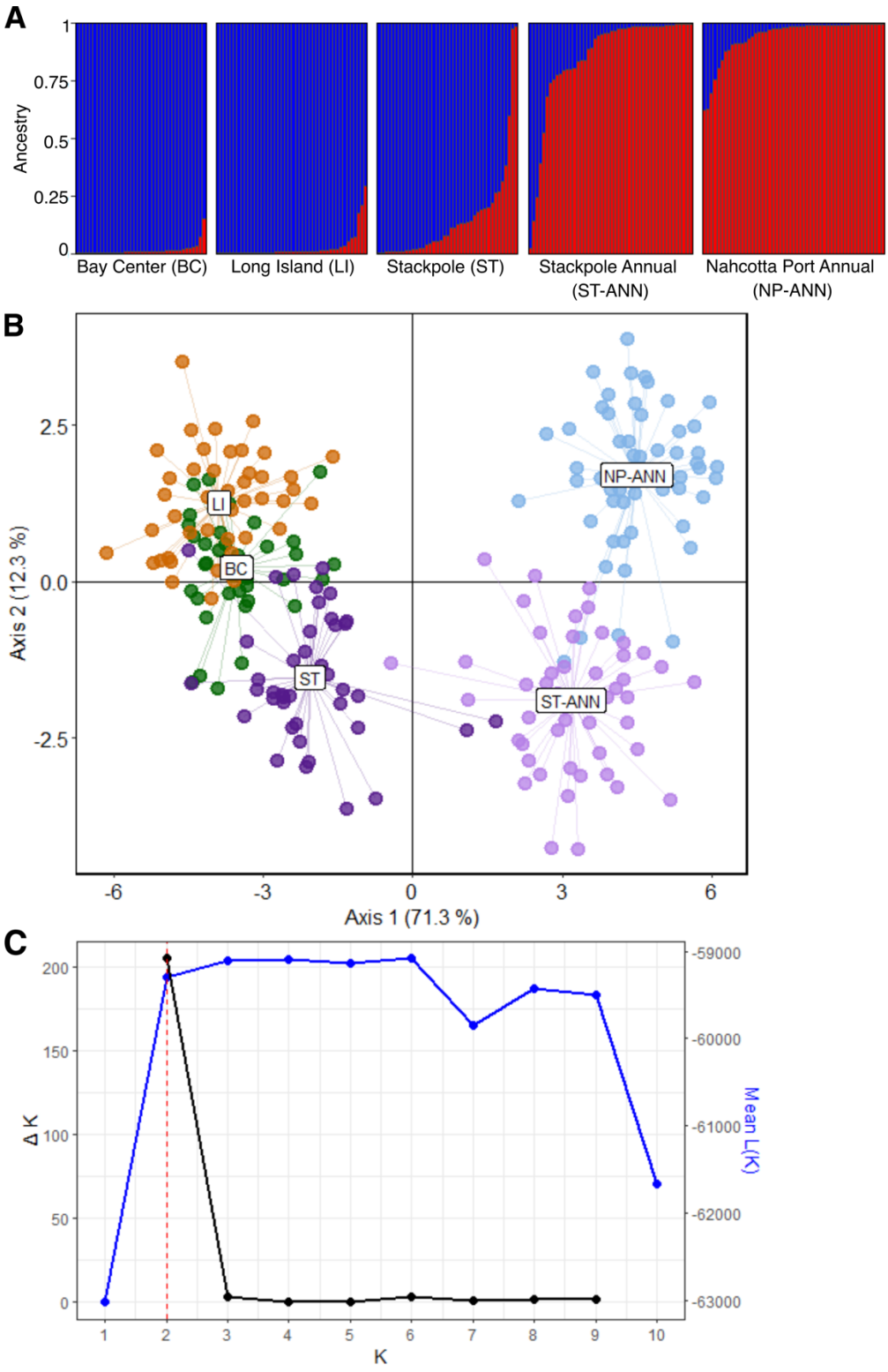

Figure S5: Population structure and genetic relationships between eelgrass populations used in our study. **(A)** Population structure inferred using ADMIXTURE analysis implemented in STRUCTURE v2.1.1.5 (admixture model with correlated allele frequencies, with a burn-in period of 10,000 iterations and 100,000 MCMC repetitions). Each individual plant is represented by a stacked column (x axis), giving the

probability of assignment to two ancestral populations (K = 2, Fig. 2C). The number of clusters (*K*) tested ranged from 1 to 10, and the most likely ancestral groups were evaluated using the mean log probability of the data, $L(K)$[2] and the ΔK statistic[3]. **(B)** Scatterplot describing genetic relationships among individuals using the first two principal components of DAPC (variance explained in parentheses). Stratified cross-validation (90% of observations used for the training dataset) was performed to identify the optimal numbers of principal components to retain for the DAPC analysis. Data points represent individuals, colors indicate source populations. **(C)** Relationship between K (the number of ancestral populations) and the Mean likelihood of the data $L(K)$ (blue) and ΔK (black) values for STRUCTURE analyses. The dashed red line indicates the suggested optimal K value based on the analyses.

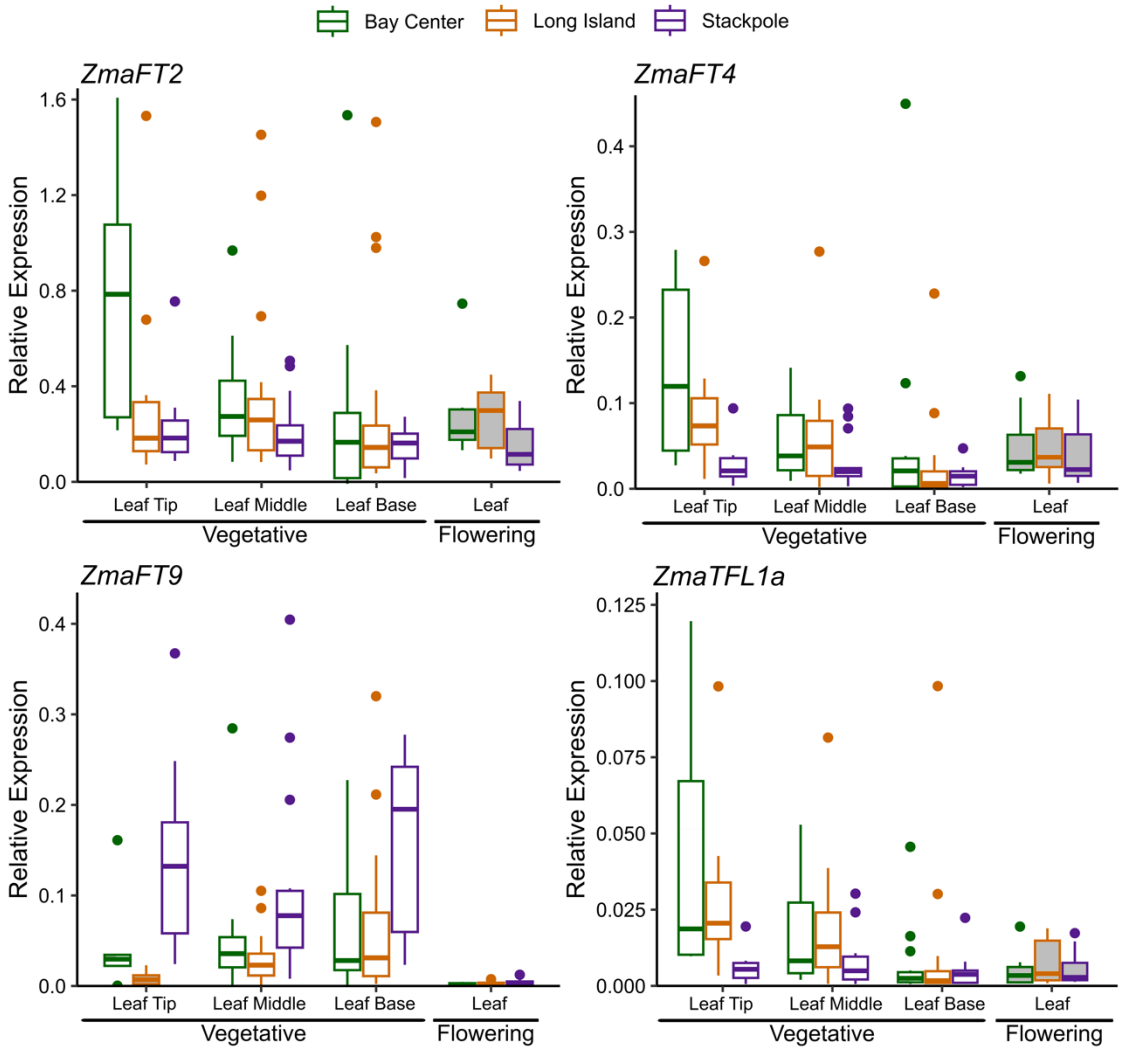

Figure S6: Relative expression levels of *ZmaFT2*, *ZmaFT4*, *ZmaFT9*, and *ZmaTFL1a* across different leaf tissues. Results from leaves on vegetative and flowering shoots are shown with white and grey boxes, respectively. Expression in tissues was measured in samples from 3 sites. All expression values are relative to 3 reference genes (*CYP2*, *ELF4A*, and *RPL28*). Median is indicated by center line in box, upper and lower quartiles by box boundaries, and highest and lowest values within two interquartile ranges by whiskers, n≥5.

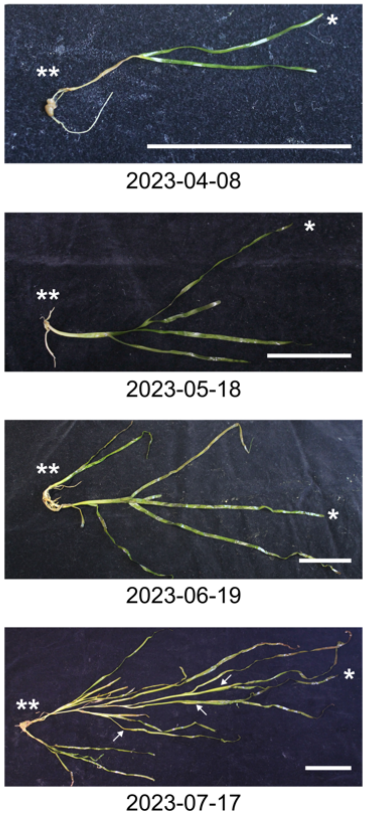

Figure S7: Representative pictures of *Z. marina* annual shoots from Stackpole Annual in April, May, June, and July timepoints. Asterisks indicate leaf (*) and rhizome and root (**) tissue sampled. Inflorescences indicated by arrows. Scale bar 5cm.

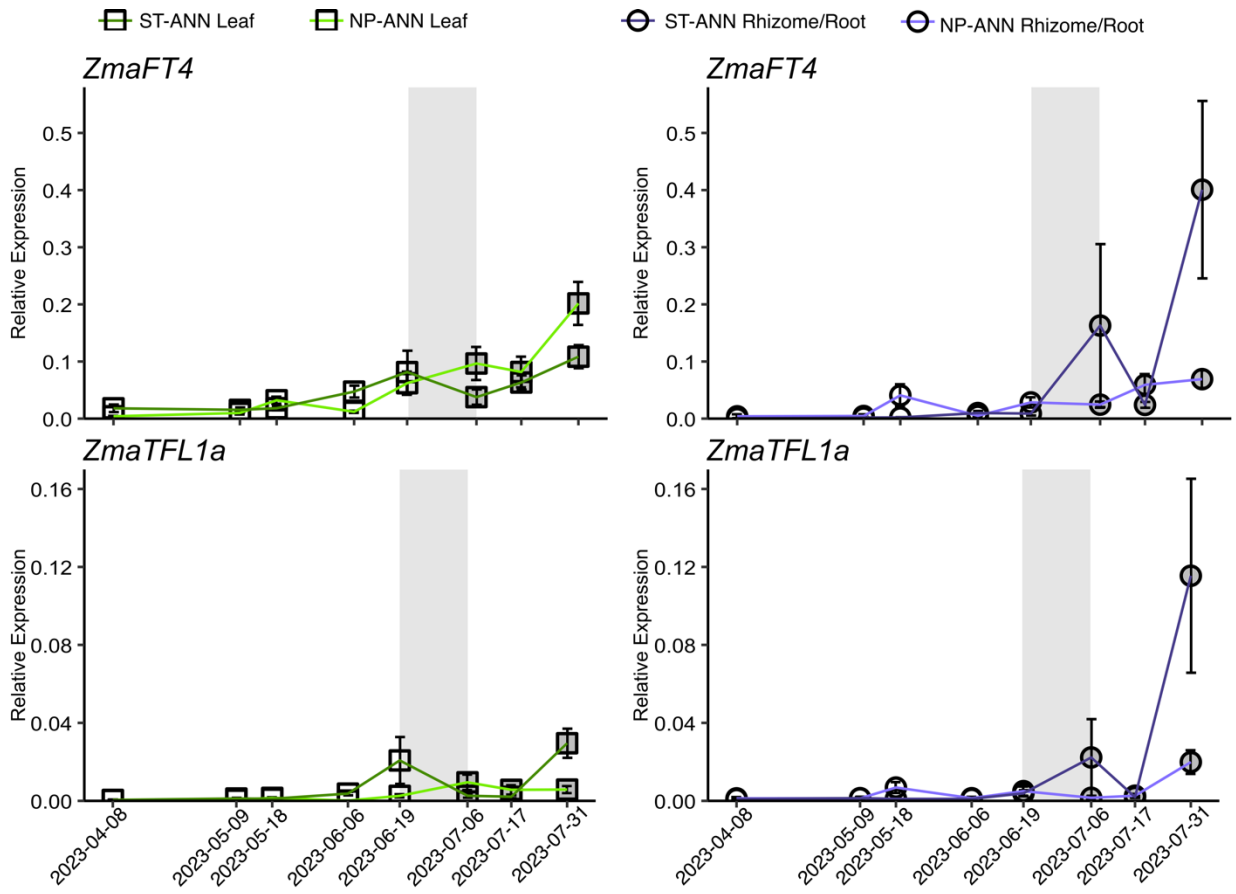

Figure S8: Expression of *ZmaFT4* and *ZmaTFL1A* genes in leaf and rhizome tissue across the 2023 growing season at ST-ANN and NP-ANN sites. Grey shaded region in each panel indicates when flowering transition occurred during growing season (April-July). Leaf (square) and rhizome/root (circle) values with lighter green and purple lines indicate NP-ANN site, while darker green and purple lines indicate ST-ANN site. Time points where shoots are vegetative shown in white and time points where shoots had flowered are filled grey. All expression values are relative to 3 reference genes (*CYP2*, *ELF4A*, and *RPL28*). Plot point represents mean, and error bars are standard error. Statistically significant groupings based on post-hoc Tukey HSD of $\log_{10}$ transformed values are listed in Table S10.

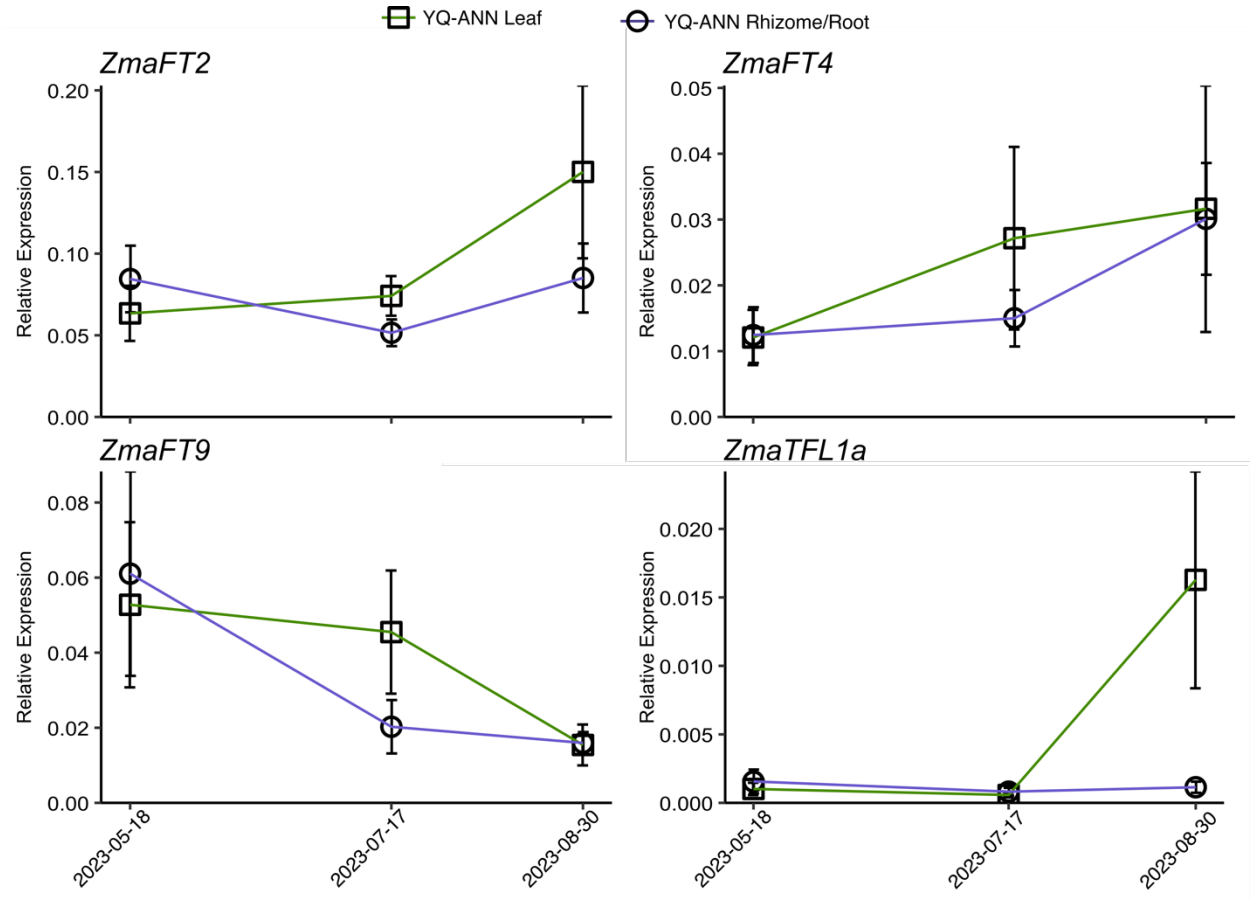

Figure S9: Expression of *ZmaFT2*, *ZmaFT4*, *ZmaFT9* and *ZmaTFL1A* genes in leaf and rhizome tissue across the 2023 growing season at YQ-ANN site. Relative expression levels across leaf (square) and rhizome and root (circle) shown throughout the growing season (May-August). All expression values are relative to 3 reference genes (*CYP2*, *ELF4A*, and *RPL28*). Plot point represents mean, and error bars are standard error. Statistically significant groupings based on post-hoc Tukey HSD of $\log_{10}$ transformed values are listed in Table S12. $n \geq 3$.

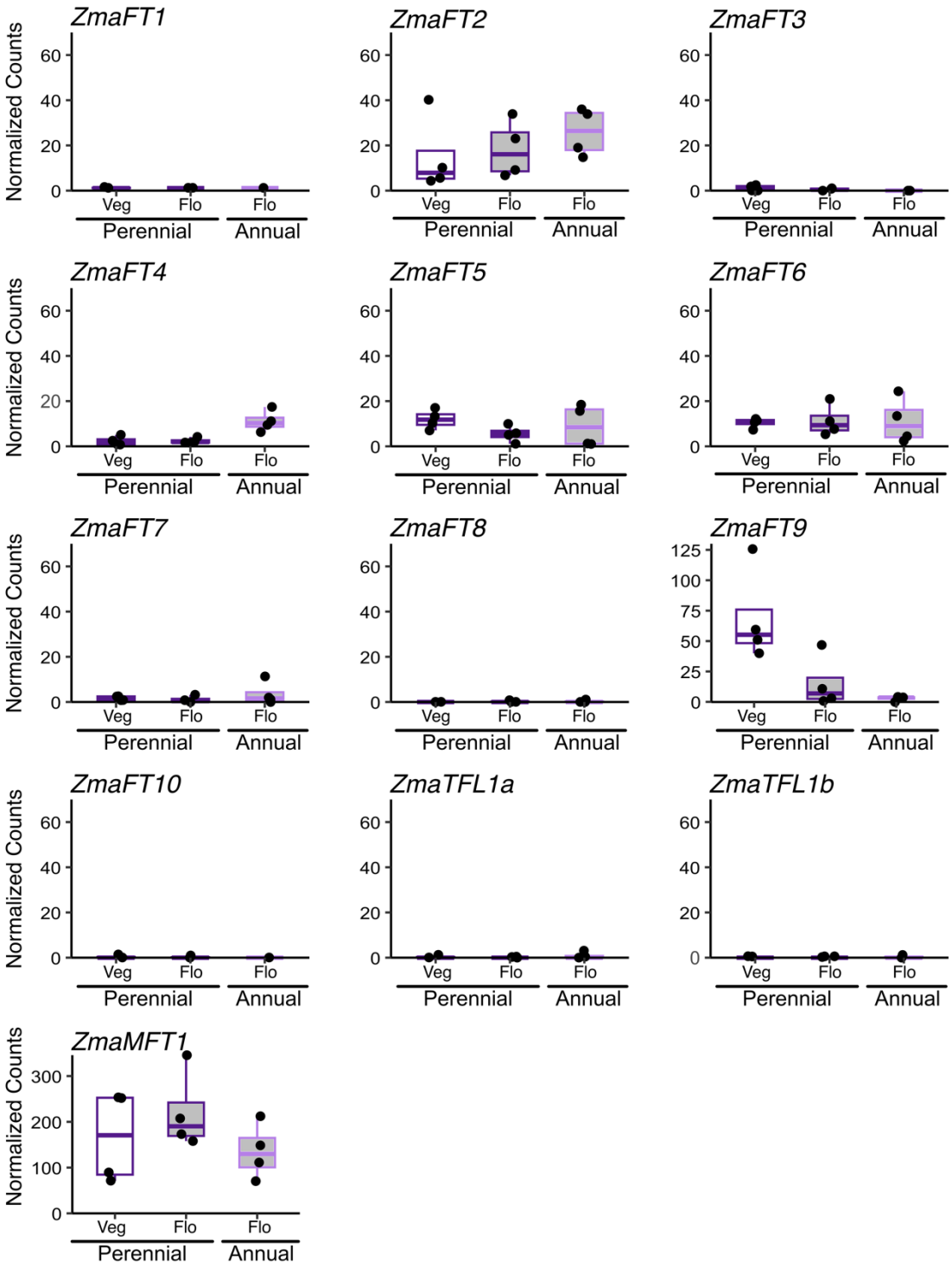

Figure S10: Normalized counts of *ZmaPEBP* genes from RNA sequencing. Stackpole leaf tissue from vegetative and flowering (Veg, white fill; Flo, grew fill) perennials (dark purple) and annual (light purple) shoots. mRNA-sequencing reads were aligned and quantified with Salmon then imported to DESeq2 for count normalization. Median is indicated by center line in box, upper and lower quartiles by box boundaries, and highest and lowest values within two interquartile ranges by whiskers. Each circle represents a biological repeat/sequencing run, n=4.

Table S1: Accession and GenBank numbers for DNA sequences used in phylogenic analysis. If gene was functionally characterized, function and reference are also included (see Supplement References.

Name	Species	Gene ID	Database	Function	Publication
ZmaFT1	*Zostera marina*	Zosma03g21100.1	Phytozome		
ZmaFT2	*Zostera marina*	Zosma01g14870	Phytozome		
ZmaFT3	*Zostera marina*	Zosma01g23380.1	Phytozome		
ZmaFT4	*Zostera marina*	Zosma04g08400.1	Phytozome		
ZmaFT5	*Zostera marina*	Zosma06g26410.1	Phytozome		
ZmaFT6	*Zostera marina*	Zosma01g37360.1	Phytozome		
ZmaFT7	*Zostera marina*	Zosma01g37330	Phytozome		
ZmaFT8	*Zostera marina*	Zosma05g25830.1	Phytozome		
ZmaFT9	*Zostera marina*	Zosma01g13540.1	Phytozome		
ZmaFT10	*Zostera marina*	Zosma06g06360.1	Phytozome		
ZmaMFT1	*Zostera marina*	Zosma06g00480.1	Phytozome		
ZmaTFL1a	*Zostera marina*	Zosma04g17290.1	Phytozome		
ZmaTFL1b	*Zostera marina*	Zosma04g24270	Phytozome		
ZmuMFT1	*Zostera muelleri*		Local (SRR1714574)		Lee et al. 2016[12]
ZmuTFL1b	*Zostera muelleri*		Local (SRR1714574)		Lee et al. 2016[12]
ZmuTFL1c	*Zostera muelleri*		Local (SRR1714574)		Lee et al. 2016[12]
ZmuTFL1a	*Zostera muelleri*		Local (SRR1714574)		Lee et al. 2016[12]
ZmuFT4	*Zostera muelleri*		Local (SRR1714574)		Lee et al. 2016[12]
ZmuFT3	*Zostera muelleri*		Local (SRR1714574)		Lee et al. 2016[12]
ZmuFT2b	*Zostera muelleri*		Local (SRR1714574)		Lee et al. 2016[12]
ZmuFT2a	*Zostera muelleri*		Local (SRR1714574)		Lee et al. 2016[12]
ZmuFT1b	*Zostera muelleri*		Local (SRR1714574)		Lee et al. 2016[12]
ZmuFT1a	*Zostera muelleri*		Local (SRR1714574)		Lee et al. 2016[12]
ZmuFT5a	*Zostera muelleri*		Local (SRR1714574)		Lee et al. 2016[12]
ZmuFT5b	*Zostera muelleri*		Local (SRR1714574)		Lee et al. 2016[12]
ZmuFT8a	*Zostera muelleri*		Local (SRR1714574)		Lee et al. 2016[12]
ZmuFT8b	*Zostera muelleri*		Local (SRR1714574)		Lee et al. 2016[12]
ZmuFT10a	*Zostera muelleri*		Local (SRR1714574)		Lee et al. 2016[12]
ZmuFT10b	*Zostera muelleri*		Local (SRR1714574)		Lee et al. 2016[12]
AtATC	*Arabidopsis thaliana*	AT2G27550	TAIR	Repressor	Mimida et al. 2001[13]
AtBFT	*Arabidopsis thaliana*	AT5G62040	TAIR	Repressor	Yoo et al. 2010[14]
AtFT	*Arabidopsis thaliana*	AT1G65480	TAIR	Activator	Kardailsky et al. 1999[15]
AtMFT	*Arabidopsis thaliana*	AT1G18100	TAIR	Activator	Yoo et al. 2004[16]
AtTFL1	*Arabidopsis thaliana*	AT5G03840	TAIR	Repressor	Kardailsky et al. 1999, Koboyashi et al. 1999[15,17]
AtTSF	*Arabidopsis thaliana*	AT4G20370	TAIR	Activator	Yamaguchi et al. 2005[18]
BdMFTA	*Brachypodium distachyon*	Bradi2g01020	Phytozome		

BdMFTBa	*Brachypodium distachyon*	Bradi2g27860	Phytozome		
BdMFTBb	*Brachypodium distachyon*	Bradi1g42510	Phytozome		
BdTCB2	*Brachypodium distachyon*	Bradi3g44860	Phytozome		
BdTCB1	*Brachypodium distachyon*	Bradi4g42400	Phytozome		
BdTCB3	*Brachypodium distachyon*	Bradi5g09270	Phytozome		
BdFT1	*Brachypodium distachyon*	Bradi1g48830	Phytozome	Activator	Lv et al. 2014[19]
BdFT2	*Brachypodium distachyon*	Bradi2g07070	Phytozome	Activator	Shaw et al. 2019[20]
BdFT3	*Brachypodium distachyon*	Bradi2g19670	Phytozome		
BdFT13	*Brachypodium distachyon*	Bradi2g49795	Phytozome	Activator (SD), Repressor (LD)	Qin et al. 2019[21]
BdFT4	*Brachypodium distachyon*	Bradi1g38150	Phytozome		
BdFT6	*Brachypodium distachyon*	Bradi3g08890	Phytozome		
BdFT7a	*Brachypodium distachyon*	Bradi4g39730	Phytozome		
BdFT7b	*Brachypodium distachyon*	Bradi4g39760	Phytozome		
BdFT7c	*Brachypodium distachyon*	Bradi4g39750	Phytozome		
BdFT9	*Brachypodium distachyon*	Bradi5g14010	Phytozome		
BdFT12	*Brachypodium distachyon*	Bradi3g48036	Phytozome		
BdFT10	*Brachypodium distachyon*	Bradi4g35040	Phytozome		
AqFT1	*Aquilegia coerulea*	Aqcoe2G432300	Phytozome		Sharma et al. 2019[22]
AqFT2	*Aquilegia coerulea*	Aqcoe4G263600	Phytozome		Sharma et al. 2019[22]
AqFT3	*Aquilegia coerulea*	Aqcoe4G257600	Phytozome		Sharma et al. 2019[22]
AqMFT	*Aquilegia coerulea*	Aqcoe3G016200	Phytozome		
AqTFL1a	*Aquilegia coerulea*	Aqcoe2G140500	Phytozome		
AqTFL1b	*Aquilegia coerulea*	Aqcoe1G447800	Phytozome		
AqTFL1c	*Aquilegia coerulea*	Aqcoe1G447700	Phytozome		
LaFTL1	*Lemna aequinoctialis*	LC625473	GenBank	Activator	Yoshida et al. 2021[23]
LaFTL2	*Lemna aequinoctialis*	LC625474	GenBank	Repressor	Yoshida et al. 2021[23]
SrMFT	*Symplocarpus renifolius*	LC030438	GenBank		Ito-Inaba et al. 2016[24]
SrFT	*Symplocarpus renifolius*	LC030437	GenBank	Activator	Ito-Inaba et al. 2016[24]
SpFT	*Spirodela polyrhiza*	Spipo19G0001700	Phytozome		
CsFTL1	*Chrysanthemum seticuspe*	AB679270	GenBank		
CsFTL2	*Chrysanthemum seticuspe*	AB679271	GenBank		
CsFTL3	*Chrysanthemum seticuspe*	AB679272	GenBank	Activator	Oda et al. 2012[25]
CsTFL1	*Chrysanthemum seticuspe*	AB839767	GenBank	Repressor	Higushi et al. 2015[26]

	Chrysanthemum seticuspe	AB770478	GenBank		
CsAFT	*Chrysanthemum seticuspe*	AB839766	GenBank	Repressor	Higuchi et al. 2013[27]
Hd3a/OsFTL2	*Oryza sativa*	Os06g06320	Phytozome	Activator	Kojima et al. 2002[28]
RFT1/OsFTL3	*Oryza sativa*	Os06g06300	Phytozome	Activator	Kojima et al. 2002[28]
OsMFT2	*Oryza sativa*	Os01g02120	Phytozome		
OsMFT1	*Oryza sativa*	Os06g30370	Phytozome		
OsRCN1	*Oryza sativa*	Os11g05470	Phytozome	Repressor	Nakagawa et al. 2002[29]
OsRCN3	*Oryza sativa*	Os12g05590	Phytozome		
OsRCN4	*Oryza sativa*	Os04g33570	Phytozome		
OsRCN2	*Oryza sativa*	Os02g32950	Phytozome	Repressor	Nakagawa et al. 2002[29]
OsFTL11	*Oryza sativa*	Os11g18870	Phytozome		
OsFTL5	*Oryza sativa*	Os02g39064	Phytozome		
OsFTL6	*Oryza sativa*	Os04g41130	Phytozome		
OsFTL7	*Oryza sativa*	Os12g13030	Phytozome		
OsFTL1	*Oryza sativa*	Os01g11940	Phytozome	Activator	Wei et al. 2025[30]
OsFTL8	*Oryza sativa*	Os01g10590	Phytozome		
OsFTL13	*Oryza sativa*	Os02g13830	Phytozome		
OsFTL12	*Oryza sativa*	Os06g35940	Phytozome	Repressor	Zheng et al. 2023[31]
OsFTL4	*Oryza sativa*	Os09g33850	Phytozome	Repressor	Gu et al. 2022[32]
OsFTL10	*Oryza sativa*	Os05g44180	Phytozome	Activator	Fang et al. 2019[33]
OsFTL9	*Oryza sativa*	Os01g54490	Phytozome		
AcFT1	*Allium cepa*	KC485348	GenBank	Activator	Lee et al. 2013[34]
AcFT2	*Allium cepa*	KC485349	GenBank	Activator	Lee et al. 2013[34]
AcFT3	*Allium cepa*	KC485350	GenBank		
AcFT4	*Allium cepa*	KC485351	GenBank	Repressor	Lee et al. 2013[34]
AcFT5	*Allium cepa*	KC485352	GenBank		
AcFT6	*Allium cepa*	KC485353	GenBank		
AtrFT	*Amborella trichopoda*	evm_27.TU.AmTr_v1.0_ scaffold00066.22 (PAC:31564108)	Phytozome		

Table S2: qPCR primers used in this study.

Name	Accession No.	Forward 5'-3'	Reverse 5'-3'
ZmaFT1	Zosma03g21100	GTTCGGATCGGTGGTGATGA	ATGGTCGGCGTTGGGTTATT
ZmaFT2	Zosma01g14870	ACACAATGCTCATGGTAGATCCT	AGCACAAACACGAAACGGTG
ZmaFT3	Zosma01g23380	GCCCAAGCAACCCTACTTCT	ACCGTCTGCCTACATGGTTG
ZmaFT4	Zosma04g08400	TGCACTGGTTGGTGGTGAA	AGCCGACTAGGTTGACGGAA
ZmaFT5	Zosma06g26410	CGAGTTGGAGGCGAGGATTT	CCGTCACCAACCAGTGTAGG
ZmaFT6	Zosma01g37360	TGCACACTCTCTTGTGCTGG	CCACGATCACCACCGTACTT
ZmaFT7	Zosma01g37330	ACCCTGGTTGGTGACGGATA	CAATCTCCGGCAACGGACTT
ZmaFT8	Zosma05g25830	CACTGGATGGTGACGGACAT	GCGGCATTGATTCGTGACAG
ZmaFT9	Zosma01g13540	TTCCTACACACTGGTTATGGTCG	GATGGATGGTTGTGGGCTCT
ZmaFT10	Zosma06g06360	AGAGTCCACAACCGAGCATC	AACCGCTACCTCTCTCCCTT
ZmaTFL1a	Zosma04g17290	TGTTCACTGGATTGTGACAGA	CCAGTGCAAATCGACGTGTG
ZmaTFL1b	Zosma04g24270	ACACACTGATCATGACTGACCC	ATCAGTTGTGCCGGGAATGT
ZmaMFT1	Zosma06g00480	TTCCTTACATGGGTCCACGC	AAACGGTAGCAACAGGGAGG
ZmaCyp2	Zosma05g32090	CACTCCACTACAAGGGATCGAAA	GGACCTGTATGCTTCTTAACGAAGT
Zmaelf4a	Zosma03g02900	TCTTTCTGCGATGCGAACAG	TGGATGTATCGGCAGAAACG
ZmaRPL28	Zosma04g25970	TTCCGCACCTAGGGTTTCG	ATATTGGCGCAGCGATTTTG
AtIPP2	AT3G02780	GTATGAGTTGCTTCTCCAGCAAAG	GAGGATGGCTGCAACAAGTGT
AtPP2AA3	AT1G13320	GCGGTTGTGGAGAACATGATACG	GAACCAAACACAATTCGTTGCTG
AtLFY	AT5G61850	ACGCCGTCATTTGCTACTCT	CTTTCTCCGTCTCTGCTGCT
AtAP1	AT1G69120	AGTGGGATCAGCAGAACCAAGGCC	TTGCAGTTGTAAACGGGTTCAAGAGTCAG
GFP	None	TGAGCAAGGGCGAGGAGCTG	TGCAGATGAACTTCAGGGTCAGCT

Table S3: Primers used for pENTR-cloning in this study, designed to be compatible with pENTR-D TOPO cloning protocol (Invitrogen).

Name	Accession No.	Forward 5'-3'	Reverse 5'-3'
ZmaFT1	Zosma03g21100	CACCATGGAAAAGAATGATCCACTTGTTC	AATCAAGTCTGAATCTTTCTACCTCCAGATC
ZmaFT2	Zosma01g14870	CACCATGTCAAAAGAAAAAAATCCCCTTG	AATCATATCCTCCTTCCTCCAGATCCA
ZmaFT3	Zosma01g23380	CACCATGGGAAAGAGTGGCA	AACTACAAGAATCGGCGACCAC
ZmaFT4	Zosma04g08400	CACCATGCCGGGATCGGA	AACTAAAAAAAAACGCCTTCCCCCA
ZmaFT5	Zosma06g26410	CACCATGGGGTTGATGATTG	AACTAGGGCATATATAAAGTCTGAAACCTT
ZmaFT6	Zosma01g37360	CACCATGGGGTTAATGATTGATTCAG	AAAATCATGTGAACCTACGGCCA
ZmaFT7	Zosma01g37330	CACCATGGTGGATCCTGATGCGCCAAATC	AATCAAGTCTGAAACCTTCTACCACTAGTA
ZmaFT8	Zosma05g25830	CACCATGCCGAGACCGGC	AATCATGTGAACCTACGGCCA
ZmaFT9	Zosma01g13540	CACCATGTCGAGGCCAGG	AATTATGCGAACCTTCGACCACCA
ZmaFT10	Zosma06g06360	CACCATGTACCGTGTTCTT	AATTAAGATGTCGATTTGAACCTTC
ZmaTFL1a	Zosma04g17290	CACCATGGCACGAGTTTC	AACTAACGTCTTCTAGCTGCAGT
ZmaTFL1b	Zosma04g24270	CACCATGAATATGACTGTTACCTACAACTC	AATTAGCGACTGCGAGCTGCAGTCTC
ZmaMFT1	Zosma06g00480	CACCATGGCGAGCTGCGT	AATCAAGTCTGAAACCTTCTACCACTAGTA

Table S4: GPS coordinates and tidal elevation of study sites including individuals sampled per site and the number of unique multilocus genotypes (MLG) used in the population genetic analyses (BC, LI, ST, ST-ANN, and NP-ANN). Tidal elevation reported in meters of mean lower low water (MLLW)

Site	Abbreviation	Individuals Sampled	Total MLGs	Position (°N, °W)	Tidal Elevation (m MLLW)
Bay Center	BC	44	38	46.652, 123.946	0.3
Long Island	LI	47	44	46.515, 123.972	0.3
Stackpole	ST	41	41	46.611, 124.038	1 ± 0.1
Stackpole Annual	ST-ANN	48	48	46.613, 124.034	1 ± 0.1
Nahcotta Port Annual	NP-ANN	53	53	46.502, 124.029	0.7
Yaquina Bay Annual	YQ-ANN	-	-	44.622, 124.042	0.3

Table S5: Filtering steps applied to the sequenced reads. Rows describe individual steps in the bioinformatic pipeline. Columns describe the number of individuals, single nucleotide polymorphic sites (SNPs), and missing data remaining in the dataset after the application of each step.

Step / Filter	Individuals	SNPs	Missing Data
Single Nucleotide Variant calling with ref_map.pl in STACKS [9]	243	10711	64.66%
Genotype depth ≥ 10	243	10711	76.68%
Genotype Allelic Balance (the proportion of reads supporting a variant site) 0.2 ≥ 0.8	243	10711	76.95%
Loci with Minor Allele Count > 1 (remove fixed loci)	243	3926	43.35%
Loci with < 20% Missing Genotypes across individuals	243	1361	6.07%
One locus per rad-tag (locus with highest Minor Allele Frequency)	243	695	5.08%
Individuals with < 20% Missing Genotypes across all loci	233	695	2.85%
Loci with Minor Allele Frequencies ≥ 0.05 in at least one subpopulation	233	330	3.81%
Loci meeting Hardy Weinberg Equilibrium expectations in at least one subpopulation	233	327	3.78%
A single individual per Identical Unique Multilocus Genotypes (MLG)	224	327	3.81%

Table S6: Pairwise genetic distances, F_{ST} (below diagonal), with corresponding 95% confidence intervals (above diagonal) among five eelgrass meadows. Confidence intervals (95%) were generated using bootstrapping with 10,000 permutations. Significant values are in bold.

	BC	LI	ST	ST-ANN	NP-ANN
BC		(-0.001, 0.005)	(0.008, 0.018)	(0.100, 0.151)	(0.112, 0.171)
LI	0.002		(0.008, 0.018)	(0.099, 0.150)	(0.113, 0.171)
ST	**0.013**	**0.013**		(0.064, 0.101)	(0.078, 0.128)
ST-ANN	**0.126**	**0.124**	**0.082**		(0.011, 0.022)
NP-ANN	**0.141**	**0.142**	**0.102**	**0.016**	

Table S7: Three-way ANOVA results of linear model testing gene expression in relation to three factors: Site was included only as a main effect, Life stage (Vegetative, Veg. vs Flowering, Flo.) and Tissue type (Leaf, Rhizome, Stem) were included as main effects and two-way interaction. Expression values were log_{10} transformed to fit assumptions of model.

		ZmaFT2			*ZmaFT4*			*ZmaFT9*			*ZmaTFL1a*		
	Df	Mean Sq	F value	Pr(>F)	Mean Sq	F value	Pr(>F)	Mean Sq	F value	Pr(>F)	Mean Sq	F value	Pr(>F)
Site	2	0.26328658	3.76413507	0.02458575	0.66584705	3.52774566	0.03092301	1.64557038	2.56810085	0.07881367	1.55594831	4.94852901	0.0078441
Developmental Stage (Veg., Flo.)	1	12.482944	178.465184	1.02E-30	16.027034	84.913343	1.73E-17	55.432046	86.50805	9.59E-18	0.95331658	3.03192254	0.08293884
Tissue type	2	0.608279	8.69639592	0.00022665	2.31443909	12.262242	8.56E-06	57.810563	90.219972	7.37E-30	3.20249286	10.18518	5.71E-05
Life stage x Tissue	2	4.1011432	58.632905	2.05E-21	3.76189104	19.930995	9.99E-09	35.919481	56.056405	1.16E-20	5.43229632	17.276838	9.90E-08
Residuals	237	0.0699461			0.18874576			0.64077327			0.31442643		

Table S8: Two-way ANOVA results of linear model testing gene expression in relation to two factors: Site and Leaf tissue type (Leaf Tip, Leaf Middle, and Leaf Base) were included as main effects. Expression values were log_{10} transformed to fit assumptions of model.

		ZmaFT2			*ZmaFT4*			*ZmaFT9*			*ZmaTFL1a*		
	Df	Mean Sq	F value	Pr(>F)	Mean Sq	F value	Pr(>F)	Mean Sq	F value	Pr(>F)	Mean Sq	F value	Pr(>F)
Site	2	0.16581393	1.28135145	0.28166476	0.62693743	2.25208832	0.10988044	7.74909151	18.0619056	1.5614E-07	1.85664635	3.29559782	0.04063748
Leaf tissue type	2	0.80581079	6.22702086	0.00271987	4.33339856	15.5664597	1.07E-06	1.38558484	3.22957892	4.33E-02	6.9162808	12.2765867	1.50E-05
Residuals	237	0.12940551			0.27838048			0.42902957			0.56337164		

Table S9: Two-way ANOVA results gene expression in relation to time in time-series at Stackpole Annual (ST-ANN) and Nahcotta Port Annual (NP-ANN) sites. Leaf tissue expression and root tissue expression data were analyzed separately. Site was included as a fixed effect, and date was included as a main effect. Date was treated as a categorical factor to account for potential non-linear change. Expression values were log_{10} transformed to fit assumptions of analysis.

ZmaFT2								
	Leaf				Rhizome/Roots			
	Df	Mean Sq	F value	Pr(>F)	Df	Mean Sq	F value	Pr(>F)
Site	1	1.695826686	20.25837067	1.36674E-05	1	0.271766091	1.13629943	0.288244726
Date	7	2.605744737	31.12826516	3.9622E-26	7	3.754810051	15.69948813	3.78125E-15
Site x Date	7	0.339047039	4.050260936	4.35E-04	7	0.34131959	1.427114227	0.198876154
Residuals	147	0.083709925			142	0.239167673	NA	NA
ZmaFT4								
	Leaf				Rhizome/Roots			
	Df	Mean Sq	F value	Pr(>F)	Df	Mean Sq	F value	Pr(>F)
Site	1	0.054492413	0.261400521	0.609926689	1	0.266466368	0.465806179	0.496034738
Date	7	4.161673425	19.96357907	1.19261E-18	7	12.71449224	22.22602831	4.25622E-20
Site x Date	7	0.717665985	3.442649188	1.93E-03	7	1.58468478	2.770165581	0.009938725
Residuals	147	0.208463293			142	0.572054173		
ZmaFT9								
	Leaf				Rhizome/Roots			
	Df	Mean Sq	F value	Pr(>F)	Df	Mean Sq	F value	Pr(>F)
Site	1	1.668719912	3.741062939	0.055011616	1	0.010529664	0.014225919	0.905228078
Date	7	17.94779202	40.23672222	3.62271E-31	7	6.370384477	8.606596338	8.88854E-09
Site x Date	7	1.347263453	3.020397454	5.39E-03	7	1.806533119	2.440684919	0.021603424
Residuals	147	0.446055022			142	0.740174655		
ZmaTFL1a								
	Leaf				Rhizome/Roots			
	Df	Mean Sq	F value	Pr(>F)	Df	Mean Sq	F value	Pr(>F)
Site	1	5.685059062	16.58488043	7.57573E-05	1	0.787561165	1.191270967	0.276921784
Date	7	6.898858101	20.12586597	9.00869E-19	7	7.702785696	11.65129183	1.17536E-11
Site x Date	7	2.561012623	7.47117799	1.10E-07	7	1.065945672	1.612357475	0.13647906
Residuals	147	0.342785653			142	0.661110013		

Table S10: Statistically significant groupings of time-points at Stackpole Annual (ST-ANN) and Nahcotta Port Annual (NP-ANN) sites based on post-hoc Tukey tests in leaves (a, b, c, d, e, f) and roots (u, v, w, x, y, z). Expression values were log_{10} transformed to fit assumptions of ANOVA.

Date	2023-04-08	2023-05-09	2023-05-18	2023-06-06	2023-06-19	2023-07-06	2023-07-17	2023-07-31
ZmaFT2								
	Leaf							
ST-ANN	abc	bcde	def	def	fg	cdef	efg	g
NP-ANN	a	ab	def	bcd	def	fg	def	fg
	Rhizome/Root							
ST-ANN	w	wx	wx	wx	wxy	wxy	xy	z
NP-ANN	wx	wx	wxy	wx	xy	wxyz	wxy	yz
ZmaFT4								
	Leaf							
ST-ANN	abcde	ab	bcdef	cdefgh	defgh	bcdefg	efgh	gh
NP-ANN	a	abc	bcdefg	abcd	cdefgh	fgh	defgh	h
	Rhizome/Root							
ST-ANN	uv	uvw	uvwx	vwxy	vwxy	wxy	xyz	z
NP-ANN	u	uvwx	wxy	uvw	wxyz	wxyz	yz	yz
ZmaFT9								
	Leaf							
ST-ANN	f	f	cdef	cd	cdef	bc	c	a
NP-ANN	def	f	cde	ef	def	cdef	bc	ab
	Rhizome/Root							
ST-ANN	z	yz	xy	xy	x	xy	xy	yz
NP-ANN	yz	xy	yz	xy	xy	xy	xy	yz
ZmaTFL1a								
	Leaf							
ST-ANN	ab	bcd	bcd	de	ef	cde	bcd	f
NP-ANN	ab	abc	bcd	a	cde	def	de	de
	Rhizome/Root							
ST-ANN	w	wx	wx	wxy	xyz	wxy	wxy	z
NP-ANN	wx	wx	xyz	wx	wxy	wxyz	wx	yz

Table S11: One-way ANOVA results gene expression in relation to time in time-series at Yaquina Bay Annual (YQ-ANN) site. Leaf tissue expression and root tissue expression data were analyzed separately. Date was treated as a categorical factor to account for potential non-linear change. Expression values were log_{10} transformed to fit assumptions of analysis.

ZmaFT2								
		Leaf				Rhizome/Roots		
	Df	Mean Sq	F value	Pr(>F)	Df	Mean Sq	F value	Pr(>F)
Date	2	0.266965246	3.444448843	0.05084795	2	0.078710562	1.177556369	0.331934457
Residuals	21	0.07750594			17	0.066842288		
ZmaFT4								
		Leaf				Rhizome/Roots		
	Df	Mean Sq	F value	Pr(>F)	Df	Mean Sq	F value	Pr(>F)
Date	2	0.327162804	0.511083633	0.60711645	2	0.078710562	1.177556369	0.331934457
Residuals	21	0.640135552			17	0.066842288		
ZmaFT9								
		Leaf				Rhizome/Roots		
	Df	Mean Sq	F value	Pr(>F)	Df	Mean Sq	F value	Pr(>F)
Date	2	0.032054783	0.020559571	0.97967003	2	0.592119052	0.544761873	0.589773426
Residuals	21	1.559117319			17	1.086931888		
ZmaTFL1a								
		Leaf				Rhizome/Roots		
	Df	Mean Sq	F value	Pr(>F)	Df	Mean Sq	F value	Pr(>F)
Date	2	3.062983934	6.229422413	0.00751515	2	0.459257127	0.770505006	0.47827979
Residuals	21	0.491696297			17	0.596046908		

Table S12: Statistically significant groupings of time-points at Yaquina Bay Annual (YQ-ANN) site based on post-hoc Tukey tests. Expression values were log_{10} transformed to fit assumptions of ANOVA.

Date	2023-05-18	2023-07-17	2023-08-30
ZmaFT2			
YQ-ANN Leaf	a	ab	b
YQ-ANN Rhizome/Root	x	x	x
ZmaFT4			
YQ-ANN Leaf	a	a	a
YQ-ANN Rhizome/Root	x	x	x
ZmaFT9			
YQ-ANN Leaf	a	a	a
YQ-ANN Rhizome/Root	x	x	x
ZmaTFL1a			
YQ-ANN Leaf	a	a	b
YQ-ANN Rhizome/Root	x	x	x

Table S13: Differential gene expression of *ZmaPEBP* genes, calculated as logFold Change from RNA sequencing of Stackpole leaf tissue samples (ST Perennial Vegetative and Flowering, ST-ANN Annual Flowering). Values were calculated with DESeq2.

Gene	baseMean	log2FoldChange	lfcSE	stat	pvalue	padj
Perennial Flowering vs Perennial Vegetative						
ZmaFT1	0.061389945	-0.448949999	3.81692888	-0.11762074	0.906368171	NA
ZmaFT2	19.73958222	0.263421259	0.719423546	0.366156015	0.714248661	NA
ZmaFT3	0.515666284	-1.29437436	2.689914959	-0.481195272	0.630377721	NA
ZmaFT4	5.234765514	0.010263584	0.83056456	0.012357358	0.990140506	NA
ZmaFT5	8.820593864	-1.093190365	0.819184905	-1.334485484	0.182044801	NA
ZmaFT6	10.9441375	0.1098815	0.631529661	0.17399262	0.861871262	NA
ZmaFT7	2.094647648	-0.70529859	1.360968308	-0.518232927	0.604295764	NA
ZmaFT8	0.153003328	0.989531482	3.81692888	0.25924808	0.795443837	NA
ZmaFT9	29.04751187	-2.185243689	0.846422241	-2.581741811	0.00983031	0.27446143
ZmaFT10	0.179857044	-0.447616944	3.811776797	-0.117429999	0.906519313	NA
ZmaMFT1	174.4123975	0.409125884	0.464236195	0.881288207	0.378161848	0.988070789
ZmaTFL1a	0.365056341	-1.109576069	3.812415502	-0.291042796	0.771018589	NA
ZmaTFL1b	0.146977557	0	3.81692888	0	1	NA
Annual Flowering vs. Perennial Vegetative						
ZmaFT1	0.061389945	0.375894457	3.81698449	0.09847943	9.22E-01	NA
ZmaFT2	19.73958222	0.767264721	0.723956937	1.059820938	0.289226069	0.485469256
ZmaFT3	0.515666284	-1.916398994	2.701388487	-0.709412586	0.478068479	NA
ZmaFT4	5.234765514	2.210147014	0.757153091	2.919022639	0.003511307	0.018244183
ZmaFT5	8.820593864	-0.491841325	0.826517149	-0.595076975	0.551792018	0.719935137
ZmaFT6	10.9441375	0.106304617	0.654716283	0.162367456	0.871016497	0.929447658
ZmaFT7	2.094647648	1.12913765	1.28129849	0.881244815	0.378185328	NA
ZmaFT8	0.153003328	1.822766396	3.81698449	0.477540949	0.632976969	NA
ZmaFT9	29.04751187	-4.517435398	0.977372429	-4.622020497	3.8002E-06	5.79438E-05
ZmaFT10	0.179857044	-0.333238372	3.811832332	-0.087422096	0.930336007	NA
ZmaMFT1	174.4123975	-0.294798558	0.468591986	-0.629115663	0.529273337	0.702916014
ZmaTFL1a	0.365056341	1.355953009	3.785415875	0.358204502	0.720190278	NA
ZmaTFL1b	0.146977557	1.818578988	3.81698449	0.476443903	0.633758163	NA
Perennial Flowering vs Annual Flowering						
ZmaFT1	0.061389945	0	3.81692888	0	1	NA
ZmaFT2	19.73958222	-0.503843462	0.723362923	-0.696529289	0.486097422	0.675849678
ZmaFT3	0.515666284	0.622024633	2.813963695	0.221049274	0.825054066	NA
ZmaFT4	5.234765514	-2.199883431	0.772003905	-2.84957552	0.004377761	0.023152472
ZmaFT5	8.820593864	-0.60134904	0.855617261	-0.702824811	0.482164933	0.673104477
ZmaFT6	10.9441375	0.003576883	0.656963028	0.005444573	0.99565588	0.998035036
ZmaFT7	2.094647648	-1.83443624	1.353783198	-1.355044325	0.175403435	NA
ZmaFT8	0.153003328	-0.833234914	3.81692888	-0.218299827	0.827195509	NA
ZmaFT9	29.04751187	2.332191709	0.98966866	2.356537903	0.018446185	0.070674899
ZmaFT10	0.179857044	-0.114378572	3.81692888	-0.029966126	0.976094069	NA
ZmaMFT1	174.4123975	0.703924442	0.468195972	1.503482482	0.132714671	0.295299904
ZmaTFL1a	0.365056341	-2.465529078	3.789906321	-0.650551457	0.515336075	NA
ZmaTFL1b	0.146977557	-1.546186721	3.81692888	-0.405086594	0.68541386	NA

Supplemental References:

1. Liu, H., Liu, X., Chang, X., Chen, F., Lin, Z., and Zhang, L. (2023). Large-scale analyses of angiosperm *Flowering Locus T* genes reveal duplication and functional divergence in monocots. Front. Plant Sci. *13*, 1039500. https://doi.org/10.3389/fpls.2022.1039500.

2. Pritchard, J.K., Stephens, M., and Donnelly, P. (2000). Inference of Population Structure Using Multilocus Genotype Data. Genetics *155*, 945–959. https://doi.org/10.1093/genetics/155.2.945.

3. Evanno, G., Regnaut, S., and Goudet, J. (2005). Detecting the number of clusters of individuals using the software structure: a simulation study. Mol. Ecol. *14*, 2611–2620. https://doi.org/10.1111/j.1365-294X.2005.02553.x.

4. Briones Ortiz, B.A., Boardman, F.C., Ruesink, J.L., and Naish, K.A. (2025). Adaptive Genetic Differentiation Between Spatially Proximate Annual and Perennial Life History Types of a Marine Foundation Species. Mol. Ecol. *n/a*, e17730. https://doi.org/10.1111/mec.17730.

5. Catchen, J., Hohenlohe, P.A., Bassham, S., Amores, A., and Cresko, W.A. (2013). Stacks: an analysis tool set for population genomics. Mol. Ecol. *22*, 3124–3140. https://doi.org/10.1111/mec.12354.

6. Olsen, J.L., Rouzé, P., Verhelst, B., Lin, Y.-C., Bayer, T., Collen, J., Dattolo, E., De Paoli, E., Dittami, S., Maumus, F., et al. (2016). The genome of the seagrass *Zostera marina* reveals angiosperm adaptation to the sea. Nature *530*, 331–335. https://doi.org/10.1038/nature16548.

7. Ma, X., Olsen, J.L., Reusch, T.B.H., Procaccini, G., Kudrna, D., Williams, M., Grimwood, J., Rajasekar, S., Jenkins, J., Schmutz, J., et al. (2021). Improved chromosome-level genome assembly and annotation of the seagrass, *Zostera marina* (eelgrass). F1000Res. *10*, 289. https://doi.org/10.12688/f1000research.38156.1.

8. Li, H. (2013). Aligning sequence reads, clone sequences and assembly contigs with BWA-MEM. ArXiv Q-BioGN.

9. Rochette, N.C., and Catchen, J.M. (2017). Deriving genotypes from RAD-seq short-read data using Stacks. Nat. Protoc. *12*, 2640–2659. https://doi.org/10.1038/nprot.2017.123.

10. DeRaad, D.A. (2022). snpfiltr: An R package for interactive and reproducible SNP filtering. Mol. Ecol. Resouces *22*, 2443–2453. https://doi.org/10.1111/1755-0998.13618.

11. Chang, C.C., Chow, C.C., Tellier, L.C., Vattikuti, S., Purcell, S.M., and Lee, J.J. (2015). Second-generation PLINK: rising to the challenge of larger and richer datasets. Gigascience *4*, 7. https://doi.org/10.1186/s13742-015-0047-8.

12. Lee, H., Golicz, A.A., Bayer, P.E., Jiao, Y., Tang, H., Paterson, A.H., Sablok, G., Krishnaraj, R.R., Chan, C.-K.K., Batley, J., et al. (2016). The genome of a southern hemisphere seagrass species (*Zostera muelleri*). Plant Physiol. *172*, 272–283. https://doi.org/10.1104/pp.16.00868.

13. Mimida, N., Goto, K., Kobayashi, Y., Araki, T., Ahn, J.H., Weigel, D., Murata, M., Motoyoshi, F., and Sakamoto, W. (2001). Functional divergence of the *TFL1*-like gene family in *Arabidopsis* revealed by characterization of a novel homologue. Genes Cells *6*, 327–336. https://doi.org/10.1046/j.1365-2443.2001.00425.x.

14. Yoo, S.J., Chung, K.S., Jung, S.H., Yoo, S.Y., Lee, J.S., and Ahn, J.H. (2010). *BROTHER OF FT AND TFL1 (BFT)* has *TFL1*-like activity and functions redundantly with *TFL1* in inflorescence meristem development in Arabidopsis. Plant J. *63*, 241–253. https://doi.org/10.1111/j.1365-313X.2010.04234.x.

15. Kardailsky, I., Shukla, V.K., Ahn, J.H., Dagenais, N., Christensen, S.K., Nguyen, J.T., Chory, J., Harrison, M.J., and Weigel, D. (1999). Activation tagging of the floral inducer *FT*. Science *286*, 1962–1965. https://doi.org/10.1126/science.286.5446.1962.

16. Yoo, S.Y., Kardailsky, I., Lee, J.S., Weigel, D., and Ahn, J.H. (2004). Acceleration of flowering by overexpression of *MFT* (MOTHER OF FT AND TFL1). Mol. Cells *17*, 95–101. https://doi.org/10.1016/S1016-8478(23)13012-3.

17. Kobayashi, Y., Kaya, H., Goto, K., Iwabuchi, M., and Araki, T. (1999). A pair of related genes with antagonistic roles in mediating flowering signals. Science *286*, 1960–1962. https://doi.org/10.1126/science.286.5446.1960.

18. Yamaguchi, A., Kobayashi, Y., Goto, K., Abe, M., and Araki, T. (2005). *TWIN SISTER OF FT (TSF)* acts as a floral pathway integrator redundantly with *FT*. Plant Cell Physiol. *46*, 1175–1189. https://doi.org/10.1093/pcp/pci151.

19. Lv, B., Nitcher, R., Han, X., Wang, S., Ni, F., Li, K., Pearce, S., Wu, J., Dubcovsky, J., and Fu, D. (2014). Characterization of *FLOWERING LOCUS T1* (*FT1*) gene in *Brachypodium* and Wheat. PLOS ONE *9*, e94171. https://doi.org/10.1371/journal.pone.0094171.

20. Shaw, L.M., Lyu, B., Turner, R., Li, C., Chen, F., Han, X., Fu, D., and Dubcovsky, J. (2019). *FLOWERING LOCUS T2* regulates spike development and fertility in temperate cereals. J. Exp. Bot. *70*, 193–204. https://doi.org/10.1093/jxb/ery350.

21. Qin, Z., Bai, Y., Muhammad, S., Wu, X., Deng, P., Wu, J., An, H., and Wu, L. (2019). Divergent roles of FT-like 9 in flowering transition under different day lengths in *Brachypodium distachyon*. Nat. Commun. *10*, 812. https://doi.org/10.1038/s41467-019-08785-y.

22. Sharma, B., Batz, T.A., Kaundal, R., Kramer, E.M., Sanders, U.R., Mellano, V.J., Duhan, N., and Larson, R.B. (2019). Developmental and molecular changes underlying the vernalization-induced transition to flowering in *Aquilegia coerulea* (James). Genes *10*, 734. https://doi.org/10.3390/genes10100734.

23. Yoshida, A., Taoka, K., Hosaka, A., Tanaka, K., Kobayashi, H., Muranaka, T., Toyooka, K., Oyama, T., and Tsuji, H. (2021). Characterization of frond and flower development and identification of FT and FD genes from duckweed *Lemna aequinoctialis* Nd. Front. Plant Sci. *12*, 697206. https://doi.org/10.3389/fpls.2021.697206.

24. Ito-Inaba, Y., Masuko-Suzuki, H., Maekawa, H., Watanabe, M., and Inaba, T. (2016). Characterization of two PEBP genes, SrFT and SrMFT, in thermogenic skunk cabbage (Symplocarpus renifolius). Sci. Rep. *6*, 29440. https://doi.org/10.1038/srep29440.

25. Oda, A., Narumi, T., Li, T., Kando, T., Higuchi, Y., Sumitomo, K., Fukai, S., and Hisamatsu, T. (2012). *CsFTL3*, a chrysanthemum *FLOWERING LOCUS T*-like gene, is a key regulator of photoperiodic flowering in chrysanthemums. J. Exp. Bot. *63*, 1461–1477. https://doi.org/10.1093/jxb/err387.

26. Higuchi, Y., and Hisamatsu, T. (2015). CsTFL1, a constitutive local repressor of flowering, modulates floral initiation by antagonising florigen complex activity in chrysanthemum. Plant Sci. *237*, 1–7. https://doi.org/10.1016/j.plantsci.2015.04.011.

27. Higuchi, Y., Narumi, T., Oda, A., Nakano, Y., Sumitomo, K., Fukai, S., and Hisamatsu, T. (2013). The gated induction system of a systemic floral inhibitor, antiflorigen, determines obligate short-day flowering in chrysanthemums. Proc. Natl. Acad. Sci. *110*, 17137–17142. https://doi.org/10.1073/pnas.1307617110.

28. Kojima, S., Takahashi, Y., Kobayashi, Y., Monna, L., Sasaki, T., Araki, T., and Yano, M. (2002). *Hd3a*, a rice ortholog of the *Arabidopsis FT* gene, promotes transition to flowering downstream of *Hd1* under short-day conditions. Plant Cell Physiol. *43*, 1096–1105. https://doi.org/10.1093/pcp/pcf156.

29. Nakagawa, M., Shimamoto, K., and Kyozuka, J. (2002). Overexpression of *RCN1* and *RCN2*, rice *TERMINAL FLOWER 1/CENTRORADIALIS* homologs, confers delay of phase transition and altered panicle morphology in rice. Plant J. *29*, 743–750. https://doi.org/10.1046/j.1365-313X.2002.01255.x.

30. Wei, S., Cheng, L., Qian, H., Li, X., Shang, L., Zhou, Y., Ye, X., Zhou, Y., Gao, Y., Cheng, L., et al. Florigen-like protein OsFTL1 promotes flowering without essential florigens Hd3a and RFT1 in rice. J. Integr. Plant Biol. *n/a*. https://doi.org/10.1111/jipb.13856.

31. Zheng, R., Meng, X., Hu, Q., Yang, B., Cui, G., Li, Y., Zhang, S., Zhang, Y., Ma, X., Song, X., et al. (2023). OsFTL12, a member of FT-like family, modulates the heading date and plant architecture by florigen repression complex in rice. Plant Biotechnol. J. *21*, 1343–1360. https://doi.org/10.1111/pbi.14020.

32. Gu, H., Zhang, K., Chen, J., Gull, S., Chen, C., Hou, Y., Li, X., Miao, J., Zhou, Y., and Liang, G. (2022). *OsFTL4*, an *FT*-like gene, regulates flowering time and drought tolerance in rice (*Oryza sativa* L.). Rice *15*, 47. https://doi.org/10.1186/s12284-022-00593-1.

33. Fang, M., Zhou, Z., Zhou, X., Yang, H., Li, M., and Li, H. (2019). Overexpression of OsFTL10 induces early flowering and improves drought tolerance in *Oryza sativa L.* PeerJ *7*, e6422. https://doi.org/10.7717/peerj.6422.

34. Lee, R., Baldwin, S., Kenel, F., McCallum, J., and Macknight, R. (2013). *FLOWERING LOCUS T* genes control onion bulb formation and flowering. Nat. Commun. *4*, 2884. https://doi.org/10.1038/ncomms3884.

Chapter 3

Accelerated flowering and differential florigen gene expression of seagrass *Zostera marina* under experimental warming

Christine T. Nolan[1], Ian McBride[2], Niyah Reid[2], Sylvia Yang*[,2,3], Takato Imaizumi[1], Jennifer L. Ruesink[1], Jeffrey L. Gaeckle[4]

[1] University of Washington, Department of Biology, Seattle, WA USA

[2] Shannon Point Marine Center, Western Washington University, Anacortes, WA USA

[3] Padilla Bay National Estuarine Research Reserve, Washington State Department of Ecology, Mount Vernon, WA USA

[4] Nearshore Habitat Program, Washington State Department of Natural Resources, Olympia, WA 98504

* Corresponding author, **Contact Information:** Sylvia Yang, Padilla Bay National Estuarine Research Reserve, Washington State Department of Ecology, 10441 Bayview-Edison Road, Mount Vernon, WA 98273, syang@padillabay.gov

Abstract:

1. Flowering is an important trait for the resilience of marine angiosperms (seagrasses) as they face rising seawater temperatures, more frequent extreme weather events, and anthropogenic disturbances.
2. Using the seagrass *Zostera marina*, we applied a common garden approach to experimentally test how flowering and its underlying molecular mechanisms responded to elevated water temperature (+3°C). We focused on developmental and reproductive traits paired with florigen gene expression to gain insight to the molecular mechanism underpinning differences in flowering responses.
3. We compared annual shoots from two source populations (Willapa Bay along the coast, and Padilla Bay in the Salish Sea, Washington, USA) to understand natural variation not only in morphological and reproductive traits, but also the gene-environment interactions governing flowering onset.
4. At the individual and population levels, annual seedlings in the +3°C heated treatment produced more spathes and accelerated development of inflorescences so seeds dispersed sooner. Seedlings from Padilla Bay flowered at greater rates and earlier than Willapa Bay, and these differences were exaggerated by the +3°C heated treatment.
5. For two predicted floral activators, *ZmaFT2* and *ZmaFT4*, expression increased throughout the summer regardless of population and showed no response to the temperature treatment. A predicted repressor of flowering onset, *ZmaFT9*, was expressed at lower levels in the shoots grown in the +3°C heated treatment, and even more so in the Padilla Bay population, which flowered earlier than the Willapa Bay population. *ZmaTFL1a*, a gene predicted to be involved with downstream flowering processes, showed no significant response to the temperature treatment.
6. Together, these results support a key role for antiflorigen (*ZmaFT9*) in the molecular control of flowering in *Z. marina*, and *ZmaFT9* expression contributes to the temperature-based response of timing of flowering onset. Other differences on flowering traits not affected by treatment were attributed to natural variation between populations. Elevated seawater temperature impacted flowering timing and spathe production, with potential consequences for seed yield and meadow resilience.

Keywords: eelgrass, *Zostera marina*, gene expression, florigen, annual life history, ecotype, angiosperm, seagrass flowering

Introduction

Seagrasses are marine angiosperms that serve as foundation species in coastal ecosystems. They provide key ecosystem services such as sediment stabilization, nutrient cycling, and habitat and feeding grounds for fish, invertebrates, and waterfowl (Orth et al., 2006). Flowering and seed production play a critical role in contributing genetic diversity and resilience and persistence within seagrass populations (Kendrick et al., 2012), and are important processes for persistence, recovery following disturbance, and population resiliency (O'Brien et al., 2018; Orth et al., 2006). Environmental factors, such as nutrient availability, tidal variation, light, salinity, and temperature have been observationally associated with flowering (Lekammudiyanse et al., 2024). Thus, elucidating the effect of environmental variation on the mechanism of flowering is important for understanding ecological resilience of seagrasses in a changing environment.

The onset of flowering processes in angiosperms is largely regulated and dictated by the phosphatidylethanolamine-binding protein (PEBP) gene family, which includes known florigen genes such as *FLOWERING LOCUS T* (*FT*) and *TWIN SISTER OF FT* (*TSF*). Within this gene family, *FT* is the primary activator of flowering and its expression is cued in response to environmental inputs and the plant's circadian clock, known as the external coincidence model (de Montaigu et al., 2010). Members of the *PEBP* gene family also include flowering repressors; for example, *TERMINAL FLOWER 1* (*TFL1*) is the main repressor in *Arabidopsis*. The *FT* pathway and the *PEBP* gene family are highly conserved across flowering plants (Bennett & Dixon, 2021; Pin & Nilsson, 2012; Wickland & Hanzawa, 2015), and recent studies have begun characterizing *FT* function and the floral pathway in aquatic and marine plants (Nolan et al., 2024; Yoshida et al., 2021). Nolan et al. identified 4 *PEBP* genes within the *Z. marina* genome that are correlated to vegetative development and reproductive stages, three of which are *FT*-like genes and cluster within the *FT* clade (Nolan et al., 2024). In this study, two genes, *ZmaFT4* and *ZmaFT2,* are likely activators. The third *FT* gene characterized, *ZmaFT9*, is likely a repressor

and the major determinant of flowering in eelgrass. The study also describes one *TFL1* homolog, *ZmaTFL1a*, whose function is suspected to be related to shoot determinacy and architecture and not to flowering onset. Their results ultimately suggest that *FT* expression is affected by environmental factors such as temperature and photoperiod, in keeping with typical cues to flower across multiple angiosperm species.

FT expression is upregulated and more easily trafficked as a signal in increased temperatures in *Arabidopsis* and results in earlier flowering (Balasubramanian et al., 2006; Blázquez et al., 2003; Kinmonth-Schultz et al., 2016; Susila et al., 2021). Previous literature in eelgrass flowering indicates that warmer temperatures over a latitudinal gradient largely result in earlier flowering onset in eelgrass (Blok et al., 2018). However, the linkage from *FT/TFL1* expression patterns to environmental temperature variation and flowering traits in seagrasses broadly is lacking or conflicting. In the seagrass *Posidonia*, heat stress led to activation of regulatory genes for flowering and stress tolerance (Marín-Guirao et al., 2019). Furthermore, there is very little known about how *FT*-driven precocious flowering affects yield or fitness. Earlier flowering time associated with warmer temperatures can lead to lower seed yields (Craufurd & Wheeler, 2009).

Temperature has been frequently identified as an important driver of flowering in seagrass (Lekammudiyanse et al., 2024). However, the response of seagrasses to elevated temperatures has varied by flowering trait, species, geographic location, and temperature regime, suggesting a mechanistic understanding of flowering is needed. Seasonal elevated temperatures have been observed to both increase and decrease flowering production (De Cock, 1980; Diaz-Almela et al., 2007; Qin et al., 2020; Thom et al., 2003) and advance flowering timing and maturation of seeds (Blok et al., 2018; Sawall et al., 2021). Understanding the mechanism of seagrass flowering onset from the level of florigen (*FT/TFL1*) gene expression to the functional level has the potential to explain the variation observed in ecological responses to elevated temperature.

Eelgrass (*Zostera marina* L.) is one of the most wide-ranging seagrasses, occupying latitudes of 30-70°N in both Atlantic and Pacific basins. Flowering frequency, timing of flowering onset, and flowering duration vary in eelgrass on both spatial and annual scales (Qin et al., 2020; Thom et al., 2003). *Z. marina* exhibits multiple ecotypes in the northeast Pacific that vary in allocation to clonal versus sexual reproduction (Backman, 1991; Ruesink et al., 2022). *Z.*

marina also uses both annual and perennial life histories (Gagnon et al., 1980; J. H. Kim et al., 2017; Muñiz-Salazar et al., 2005). Annual and perennial ecotypes of eelgrass undergo sexual reproduction and flowering at different rates, with perennial meadows primarily persisting through clonal rhizomal branching, and annual populations through flowering (Ruesink et al., 2022). Variation in sensitivity and response to temperature stress may also be due to local adaptation (DuBois et al., 2022). Thus, variation in flowering response to temperature may be derived from any level of biological organization and requires an experimental set-up to disentangle effects of temperature and genotype on flowering traits and florigen expression in eelgrass.

In this study, we use a common garden approach to experimentally test the effect of +3°C elevated seawater temperature on *Z. marina PEBP* gene (*ZmaPEBP*) expression and individual and population-level flowering traits. We predicted that:

1) Flowering onset would occur earlier in the +3°C treatment and could influence the timing and amount of seed production;
2) Treatments with earlier or more frequent flowering would have lower expression of the antiflorigen repressor of flowering (*ZmaFT9*) and higher expression of activators (*ZmaFT2* and *ZmaFT4*);
3) Natural variation in populations resulting from local adaptation likely play a role in the response of flowering to environmental cues broadly.

These traits are directly linked to plant fitness and population resilience of these aquatic foundation species.

Materials and Methods

Study Species: Eelgrass, *Zostera marina* L., is a seagrass species that is widely distributed across the northern hemisphere in nearshore soft-sediment habitats. In eelgrass, flowering traits are complex and include prevalence and intensity of flowering, timing of transition from vegetative growth to flowering, speed of spathe (inflorescence) development, spathe and seed production, seed yield, and timing of seed dispersal. Primarily a perennial, *Z. marina* also reproduces sexually. More rarely, *Z. marina* can also exhibit an annual life history,

in which seeds germinate, grow as seedlings, then flower, disperse seed, and senesce each year. This annual ecotype of *Z. marina* has been associated with environments characterized by high stress, such as seasonal low light or extreme temperatures (Jarvis & Moore, 2015; Keddy & Patriquin, 1978; S. H. Kim et al., 2014; Meling-López & Ibarra-Obando, 1999; Morita et al., 2010; Nelson & Sullivan, 2018; Phillips et al., 1983; van Katwijk & van Tussenbroek, 2023; van Lent & Verschuure, 1994). We use this annual life history ecotype as a model system for investigating flowering timing in this study since plant individuals will predictably flower within a growing season.

Field Sites and Collection: To investigate potential variation in flowering mechanisms, we collected *Z. marina* seedlings from two locations in Washington state (USA) where annuals are known to be found, Padilla and Willapa Bays (Figure 1, Table S1). Willapa Bay (WB) is located on the coast of Washington state and is estuarine, whereas Padilla Bay (PB) is in the central Salish Sea and has a highly modified shoreline and orphaned from riverine influences. This difference in geographic location leads to differences in temperature and tidal regimes at the two embayments (Figure 2a).

Z. marina seedlings were collected April 26, 2024, from intertidal locations where annual life history has previously been found in the two embayments, co-occurring with perennial *Z. marina* (Table S1). Thus, seedlings could not be identified as annual or perennial until they flowered during the duration of this experiment. Seedlings were carefully extracted from the sediment to preserve roots and were soaked for 2-4 hours in <10 ppt seawater to reduce transfer of *Labyrinthula* sp. and other hitch-hikers. Seedlings were planted into separate tubs of masonry sand in flow-through seawater mesocosms within 8-24 hours.

Experimental Design: *Z. marina* seedlings from each bay were planted into replicate tubs of masonry sand conditioned for one week (32 seedlings per tub, 51 cm L x 38 cm W x 10 cm sediment depth). One tub per source population was placed in each of eight flow-through seawater mesocosms at the Shannon Point Marine Center (SPMC; Table S1). Seawater was piped into these mesocosms from an offshore source with a flow rate of 10 L/min. Four of the mesocosms held custom-built heat exchangers (Breiter et al., 2024) to achieve a +3°C temperature increase (+2.73 ± 0.02°C (mean ± s.e.), Figure 2a). We chose a +3°C temperature

increase based on predicted global warming trends (Intergovernmental Panel on Climate Change (IPCC), 2023) and predicted warming trends of the Salish Sea (Khangaonkar et al., 2019; Mote & Salathé, 2010). Seedlings were reared continuously in the heated and ambient mesocosm conditions for approximately 3.6 months (108 days) to observe effects of increased seawater temperature on phenology, quantity, and morphology of seedlings as they developed into flowering shoots. See Replication table (Table 1).

Population & Morphological Traits: Every week, seedlings were counted in each tub as non-flowering or flowering, and every other week, morphological measurements were recorded: shoot length, number of leaves, and leaf width for 3 haphazardly selected non-flowering seedlings (if present); and flowering shoot length, number of spathes, and developmental stage of each spathe (de Cock 1980) for 3 flowering seedlings (if present). Seedlings were considered 'flowering' as soon as they began to bolt. At the end of the experiment, all flowering shoots were scored for developmental stage. Below-ground parameters were obtained from biweekly destructive sampling, described below.

ZmaPEBP Gene Expression & Individual Traits: Two plants from each population and replicate tub were destructively sampled for gene expression analysis on a weekly basis from 2024-05-06 until 2024-06-05, and on a biweekly basis between 2024-06-05 and 2024-07-29. Plants (with roots and rhizome intact) were collected between ZT3-5 (Zeitgeber time: hours from sunrise) (Song et al., 2018). All collected plant tissue was stored in RNAlater stabilization solution (ThermoFisher, Waltham MA). Samples were stored at -20°C until processing, at which point individual morphological measurements were taken for shoot length, number of leaves or spathes, leaf width, number of branches, rhizome length, number of rhizome internodes, and root length, as well as developmental state (vegetative, bolting, and flowering). Number of internodes at the beginning of the experiment was used as a proxy for age at time of collection. Frozen tissue was frozen at -80°C for long term storage.

Gene expression analysis was conducted in the manner as described in Nolan et al., (Nolan et al., 2024). Total RNA was extracted with the RNeasy Plant Mini Kit (Qiagen, Hilden Germany) with an on-column DNA digestion incubation. Complementary DNA (cDNA) was made with iScript cDNA synthesis kit (Bio-Rad, Hercules CA). Locus specific primers to detect

expression of *ZmaFT2*, *ZmaFT4*, *ZmaFT9*, and *ZmaTFL1a* are described in Nolan et al. (Table S2) (Nolan et al., 2024). For reference genes, locus specific primers to detect expression of *CYCLOPHILIN 2* (*CYP2*), *EUKARYOTIC INITIATION FACTOR4A* (*ELF4A*), and *RIBOSOME STRUCTURAL PROTEIN L28* (*RPL28*) are described in Ransbotyn and Reusch (Ransbotyn & Reusch, 2006). For all qPCR (quantitative PCR) runs, we set a baseline threshold of relative fluorescence units (RFU) for consistency across primers and to ensure that plates were comparable. Samples with no detectable expression were given a cycle threshold (C_T) value of 40 ($C_T = 40$). C_T values were analyzed using the ΔC_T method, and average C_T values for the three reference genes were used for calculation.

Replication Statement

Table 1. Replication Statement

Scale of inference	**Scale at which factor of interest is applied**	**Number of replicates at the appropriate scale**
Individual (gene expression, morphology, or life stage related to temperature)	Tank	4 tank replicates of each temperature-source combination

Statistical Analyses: Although seedlings were collected where annuals were present the previous summer, seedlings could not be identified as annual or perennial when they were collected. Therefore, population-level flowering could be reduced by annuals that did not flower or by perennial plants. Perennial seedlings were not expected to flower within the first growing season and instead produce clonal branches.

We aimed to quantify differences in the morphological traits between the two populations (WB and PB) and the two treatments (Ambient and +3°C heated) to capture effects of increased temperature on growth, reproductive timing, and variability of response by population.

To estimate differences in flowering timing, proportion flowering was fit to a 3-parameter log-logistic model using the *drm* function in R (Ritz et al., 2015). Proportion flowering was calculated per tub from the number of flowering shoots divided by the total number of remaining shoots at each time point. The location parameter *e* (the time to reach 50% of total flowering) was used to estimate relative differences in flowering time between populations and temperature treatments. The parameter *d* was used to assess fraction of seedlings that were annual and flowered (versus pre-flowering annuals or perennials that would not be

expected to flower during the experiment). The parameter *b* was used to represent synchronicity of the flowering event. The *compParm* function was used to compare model coefficients amongst treatment-population combinations.

To test the effect of population and temperature treatment on morphological traits, 3-way mixed effects ANOVAs were conducted using the *aov* function in R (R Core Team., 2021) with the following model construction: response ~ treatment * population * census date as fixed effects and tank as a random effect to account for repeated measures of each mesocosm replicate. Date was assumed categorical. Morphological traits of the non-flowering or flowering seedlings were averaged by population and mesocosm replicate prior to analysis. For final spathe developmental stage and initial and final rhizome internode counts, individual data was analyzed with a 2-way ANOVA using population * treatment as fixed effects. Post-hoc pairwise comparisons were conducted using the *emmeans_test* function (Searle et al., 1980) with Bonferroni correction to account for multiple testing.

We used a generalized additive mixed effect model (GAMM) to analyze the expression of *ZmaPEBP* genes across time. GAMMs are able account for the non-unidirectional response of gene expression over time. We used gene expression values as response variable and temperature treatment (Ambient or +3°C Heated) and population (Willapa Bay, WB, and Padilla Bay, PB) as main effects. Date (continuous) was included as a global thin-plate regression spline smooth term. As an additional smooth term, the interaction between date and treatment was included to account for possible changes in the timing of expression. Tank number also was included as a random effect smooth term, since two individuals were sampled per mesocosm on each date. Expression values were log10 transformed to fit assumptions of model. Statistical models were built in R (R Core Team, 2024) using *gam* function from the package *mgcv* (Wood, 2011).

Results

Population & Morphological Traits:

Flowering timing: A higher proportion of seedlings from Padilla Bay flowered under +3°C heated conditions, but temperature treatment did not have an effect on the proportion of flowering seedlings from Willapa Bay over the duration of the experiment. Annual seedlings

from Padilla Bay flowered approximately 9 days earlier in the heated treatment compared to ambient, and 50% of the seedlings in the heated treatment from Padilla Bay flowered approximately 30 days before that of seedlings from Willapa Bay (Figure 2b, Table S3 parameter *e*). Nearly all seedlings from Padilla Bay flowered in heated tanks compared to 90% of seedlings in ambient tanks, which was greater than Willapa Bay seedlings (40-60%), which were not affected by temperature treatment (Figure 2b, Table S3 parameter *d*). Willapa Bay's maximum flowering was probably reduced by contamination from perennial seedlings. Synchronicity of flowering (parameter *b*) did not differ amongst temperature treatments or populations.

Morphological traits: Non-flowering seedling length and width increased over time prior to flowering but did not differ between treatments or populations (Figure 3a-b, Table S4). Width of leaves on non-flowering seedlings increased over time due to treatment (becoming wider in heated treatment after day 94) (Figure 3c, Table S4). Non-flowering seedlings were primarily limited to the Willapa population by the end of the experiment since the majority of Padilla seedlings flowered by day 80 (Figure 3c).

Flowering seedling length and spathe developmental stage increased over time but did not differ by temperature treatment. Number of spathes also increased over time and differed between populations and temperature treatment. Flowering seedlings in the heated treatment produced 0.8 more spathes than those in the ambient treatment. Flowering seedlings from Padilla Bay showed longer leaf length regardless of temperature treatment and produced 1.2 more spathes than those from Willapa Bay (Figure 3d-f, Table S4).

Rhizome and root length of the seedlings also increased over time (flowering and non-flowering seedlings combined) but did not differ by treatment or population (Figure 3g-h, Table S4). The number of rhizome internodes exhibited a significant site effect, with post-hoc pairwise comparisons demonstrating Willapa seedlings having more internodes than Padilla seedlings at the end of the experiment (Figure 3i, Table S4). The number of internodes did not differ between populations or treatments at the beginning of the experiment. By the last destructive sampling (day 94), Willapa Bay plants had 2.6 more internodes than Padilla Bay plants (Figure 3i, Table S4). Thus, temperature treatment did not have an effect on rhizome length or rate of internode production, but internode production rate was different between populations.

Flower development: At the end of the experiment (day 108), spathe developmental stage was 0.9 stages further along in the heated treatment for both populations compared to ambient,

and Padilla Bay spathes were 0.4 developmental stages ahead of Willapa Bay spathes (Figure 3f, Table S4). Peak pollination also occurred approximately 2 weeks earlier in heated tanks (Figure S1).

Gene Expression & Individual Traits: To gain insight into how sustained increased temperature affects the genes involved in eelgrass flowering, we characterized expression of *ZmaFT2*, *ZmaFT4*, *ZmaFT9*, and *ZmaTFL1a* at various time points during the annual shoot's lifespan in both populations. We focused our sampling to the timeframe we expected would correspond to prior to and during the onset of flowering in these populations, thereby aiming to capture the window in which flowering is induced. *ZmaFT2* and *ZmaFT4* showed increased expression over time in both Padilla Bay and Willapa populations (Figure 4a-d, Figure S2a-d, Table S5). *ZmaFT2* expression peaked in early July (2024-07-01), and *ZmaFT4* expression peaked two weeks after at the following collection (2024-07-15). Gene expression patterns in both genes did not differ between temperature treatments or between source populations. Expression of *ZmaFT9* was statistically lower in the +3°C treatment and was lower in shoots from Padilla Bay (Figure 4e-f, Figure S2e-f), which flowered earlier compared to Willapa Bay (Figure 2b). In Padilla Bay samples, *ZmaFT9* showed higher levels in expression in earlier stages in vegetative development, and an overall decrease before and after flowering onset. *ZmaFT9* expression decreased approximately 7 days earlier in the +3°C heated treatment compared to the ambient treatment (2024-05-20 and 2024-05-27, respectively) (Figure 2b), which may contribute to the significant interaction effect between temperature treatment and date in the GAMM results (Table S5). *ZmaTFL1a* expression, in both populations, showed no temporal trend or change due to temperature treatment (Figure 4g-h).

Discussion

In this study, we characterized the effects of elevated temperature on *Z. marina* flowering from *ZmaPEBP* gene expression (*ZmaFT* and *ZmaTFL1a*) *to* functional ecological traits. We observed earlier flowering and an acceleration of flowering shoot growth and spathe development in shoots from Padilla Bay in the +3°C treatment. Our results suggest that among

the four *ZmaPEBP* genes we analyzed, only the antiflorigen gene, *ZmaFT9* is regulated by temperature inputs and that expression of *ZmaFT2*, *ZmaFT4*, and *ZmaTFL1a* are all unaffected by an increase in temperature. Combined with our results that flowering occurred earlier in the heated treatment (9 days in Padilla Bay shoots), we expect that *ZmaFT9* may be an upstream regulator of flowering relative to *ZmaFT2*, *ZmaFT4*, and *ZmaTFL1a*, and ultimately may be a major determinant of when flowering onset occurs in eelgrass.

Elevated temperatures result in earlier flowering in eelgrass annuals:

Previous studies have shown that warmer temperatures, both artificially manipulated in mesocosms and naturally over a latitudinal gradient, drive flowering processes in *Z. marina* populations broadly (Blok et al., 2018; Sawall et al., 2021). In our study focused on annual populations, our results similarly showed that a temperature increase of +3°C resulted in earlier flowering and flowering-related developmental changes. We observed an overall increase in flowering proportion, specifically in the Padilla Bay population, which was composed predominantly of annuals. However, the lack of difference in flowering proportion between heated and ambient for Willapa seedlings could have been due to the low number of annual seedlings represented from this population due to contamination by perennial seedlings (Figure 3, Table S4). The presence of perennials was confirmed by the end of the experiment, with Willapa Bay shoots having more internodes and longer rhizomes, despite starting with the same number of internodes initially, which is more characteristic of perennial shoots (Figure 3i). Additionally, increased leaf width and rate of leaf production of the Willapa seedlings late in the experiment is also consistent with the response of perennial *Z. marina* to elevated temperature in Breiter et al.'s study (Breiter et al., 2024).

In the annual shoots that did flower, this acceleration in flowering was not only observed in the timing of the emergence of flowering shoots, but in the earlier development and production of spathes and seeds (Figure S1). Spathes on shoots in the +3°C treatment had more time to develop, compared to their ambient counterparts, and thus developed earlier (De Cock, 1980). Thus, with warming, annual seedlings produced earlier and potentially higher seed yields, though number of seeds per spathe remains to be enumerated.

ZmaFT9 expression is decreased in elevated temperature and may be determinant of earlier flowering in warmer conditions

PEBP genes are largely regulated by temperature, among other stimuli, so temperature thereby regulates flowering time. In *Arabidopsis*, *FT* gene expression is activated by increased temperature (Balasubramanian et al., 2006; Blázquez et al., 2003; Kinmonth-Schultz et al., 2016; Susila et al., 2021). In rice, *Ghd7* regulates flowering via repression of rice *FT*-homolog, *Hd3a*, in a temperature-dependent manner in short day conditions (Nagalla et al., 2021). Given that eelgrass flowering occurs earlier under warmer conditions (Blok et al., 2018; Sawall et al., 2021), we would expect that *ZmaFT* homologs are similarly regulated by temperature and that activators of flowering would experience an increase in expression in heated conditions. However, in the four eelgrass *PEBP* genes that we tested, only *ZmaFT9* expression, the antiflorigen gene with apparent repressive function, is affected by the +3°C treatment. *ZmaFT9* was previously described to be a repressor of flowering and speculated to be the main determinant of flowering in eelgrass due to a decrease in expression occurring prior to flowering onset (Nolan et al., 2024). Shoots grown in the heated treatment showed lower expression of *ZmaFT9* throughout the entire season in both populations. The decrease in expression over time which is expected to precede the onset of flowering seems to occur earlier in the Padilla Bay population in the +3°C treatment compared to the ambient, by approximately 7 day, though we were unable to resolve this difference statistically given the variation within our datasets. Nonetheless, temperature is a key factor in the regulation of *ZmaFT9* expression.

ZmaFT2 and *ZmaFT4* expression is unaffected by temperature increase

ZmaFT2 and *ZmaFT4*, two of the four *ZmaPEBP* genes examined, are described as activators of flowering and expression generally increases over time (Nolan et al., 2024). While our findings confirm that expression of *ZmaFT2* and *ZmaFT4* increase over time as the plant reaches maturity and flowers, we observed no significant difference in expression between treatments, contradicting our original hypothesis. Our finding that *ZmaFT2* and *ZmaFT4* are seemingly unregulated by temperature is an unexpected finding given effects of increased temperature on florigen in other angiosperms (Balasubramanian et al., 2006; Blázquez et al., 2003; Kinmonth-Schultz et al., 2016). However, it is not entirely novel for flowering-related gene expression to be regulated independently of temperature. For example, the Cape Verde

Islands accession of *Arabidopsis* is temperature insensitive due to a hyperactive gain-of-function allele of in *CRYPTOCHROME2* (*CRY2*) (Sanchez-Bermejo et al., 2015), which activates *FT* expression via interaction with CIB1, a blue-light mediated basic-helix-loop-helix (bHLH) transcription factor (Liu et al., 2013). Also, most studies into temperature-dependent regulation of *FT* are conducted in constant temperature conditions, rather than elevated temperatures relative to the ambient environment, which may introduce differences in diurnal regulation of *FT* genes, which already have been shown to be affected by standard light regimens within artificial conditions (Song et al., 2018). Given our results, we cannot determine how expression of *ZmaFT2* and *ZmaFT4* was unaffected by increased temperature. Nonetheless, we can conclude that *Z. marina* flowering includes another mechanism for incorporating temperature signals involving *ZmaFT9* regulation. We speculate that this may be the result of *Zostera*'s adaptation to an intertidal or subtidal environment, because intertidal *Z. marina* populations, such as those occupying the Northwestern coasts of the United States, must account for a highly variable thermal regime which includes both water and air temperatures, such as those described for the Willapa Bay population in Nolan et al. (Nolan et al., 2024). It is possible that having a repressor present at stages of vegetative growth, when flowering is not advantageous, more effectively prevents precocious flowering as a result from a temperature-sensitive flowering activator.

Natural variation in populations affects flowering response and related morphology

Beyond the difference in flowering morphology, development, and gene expression because of the +3°C treatment, we also observed differences on flowering traits that were attributed to natural variation between populations. Flowering shoot length was longer across both treatments in Padilla Bay shoots, and these produced overall more spathes than compared to Willapa (Figure 3d-e, Table S4). Lateral roots were longer in the Padilla Bay shoots as well (Figure 3h, Table S4). Also, Padilla Bay shoots showed overall lower expression of *ZmaFT9* compared to Willapa Bay (Figure 4e-f, Table S5). In fact, *ZmaFT9* expression in Willapa shoots is approximately double that of Padilla Bay. This variation is, in part, likely due to the presence of vegetative perennial seedlings in the Willapa Bay population, but also may indicate that the expected decrease in *ZmaFT9* was not captured in the Willapa Bay samples, since annual seedlings in early vegetative stages described in Nolan et al. (Nolan et al., 2024) had *ZmaFT9* expression at even higher levels than what was captured in our study. We attribute these different

overall amounts of expression to genetic differences between the populations, which could also account for the morphological phenotype differences we observed. Briones Ortiz et al. described genetic differences and population structure between Salish Sea and coastal populations in Washington (Briones Ortiz et al., 2025). These two population sites experience different thermal conditions, with overall higher and more variation in temperature experienced at Willapa Bay (Figure 2a), and local adaptation can contribute to differential responses to environmental stimuli (Lasky et al., 2014).

Plants in our study remained submerged throughout the experiment, and therefore we were unable to account for effects of tide or exposure to air and aerial temperatures. Temperatures in the mesocosms were lower than typically experienced by these intertidal populations in the field (Figure 2), limiting the conclusions that can be drawn about still higher temperatures, which might impair sexual reproduction. Further, it is possible that seedlings could have been compromised by transplant shock, so differences between treatments should be considered relative. Nonetheless, it is clear that temperature affects development and accelerates reproduction through genetic mechanisms, likely including *ZmaFT9* expression and function. Further study will be needed to evaluate the effects of heat on flowering abundance, since this was not testable in our annual system which have obligate flowering within one year, but we expect that flowering frequency of perennials could also increase with warming over this range, given that *ZmaFT9* expression was overall lower in the heated treatment.

Our findings present insight into how eelgrass populations may respond to warming temperatures predicted to occur in Washington state over the next 100 years (Khangaonkar et al., 2019; Mote & Salathé, 2010). The acceleration of sexual reproductive processes in eelgrass highlights potential ecological consequences, especially in areas where annual and perennials life history types coexist, and timing of reproductive events may begin to overlap. There is evidence of a mixed-annual life history type present at a well-studied perennial site at the southern limit of Atlantic *Z. marina*, possibly as a result of continued environmental stress (Jarvis et al., 2012). Ecological consequences may also arise from the increased frequency in marine heatwaves (Hobday et al., 2018), now accompanying the general increasing trends in both air and water temperatures. Collectively, this work highlights the need for continued investigation into

changing environmental conditions and their effects on reproduction and, ultimately, resiliency and persistence in eelgrass populations.

Implications

Globally, seagrasses are experiencing annual decline rates of greater than 7%, which threaten the persistence of coastal ecosystems and can have major ecological ramifications (Orth et al., 2006; Waycott et al., 2009) Seed dispersal and recruitment contributes to persistence and resiliency in seagrass populations (Kendrick et al., 2012), and understanding ecological consequences of warming trends for flowering and seed production are key knowledge gaps that, if addressed, would provide insight into how seagrass, like eelgrass, will survive and persist under a changing climate.

Seeds have shown promise as a tool for restoration of eelgrass populations (Jarvis et al., 2014; Kendrick et al., 2012; Marion & Orth, 2010; Orth et al., 2012, 2020; van Katwijk et al., 2016). However not all populations flower and produce seeds at equal rates, and flowering rates can be especially low in perennial populations (Ruesink et al., 2022). Our findings imply that warmer temperatures may ultimately increase seed production in populations, and that annuals may experience greater seed yield if inflorescences are pollinated earlier, and ultimately have a longer period of time to develop, produce and disperse seeds. Interestingly, this contrasts with the response of many terrestrial annual crops to warming, where earlier flowering led to lower seed yield (Bassu et al., 2021; Ullah et al., 2022). The warmed conditions in this experiment are evidently below the damaging levels for these *Z. marina* populations. We expect that further study on the viability of resulting seeds from shoots experiencing warmer temperatures will ultimately answer the question of whether increased temperature increases seed yield in eelgrass as well as implications of elevated temperature on seed-based restoration.

Acknowledgements: We would like to thank M. Garcia, H. Mawson, R. Wells and D. Nikitin for technical assistance, M. Scheuerell for analysis feedback, R. Skubel and C. Catton for project feedback and funding coordination, and K. A. Naish for manuscript feedback. We thank Shannon Point Marine Station and Western Washington University for use of mesocosm facilities, and Padilla Bay National Estuarine Research Reserve (PBNERR), K. Wiegardt (Jolly

Roger Oysters), and the Port of Peninsula for granting site access for seedling collections. This research was funded by Washington Department of Natural Resources interagency agreements (93-106455 to T. Imaizumi and 93-102512 to S. Yang), and U.S. Geological Survey Northwest Climate Science Adaptation Center award G17AC00218 to C. T. Nolan.

Conflict of Interest: No authors have any sources of conflict of interest.

Author Contributions: Authors C. T. Nolan, I. McBride, T. Imaizumi, J. L. Ruesink, S. Yang, and J. L. Gaeckle conceived the ideas and designed methodology; C. T. Nolan, I. McBride, N. Reid, and S. Yang collected the data; C. T. Nolan, S. Yang, I. McBride, and N. Reid analyzed the data; C. T. Nolan and S. Yang led the writing of the manuscript. All authors contributed critically to the drafts and gave final approval for publication.

Data availability statement:
All data and code are available on Dryad at the following link: 10.5061/dryad.612jm64hd

References:

Backman, T. W. H. (1991). Genotypic and phenotypic variability of Zostera marina on the west coast of North America. *Canadian Journal of Botany*, *69*(6), 1361–1371. https://doi.org/10.1139/b91-176

Balasubramanian, S., Sureshkumar, S., Lempe, J., & Weigel, D. (2006). Potent induction of *Arabidopsis thaliana* flowering by elevated growth temperature. *PLOS Genetics*, *2*(7), e106. https://doi.org/10.1371/journal.pgen.0020106

Bassu, S., Fumagalli, D., Toreti, A., Ceglar, A., Giunta, F., Motzo, R., Zajac, Z., & Niemeyer, S. (2021). Modelling potential maize yield with climate and crop conditions around flowering. *Field Crops Research*, *271*, 108226. https://doi.org/10.1016/j.fcr.2021.108226

Bennett, T., & Dixon, L. E. (2021). Asymmetric expansions of FT and TFL1 lineages characterize differential evolution of the EuPEBP family in the major angiosperm lineages. *BMC Biology*, *19*(1), 181. https://doi.org/10.1186/s12915-021-01128-8

Blázquez, M. A., Ahn, J. H., & Weigel, D. (2003). A thermosensory pathway controlling flowering time in *Arabidopsis thaliana*. *Nature Genetics*, *33*(2), Article 2. https://doi.org/10.1038/ng1085

Blok, S. E., Olesen, B., & Krause-Jensen, D. (2018). Life history events of eelgrass *Zostera marina L.* populations across gradients of latitude and temperature. *Marine Ecology Progress Series*, *590*, 79–93. https://doi.org/10.3354/meps12479

Breiter, A. L., Sokoloski, C. T., Yang, S., & Gaeckle, J. L. (2024). Effect of prolonged seawater warming on *Zostera marina* ecotypes of the northeast Pacific. *Journal of Experimental Marine Biology and Ecology*, *578*, 152036. https://doi.org/10.1016/j.jembe.2024.152036

Briones Ortiz, B. A., Boardman, F. C., Ruesink, J. L., & Naish, K. A. (2025). Adaptive genetic differentiation between spatially proximate annual and perennial life history types of a marine foundation species. *Molecular Ecology*, *n/a*(n/a), e17730. https://doi.org/10.1111/mec.17730

Craufurd, P. Q., & Wheeler, T. R. (2009). Climate change and the flowering time of annual crops. *Journal of Experimental Botany*, *60*(9), 2529–2539. https://doi.org/10.1093/jxb/erp196

De Cock, A. W. A. M. (1980). *Flowering biology of the seagrass* Zostera marina *L.*

de Montaigu, A., Tóth, R., & Coupland, G. (2010). Plant development goes like clockwork. *Trends in Genetics*, *26*(7), 296–306. https://doi.org/10.1016/j.tig.2010.04.003

Diaz-Almela, E., Marbà, N., & Duarte, C. M. (2007). Consequences of Mediterranean warming events in seagrass (*Posidonia oceanica*) flowering records. *Global Change Biology*, *13*(1), 224–235. https://doi.org/10.1111/j.1365-2486.2006.01260.x

DuBois, K., Pollard, K. N., Kauffman, B. J., Williams, S. L., & Stachowicz, J. J. (2022). Local adaptation in a marine foundation species: Implications for resilience to future global change. *Global Change Biology*, *28*(8), 2596–2610. https://doi.org/10.1111/gcb.16080

Gagnon, P. S., Vadas, R. L., Burdick, D. B., & May, B. (1980). Genetic identity of annual and perennial forms of *Zostera marina* L. *Aquatic Botany*, *8*, 157–162. https://doi.org/10.1016/0304-3770(80)90047-9

Hobday, A. J., Oliver, E. C. J., Gupta, A. S., Benthuysen, J. A., Burrows, M. T., Donat, M. G., Holbrook, N. J., Moore, P. J., Thomsen, M. S., Wernberg, T., & Smale, D. A. (2018). Categorizing and naming marine heatwaves. *Oceanography*, *31*(2), 162–173.

Intergovernmental Panel on Climate Change (IPCC) (Ed.). (2023). Future Global Climate: Scenario-based Projections and Near-term Information. In *Climate Change 2021 – The Physical Science Basis: Working Group I Contribution to the Sixth Assessment Report of the Intergovernmental Panel on Climate Change* (pp. 553–672). Cambridge University Press. https://doi.org/10.1017/9781009157896.006

Jarvis, J. C., Brush, M. J., & Moore, K. A. (2014). Modeling loss and recovery of *Zostera marina* beds in the Chesapeake Bay: The role of seedlings and seed-bank viability. *Aquatic Botany*, *113*, 32–45. https://doi.org/10.1016/j.aquabot.2013.10.010

Jarvis, J. C., & Moore, K. A. (2015). Effects of seed source, sediment type, and burial depth on mixed-annual and perennial *Zostera marina l.* seed germination and seedling establishment. *Estuaries and Coasts*, *38*(3), 964–978. https://doi.org/10.1007/s12237-014-9869-3

Jarvis, J. C., Moore, K. A., & Kenworthy, W. J. (2012). Characterization and ecological implication of -eelgrass life history strategies near the species' southern limit in the western North Atlantic. *Marine Ecology Progress Series*, *444*, 43–56. https://doi.org/10.3354/meps09428

Keddy, C. J., & Patriquin, D. G. (1978). An annual form of eelgrass in Nova Scotia. *Aquatic Botany*, *5*, 163–170. https://doi.org/10.1016/0304-3770(78)90059-1

Kendrick, G. A., Waycott, M., Carruthers, T. J. B., Cambridge, M. L., Hovey, R., Krauss, S. L., Lavery, P. S., Les, D. H., Lowe, R. J., Vidal, O. M. i, Ooi, J. L. S., Orth, R. J., Rivers, D. O., Ruiz-Montoya, L., Sinclair, E. A., Statton, J., van Dijk, J. K., & Verduin, J. J. (2012). The central role of dispersal in the maintenance and persistence of seagrass populations. *BioScience*, *62*(1), 56–65. https://doi.org/10.1525/bio.2012.62.1.10

Khangaonkar, T., Nugraha, A., Xu, W., & Balaguru, K. (2019). Salish sea response to global climate change, sea level rise, and future nutrient loads. *Journal of Geophysical Research: Oceans*, *124*(6), 3876–3904. https://doi.org/10.1029/2018JC014670

Kim, J. H., Kang, J. H., Jang, J. E., Choi, S. K., Kim, M. J., Park, S. R., & Lee, H. J. (2017). Population genetic structure of eelgrass (Zostera marina) on the Korean coast: Current status and conservation implications for future management. *PLOS ONE*, *12*(3), e0174105. https://doi.org/10.1371/journal.pone.0174105

Kim, S. H., Kim, J.-H., Park, S. R., & Lee, K.-S. (2014). Annual and perennial life history strategies of Zostera marina populations under different light regimes. *Marine Ecology Progress Series*, *509*, 1–13. https://doi.org/10.3354/meps10899

Kinmonth-Schultz, H. A., Tong, X., Lee, J., Song, Y. H., Ito, S., Kim, S.-H., & Imaizumi, T. (2016). Cool night-time temperatures induce the expression of *CONSTANS* and *FLOWERING LOCUS T* to regulate flowering in *Arabidopsis*. *New Phytologist*, *211*(1), 208–224. https://doi.org/10.1111/nph.13883

Lasky, J. R., Des Marais, D. L., Lowry, D. B., Povolotskaya, I., McKay, J. K., Richards, J. H., Keitt, T. H., & Juenger, T. E. (2014). Natural variation in abiotic stress responsive gene expression and local adaptation to climate in *Arabidopsis thaliana*. *Molecular Biology and Evolution*, *31*(9), 2283–2296. https://doi.org/10.1093/molbev/msu170

Lekammudiyanse, M. U., Saunders, M. I., Flint, N., Irving, A., Aiken, C., Clark, D. E., Berthelsen, A., Hindmarsh, B., Hooks, R., Connolly, R. M., Sievers, M., Rasheed, M. A., Smith, T. M., Glasby, T. M., Sherman, C. D. H., & Jackson, E. L. (2024). Environmental drivers of flowering in the genus Zostera and spatio-temporal variability of *Zostera*

muelleri flowering in Australasia. *Aquatic Conservation: Marine and Freshwater Ecosystems*, *34*(2), e4068. https://doi.org/10.1002/aqc.4068

Liu, Y., Li, X., Li, K., Liu, H., & Lin, C. (2013). Multiple bHLH proteins form heterodimers to mediate CRY2-dependent regulation of flowering-time in *Arabidopsis*. *PLOS Genetics*, *9*(10), e1003861. https://doi.org/10.1371/journal.pgen.1003861

Marín-Guirao, L., Entrambasaguas, L., Ruiz, J. M., & Procaccini, G. (2019). Heat-stress induced flowering can be a potential adaptive response to ocean warming for the iconic seagrass Posidonia oceanica. *Molecular Ecology*, *28*(10), 2486–2501. https://doi.org/10.1111/mec.15089

Marion, S. R., & Orth, R. J. (2010). Innovative techniques for large-scale seagrass restoration using *Zostera marina* (eelgrass) seeds. *Restoration Ecology*, *18*(4), 514–526. https://doi.org/10.1111/j.1526-100X.2010.00692.x

Meling-López, A. E., & Ibarra-Obando, S. E. (1999). Annual life cycles of two *Zostera marina* L. populations in the Gulf of California: Contrasts in seasonality and reproductive effort. *Aquatic Botany*, *65*(1), 59–69. https://doi.org/10.1016/S0304-3770(99)00031-5

Morita, T., Kakinuma, M., Mizuno, G., Okumura, I., Kokubu, H., Kurashima, A., & Maegawa, M. (2010). Morphological characteristics of annual *Zostera marina* shoots at various germination temperatures. *Aquatic Botany*, *92*(1), 49–54. https://doi.org/10.1016/j.aquabot.2009.10.001

Mote, P. W., & Salathé, E. P. (2010). Future climate in the Pacific Northwest. *Climatic Change*, *102*(1), 29–50. https://doi.org/10.1007/s10584-010-9848-z

Muñiz-Salazar, R., Talbot, S. L., Sage, G. K., Ward, D. H., & Cabello-Pasini, A. (2005). Population genetic structure of annual and perennial populations of Zostera marina L. along the Pacific coast of Baja California and the Gulf of California. *Molecular Ecology*, *14*(3), 711–722. https://doi.org/10.1111/j.1365-294X.2005.02454.x

Nagalla, A. D., Nishide, N., Hibara, K., & Izawa, T. (2021). High ambient temperatures inhibit Ghd7-mediated flowering repression in rice. *Plant and Cell Physiology*, *62*(11), 1745–1759. https://doi.org/10.1093/pcp/pcab129

Nelson, W. G., & Sullivan, G. (2018). Effects of microtopographic variation and macroalgal cover on morphometrics and survival of the annual form of eelgrass (*Zostera marina*). *Aquatic Botany*, *145*, 37–44. https://doi.org/10.1016/j.aquabot.2017.11.008

Nolan, C. T., Campbell, I., Farrell-Sherman, A., Ortiz, B. A. B., Naish, K. A., Stilio, V. D., Kaldy, J. E., Donoghue, C., Ruesink, J. L., & Imaizumi, T. (2024). Florigen and antiflorigen gene expression correlates with reproductive state in a marine angiosperm, Zostera marina. *bioRxiv*, 2024.11.09.622789. https://doi.org/10.1101/2024.11.09.622789

O'Brien, K. R., Waycott, M., Maxwell, P., Kendrick, G. A., Udy, J. W., Ferguson, A. J. P., Kilminster, K., Scanes, P., McKenzie, L. J., McMahon, K., Adams, M. P., Samper-Villarreal, J., Collier, C., Lyons, M., Mumby, P. J., Radke, L., Christianen, M. J. A., & Dennison, W. C. (2018). Seagrass ecosystem trajectory depends on the relative timescales of resistance, recovery and disturbance. *Marine Pollution Bulletin*, *134*, 166–176. https://doi.org/10.1016/j.marpolbul.2017.09.006

Orth, R. J., Carruthers, T. J. B., Dennison, W. C., Duarte, C. M., Fourqurean, J. W., Heck, K. L., Hughes, A. R., Kendrick, G. A., Kenworthy, W. J., Olyarnik, S., Short, F. T., Waycott, M., & Williams, S. L. (2006). A global crisis for seagrass ecosystems. *BioScience*, *56*(12), 987–996. https://doi.org/10.1641/0006-3568(2006)56[987:AGCFSE]2.0.CO;2

Orth, R. J., Lefcheck, J. S., McGlathery, K. S., Aoki, L., Luckenbach, M. W., Moore, K. A., Oreska, M. P. J., Snyder, R., Wilcox, D. J., & Lusk, B. (2020). Restoration of seagrass habitat leads to rapid recovery of coastal ecosystem services. *Science Advances*, *6*(41), eabc6434. https://doi.org/10.1126/sciadv.abc6434

Orth, R. J., Moore, K. A., Marion, S. R., Wilcox, D. J., & Parrish, D. B. (2012). Seed addition facilitates eelgrass recovery in a coastal bay system. *Marine Ecology Progress Series*, *448*, 177–195. https://doi.org/10.3354/meps09522

Phillips, R. C., Stewart Grant, W., & Peter McRoy, C. (1983). Reproductive strategies of eelgrass (*Zostera marina* L.). *Aquatic Botany*, *16*(1), 1–20. https://doi.org/10.1016/0304-3770(83)90047-5

Pin, P. A., & Nilsson, O. (2012). The multifaceted roles of FLOWERING LOCUS T in plant development. *Plant, Cell & Environment*, *35*(10), 1742–1755. https://doi.org/10.1111/j.1365-3040.2012.02558.x

Qin, L.-Z., Kim, S. H., Song, H.-J., Suonan, Z., Kim, H., Kwon, O., & Lee, K.-S. (2020). Influence of regional water temperature variability on the flowering phenology and sexual reproduction of the seagrass *Zostera marina* in Korean coastal waters. *Estuaries and Coasts*, *43*(3), 449–462. https://doi.org/10.1007/s12237-019-00569-3

R Core Team. (2021). *R: A language and environment for statistical computing [Computer software]* (zis-RCoreTeam.2021R).

R Core Team. (2024). *A language and environment for statistical computing_* [Computer software]. R Foundation for Statistical Computing.

Ransbotyn, V., & Reusch, T. B. H. (2006). Housekeeping gene selection for quantitative real-time PCR assays in the seagrass *Zostera marina* subjected to heat stress. *Limnology and Oceanography: Methods*, *4*(10), 367–373. https://doi.org/10.4319/lom.2006.4.367

Ritz, C., Baty, F., Streibig, J. C., & Gerhard, D. (2015). Dose-response analysis using R. *PLOS ONE*, *10*(12), e0146021. https://doi.org/10.1371/journal.pone.0146021

Ruesink, J. L., Ortiz, B. A. B., Mawson, C. H., & Boardman, F. C. (2022). Tradeoffs in life history investment of eelgrass *Zostera marina* across estuarine intertidal conditions. *Marine Ecology Progress Series*, *686*, 61–70. https://doi.org/10.3354/meps14000

Sanchez-Bermejo, E., Zhu, W., Tasset, C., Eimer, H., Sureshkumar, S., Singh, R., Sundaramoorthi, V., Colling, L., & Balasubramanian, S. (2015). Genetic architecture of natural variation in thermal responses of *Arabidopsis*. *Plant Physiology*, *169*(1), 647–659. https://doi.org/10.1104/pp.15.00942

Sawall, Y., Ito, M., & Pansch, C. (2021). Chronically elevated sea surface temperatures revealed high susceptibility of the eelgrass Zostera marina to winter and spring warming. *Limnology and Oceanography*, *66*(12), 4112–4124. https://doi.org/10.1002/lno.11947

Searle, S. R., Speed, F. M., & Milliken, G. A. (1980). Population marginal means in the linear model: An alternative to least squares means. *The American Statistician*. https://www.tandfonline.com/doi/abs/10.1080/00031305.1980.10483031

Song, Y. H., Kubota, A., Kwon, M. S., Covington, M. F., Lee, N., Taagen, E. R., Laboy Cintrón, D., Hwang, D. Y., Akiyama, R., Hodge, S. K., Huang, H., Nguyen, N. H., Nusinow, D. A., Millar, A. J., Shimizu, K. K., & Imaizumi, T. (2018). Molecular basis of flowering under natural long-day conditions in *Arabidopsis*. *Nature Plants*, *4*(10), Article 10. https://doi.org/10.1038/s41477-018-0253-3

Susila, H., Jurić, S., Liu, L., Gawarecka, K., Chung, K. S., Jin, S., Kim, S.-J., Nasim, Z., Youn, G., Suh, M. C., Yu, H., & Ahn, J. H. (2021). Florigen sequestration in cellular

membranes modulates temperature-responsive flowering. *Science*, *373*(6559), 1137–1142. https://doi.org/10.1126/science.abh4054

Thom, R. M., Borde, A. B., Rumrill, S., Woodruff, D. L., Williams, G. D., Southard, J. A., & Sargeant, S. L. (2003). Factors influencing spatial and annual variability in eelgrass (*Zostera marina* L.) meadows in Willapa Bay, Washington, and Coos Bay, Oregon, estuaries. *Estuaries*, *26*(4), 1117–1129. https://doi.org/10.1007/BF02803368

Ullah, A., Nadeem, F., Nawaz, A., Siddique, K. H. M., & Farooq, M. (2022). Heat stress effects on the reproductive physiology and yield of wheat. *Journal of Agronomy and Crop Science*, *208*(1), 1–17. https://doi.org/10.1111/jac.12572

van Katwijk, M. M., Thorhaug, A., Marbà, N., Orth, R. J., Duarte, C. M., Kendrick, G. A., Althuizen, I. H. J., Balestri, E., Bernard, G., Cambridge, M. L., Cunha, A., Durance, C., Giesen, W., Han, Q., Hosokawa, S., Kiswara, W., Komatsu, T., Lardicci, C., Lee, K.-S., … Verduin, J. J. (2016). Global analysis of seagrass restoration: The importance of large-scale planting. *Journal of Applied Ecology*, *53*(2), 567–578. https://doi.org/10.1111/1365-2664.12562

van Katwijk, M. M., & van Tussenbroek, B. I. (2023). Facultative annual life cycles in seagrasses. *Plants*, *12*(10), Article 10. https://doi.org/10.3390/plants12102002

van Lent, F., & Verschuure, J. M. (1994). Intraspecific variability of *Zostera marina* L. (eelgrass) in the estuaries and lagoons of the southwestern Netherlands. I. Population dynamics. *Aquatic Botany*, *48*(1), 31–58. https://doi.org/10.1016/0304-3770(94)90072-8

Waycott, M., Duarte, C. M., Carruthers, T. J. B., Orth, R. J., Dennison, W. C., Olyarnik, S., Calladine, A., Fourqurean, J. W., Heck, K. L., Hughes, A. R., Kendrick, G. A., Kenworthy, W. J., Short, F. T., & Williams, S. L. (2009). Accelerating loss of seagrasses across the globe threatens coastal ecosystems. *Proceedings of the National Academy of Sciences*, *106*(30), 12377–12381. https://doi.org/10.1073/pnas.0905620106

Wickland, D. P., & Hanzawa, Y. (2015). The *FLOWERING LOCUS T/TERMINAL FLOWER 1* gene family: Functional evolution and molecular mechanisms. *Molecular Plant*, *8*(7), 983–997. https://doi.org/10.1016/j.molp.2015.01.007

Wood, S. N. (2011). Fast stable restricted maximum likelihood and marginal likelihood estimation of semiparametric generalized linear models. *Journal of the Royal Statistical Society Series B: Statistical Methodology*, *73*(1), 3–36. https://doi.org/10.1111/j.1467-9868.2010.00749.x

Yoshida, A., Taoka, K., Hosaka, A., Tanaka, K., Kobayashi, H., Muranaka, T., Toyooka, K., Oyama, T., & Tsuji, H. (2021). Characterization of frond and flower development and identification of FT and FD genes from duckweed *Lemna aequinoctialis* Nd. *Frontiers in Plant Science*, *12*, 697206. https://doi.org/10.3389/fpls.2021.697206

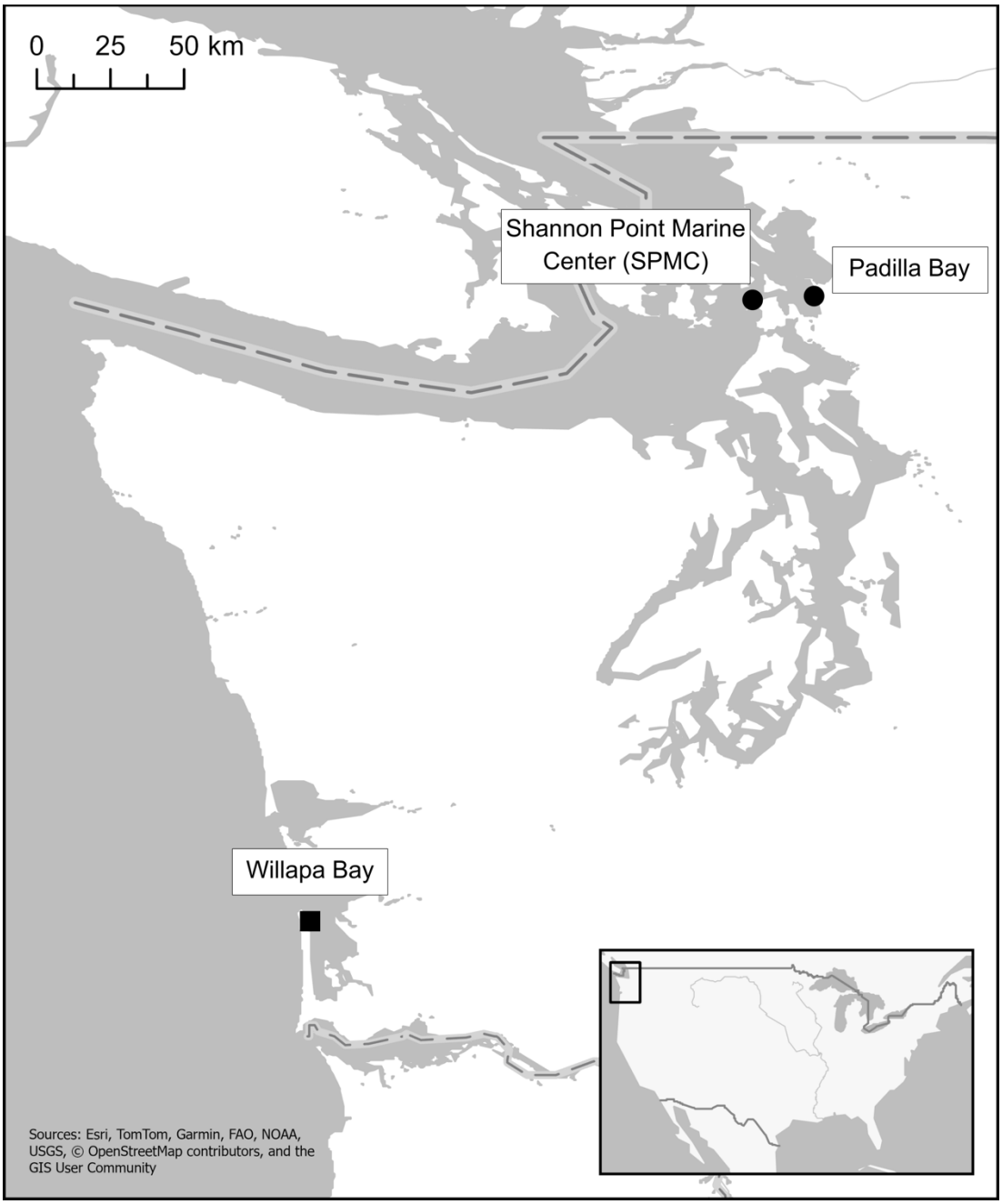

Figure 1: Map of source populations used in study (Willapa Bay, square, and Padilla Bay, circle). Mesocosm facility also shown (Shannon Point Marine Center, circle).

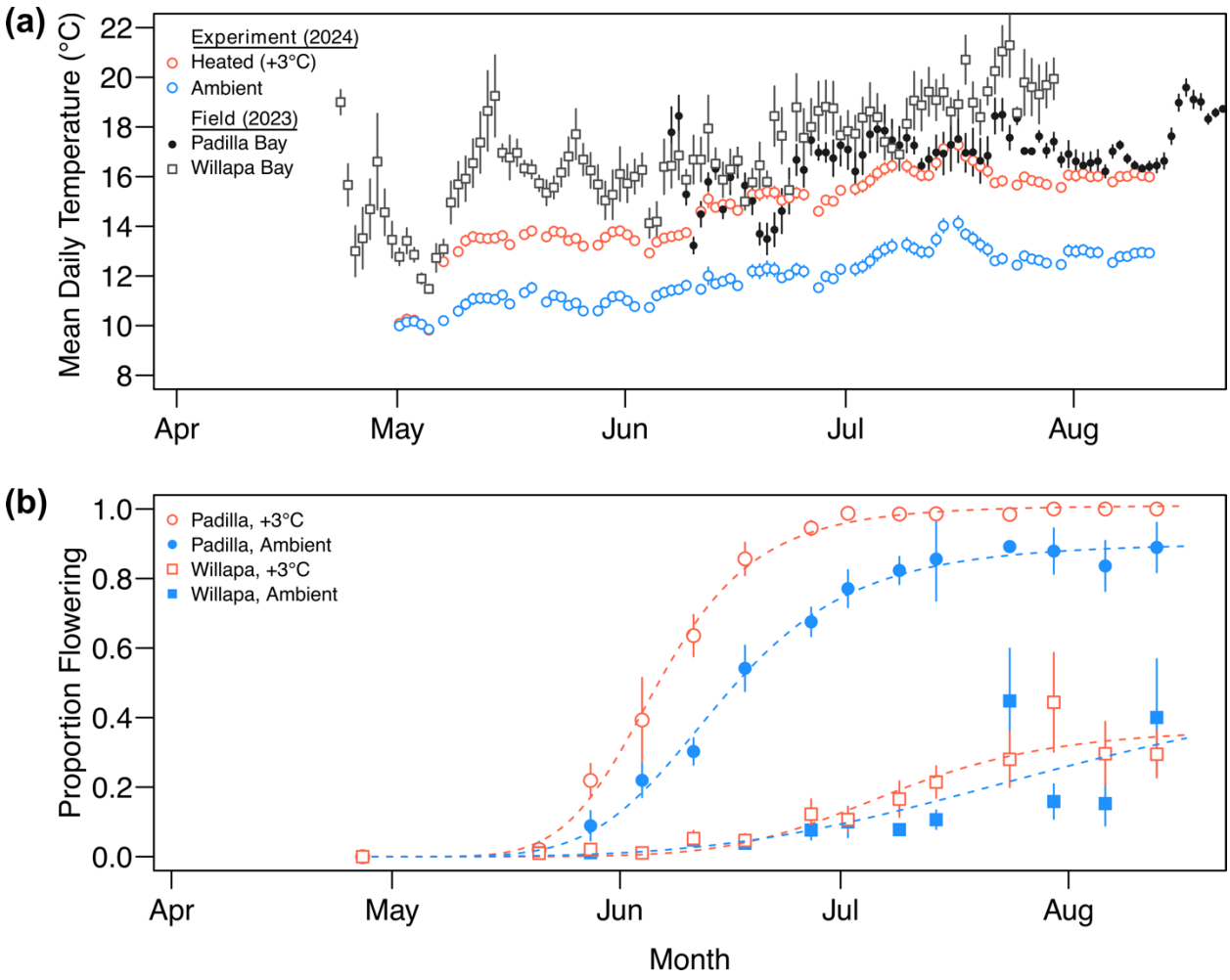

Figure 2: Temperature regimes and flowering proportion in mesocosm set-up. a) Mean daily temperatures (mean ± s.e.) at each field collection site in 2023 and in the experimental tanks over the duration of the common garden experiment in 2024. Field sites are intertidal, so temperatures are a combination of water and air temperatures. b) Proportion of seedlings flowering over the duration of the experiment. Dashed lines show log-logistic model fit for each combination of population (Willapa or Padilla Bay) and temperature treatment (+3°C or ambient).

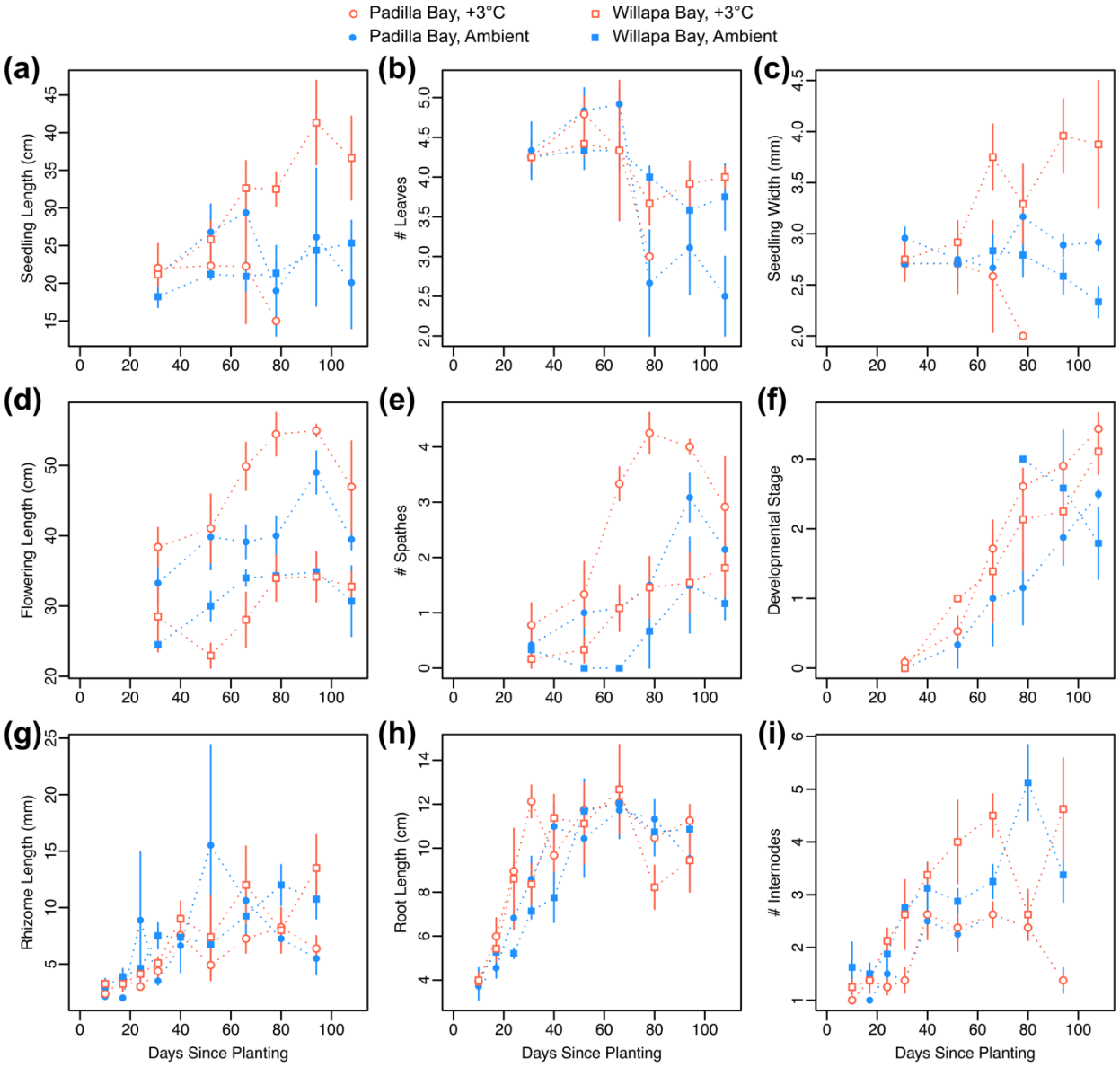

Figure 3: Mean above-ground seedling morphology prior to flowering (a-c): non-flowering seedling length, number of leaves, leaf width; and for shoots with flowers (d-f): flowering shoot length, mean number of spathes per flowering shoot, mean developmental stage of spathes per flowering shoot. Mean below-ground seedling morphology (g-i): rhizome length, root length, and number of rhizome internodes. For below-ground measurements, flowering and non-flowering seedlings are combined. All seedlings were planted on 2024-04-26. Symbology: Padilla Bay (circle); WB = Willapa Bay (square); H = heated (open, red); A = ambient (filled, blue).

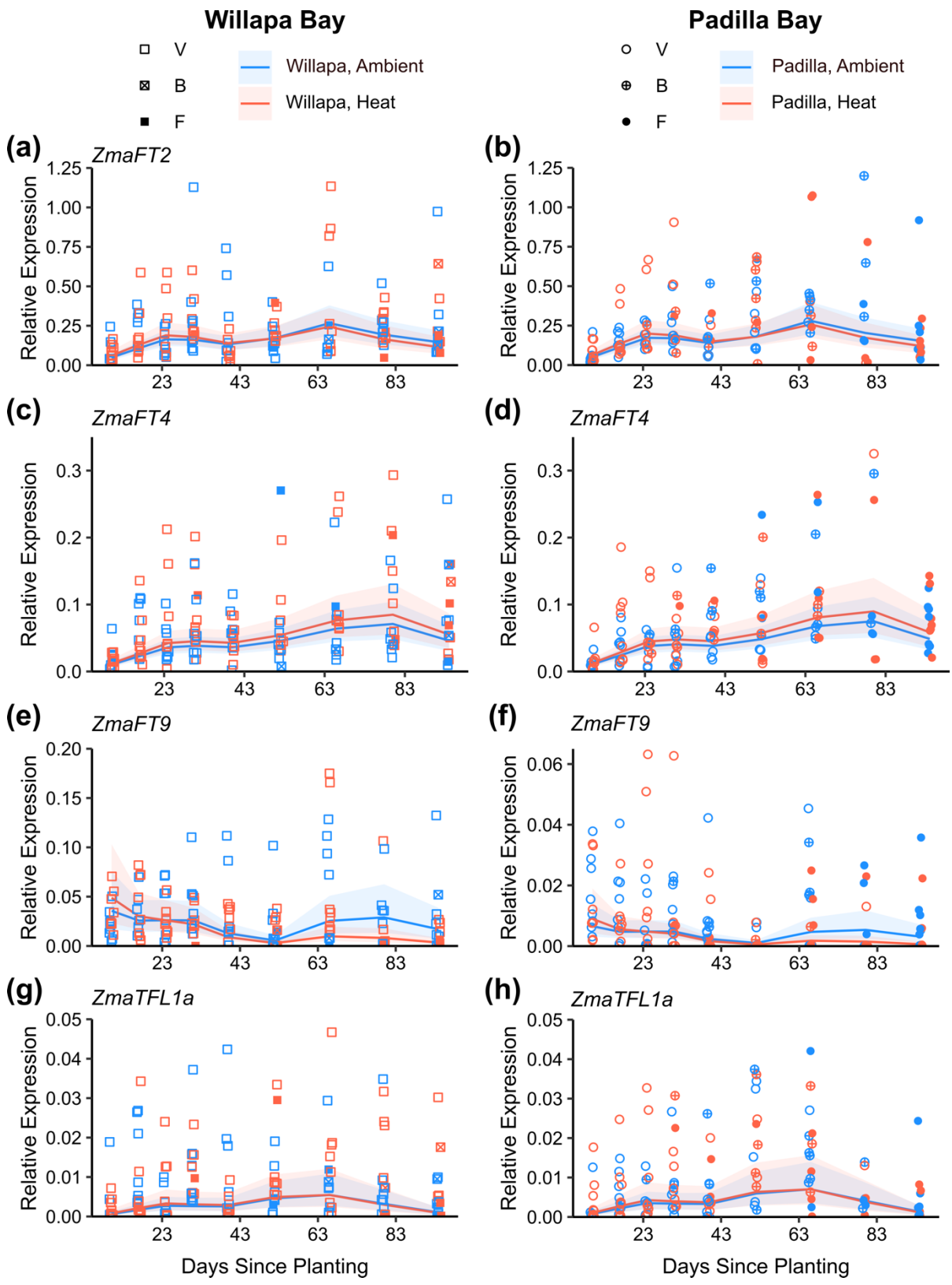

Figure 4: Relative expression of *ZmaFT2* (a, b), *ZmaFT4* (c, d), *ZmaFT9* (e, f), and *ZmaTFL1a* (g, h) genes in leaf tissue during annual growing season (May-July, shown as days since

planting, which took place 2024-04-26) from both populations (Willapa, square, left; Padilla, circle right) within the mesocosm, plotted with predicted expression trends based on general additive mixed effect model (GAMM). Blue lines represent ambient treated samples, and red lines indicate +3°C treated samples, and the respective ribbons indicate confidence interval. Point shape represents the development state at the time of collection; vegetative (V), bolted (B), flowering (F). Data points above respective axis limits not shown to better visualize model fit, but included in model analysis (*ZmaFT2*, 1.25; *ZmaFT4*, 0.35; *ZmaFT9*, 0.2 for WB and 0.065 for PB; and *ZmaTFL1a*, 0.5). All expression values are relative to 3 reference genes (*CYP2*, *ELF4A*, and *RPL28*).

Supplemental Information

Table S1: GPS coordinates and tidal elevation of study sites
Table S2: qPCR primers used in this study for gene expression analysis
Table S3: Log-logistic model parameter estimates for time to reach 50% (a) and pairwise comparisons (b)
Table S4: Results from mixed-effects ANOVA tests for morphological measurements
Table S5: Generalized additive model (GAM) results with gene expression values as response variable and temperature treatment (Ambient or +3°C Heated) and population (Willapa Bay, WB, and Padilla Bay, PB) as main effects.

Figure S1: Developmental stage of spathes in each temperature treatment and population over the duration of the experiment
Figure S2: Relative expression of *ZmaFT2*, *ZmaFT4*, *ZmaFT9*, and *ZmaTFL1a* genes in leaf tissue during annual growing season

Table S1: GPS coordinates and tidal elevation of study sites.

Site	Abbreviation	Position (°N, °W)	Tidal Elevation (m MLLW)
Stackpole Annual, Willapa Bay WA USA	WB	46.613, 124.034	1.1 ± 0.1
Joe Leary Annual, Padilla Bay WA USA	PB	48.520, 122.495	0.3
Shannon Point Marine Center, Anacortes WA USA (mesocosm facility)	SPMC	48.508, 122.683	NA

Table S2: qPCR primers used in this study for gene expression analysis (Nolan et al., 2024; Ransbotyn & Reusch, 2006)

Name	Accession No.	Forward 5'-3'	Reverse 5'-3'	Reference
ZmaFT2	Zosma01g14870	ACACAATGCTCATGGTAGATCCT	AGCACAAACACGAAACGGTG	Nolan et al.
ZmaFT4	Zosma04g08400	TGCACTGGTTGGTGGTGAA	AGCCGACTAGGTTGACGGAA	Nolan et al.
ZmaFT9	Zosma01g13540	TTCCTACACACTGGTTATGGTCG	GATGGATGGTTGTGGGCTCT	Nolan et al.
ZmaTFL1a	Zosma04g17290	TGTTCACTGGATTGTGACAGA	CCAGTGCAAATCGACGTGTG	Nolan et al.
ZmaCyp2	Zosma05g32090	CACTCCACTACAAGGGATCGAAA	GGACCTGTATGCTTCTTAACGAAGT	Ransbotyn and Reusch
Zmaelf4a	Zosma03g02900	TCTTTCTGCGATGCGAACAG	TGGATGTATCGGCAGAAACG	Ransbotyn and Reusch
ZmaRPL28	Zosma04g25970	TTCCGCACCTAGGGTTTCG	ATATTGGCGCAGCGATTTTG	Ransbotyn and Reusch

Table S3: a) Log-logistic model parameter estimates for time to reach 50% flowering (parameter *e*), fraction of seedlings that flowered (parameter *d*), and flowering synchronicity (parameter *b*), by each population in heated versus ambient conditions. b) Pairwise comparisons of parameter estimates for each treatment-population combination.

a)

Parameter	Site	Treatment	Estimate	Std. Error	t-value	p-value
b	PB	ambient	-5.402	0.864	-6.251	0.00
b	PB	heated	-6.027	0.854	-7.055	0.00
b	WB	ambient	-3.742	2.569	-1.457	0.15
b	WB	heated	-6.378	3.113	-2.049	0.04
d	PB	ambient	0.903	0.036	25.417	0.00
d	PB	heated	1.010	0.025	40.305	0.00
d	WB	ambient	0.552	0.651	0.848	0.40
d	WB	heated	0.371	0.071	5.238	0.00
e	PB	ambient	48.861	1.603	30.480	0.00
e	PB	heated	40.365	1.069	37.754	0.00
e	WB	ambient	98.948	63.099	1.568	0.12
e	WB	heated	72.207	6.182	11.680	0.00

b)

Comparison for parameter *d*				
Ratio	**Estimate**	**Std. Error**	**t-value**	**p-value**
PB ambient/PB heated	0.89	0.04	-2.56	0.01
WB ambient/WB heated	1.49	1.78	0.27	0.78
PB ambient/WB ambient	1.64	1.93	0.33	0.74
PB heated/WB heated	2.72	0.52	3.29	0.00
PB ambient/WB heated	2.43	0.47	3.02	<0.01
WB ambient/PB heated	0.55	0.64	-0.70	0.48
Comparison for parameter *e*				
Ratio	**Estimate**	**Std. Error**	**t-value**	**p-value**
PB ambient/PB heated	1.21	0.05	4.12	<0.01
WB ambient/WB heated	1.37	0.88	0.42	0.67
PB ambient/WB ambient	0.49	0.32	-1.61	0.11
PB heated/WB heated	0.56	0.05	-8.80	<0.01
PB ambient/WB heated	0.68	0.06	-5.21	<0.01
WB ambient/PB heated	2.45	1.56	0.93	0.35
Comparison for parameter *b*				
Ratio	**Estimate**	**Std. Error**	**t-value**	**p-value**
PB ambient/PB heated	0.90	0.19	-0.54	0.59
WB ambient/WB heated	0.59	0.49	-0.84	0.40
PB ambient/WB ambient	1.44	1.02	0.44	0.66
PB heated/WB heated	0.94	0.48	-0.11	0.91
PB ambient/WB heated	0.85	0.44	-0.35	0.73
WB ambient/PB heated	0.62	0.44	-0.87	0.39

Table S4: Results from mixed-effects ANOVA tests for morphological measurements, with temperature treatment ('trt'), site, census date ('days'), and their interactions as explanatory variables, and with tank replicate as a random effect (repeated measures). Relevant post-hoc pairwise comparisons are shown with p-values adjusted using the Bonferroni correction.

Non-flowering seedling: Shoot Length (cm)

Error: tank

	Df	Sum Sq.	Mean Sq.	F value	Pr(>F)
trt	1	543.1	543.1	5.16	0.0528
site	1	151.4	151.4	1.438	0.2647
days	4	953.8	238.4	2.266	0.151
trt:site	1	506.4	506.4	4.812	0.0596
Residuals	8	841.9	105.2		

Error: Within

	Df	Sum Sq.	Mean Sq.	F value	Pr(>F)
days	5	884	176.79	5.809	0.00032
trt:days	5	285.7	57.13	1.877	0.11722
site:days	5	62.5	12.5	0.411	0.83871
trt:site:days	3	121.8	40.61	1.334	0.27504
Residuals	45	1369.4	30.43		

Non-flowering seedling: Number of leaves

Error: tank

	Df	Sum Sq.	Mean Sq.	F value	Pr(>F)
trt	1	0.485	0.4848	1.148	0.315
site	1	0.13	0.1305	0.309	0.594
days	4	7.769	1.9421	4.597	0.032
trt:site	1	0.085	0.0847	0.2	0.666
Residuals	8	3.38	0.4225		

Error: Within

	Df	Sum Sq.	Mean Sq.	F value	Pr(>F)
days	5	11.522	2.3043	6.178	0.000194
trt:days	5	1.604	0.3207	0.86	0.515354
site:days	5	3.631	0.7263	1.947	0.105171
trt:site:days	3	0.705	0.2351	0.63	0.599202
Residuals	45	16.784	0.373		

Non-flowering seedling: Leaf Width (mm)

Error: tank

	Df	Sum Sq.	Mean Sq.	F value	Pr(>F)
trt	1	3.246	3.246	5.071	0.0544
site	1	1.005	1.005	1.57	0.2456
days	4	4.522	1.131	1.766	0.2288
trt:site	1	1.714	1.714	2.678	0.1404
Residuals	8	5.122	0.64		

Error: Within

	Df	Sum Sq.	Mean Sq.	F value	Pr(>F)
days	5	1.169	0.2339	1.066	0.3915
trt:days	5	3.22	0.644	2.937	0.0223
site:days	5	1.7	0.3399	1.55	0.1937
trt:site:days	3	0.73	0.2432	1.109	0.3554
Residuals	45	9.869	0.2193		

Post-hoc test by treatment (A=ambient, H=heated)

Days	H-A	df	statistic	p	p.adjusted
31	-0.1	67	0.369	0.713	0.713
52	0.08	67	-0.295	0.769	0.769
66	0.5	67	-1.71	0.0915	0.0915

78	0.12	67	-0.341	0.734	0.734
94	1.24	67	-3.52	0.000789	<0.001
108	1.35	67	-3.7	0.00044	<0.001

Flowering seedling: Flowering shoot length (cm)

Error: tank

	Df	Sum Sq.	Mean Sq.	F value	Pr(>F)
trt	1	148	148	1.009	0.34449
site	**1**	**3637**	**3637**	**24.871**	**0.00107**
days	2	145	73	0.497	0.6262
trt:site	1	436	436	2.98	0.12258
trt:days	1	59	59	0.402	0.54356
site:days	1	8	8	0.058	0.81562
Residuals	8	1170	146		

Error: Within

	Df	Sum Sq.	Mean Sq.	F value	Pr(>F)
days	5	1377.7	275.55	9.055	<<0.0001
trt:days	5	209.8	41.96	1.379	0.247
site:days	5	140.2	28.04	0.922	0.475
trt:site:days	5	115.4	23.08	0.758	0.584
Residuals	52	1582.4	30.43		

Post-hoc test by site (PB=Padilla, WB=Willapa)

PB-WB	df	statistic	p	p.adjusted
12.75	86	7.48	<<0.0001	<<0.0001

Flowering seedling: Number of spathes

Error: tank

	Df	Sum Sq.	Mean Sq.	F value	Pr(>F)
trt	**1**	**15.04**	**15.04**	**6.732**	**0.0357**
site	**1**	**35.34**	**35.34**	**15.816**	**0.00535**
days	3	3.64	1.21	0.542	0.66851
trt:site	1	3.07	3.07	1.373	0.27959
trt:days	1	1.92	1.92	0.86	0.3846
site:days	1	1.39	1.39	0.624	0.45544
Residuals	7	15.64	2.23		

Error: Within

	Df	Sum Sq.	Mean Sq.	F value	Pr(>F)
days	5	50.91	10.183	14.42	<<0.0001
trt:days	5	8.42	1.684	2.385	0.0509
site:days	5	5.91	1.182	1.673	0.1579
trt:site:days	5	2.76	0.551	0.781	0.5683
Residuals	51	36.01	0.706		

Post-hoc test by site (PB=Padilla, WB=Willapa)

PB-WB	df	statistic	p	p.adjusted
1.2	85	4.33	<<0.0001	<<0.0001

Post-hoc test by treatment (A=ambient, H=heated)

H-A	df	statistic	p	p.adjusted
0.8	85	-2.78	0.00662	0.00662

Flowering seedling: Mean developmental stage of spathes (final timepoint only)

	Df	Sum Sq.	Mean Sq.	F value	Pr(>F)
trt	**1**	**21.42**	**21.417**	**16.225**	**0.000108**
site	**1**	**8.07**	**8.073**	**6.116**	**0.015031**
trt:site	1	0.06	0.063	0.048	0.827732
Residuals	103	135.96	1.32		

Post-hoc test by treatment (A=ambient, H=heated)

H-A	df	statistic	p	p.adjusted
0.9	105	-3.95	0.000142	0.000142

Post-hoc test by site (PB=Padilla, WB=Willapa)

PB-WB	df	statistic	p	p.adjusted
0.4	105	1.56	0.121	0.121

Seedling rhizome length (mm, includes both flowering and non-flowering)

Error: tank

	Df	Sum Sq.	Mean Sq.	F value	Pr(>F)
trt	1	21.1	21.12	0.513	0.487
site	1	48.8	48.83	1.186	0.297
trt:site	1	24.4	24.38	0.592	0.456
Residuals	12	493.8	41.15		

Error: Within

	Df	Sum Sq.	Mean Sq.	F value	Pr(>F)
days	8	921.5	115.19	5.599	<<0.0001
trt:days	8	150.7	18.83	0.916	0.507
site:days	8	218.1	27.26	1.325	0.24
trt:site:days	8	214	26.75	1.301	0.253
Residuals	96	1974.9	20.57		

Seedling root length (cm, includes both flowering and non-flowering)

Error: tank

	Df	Sum Sq.	Mean Sq.	F value	Pr(>F)
trt	1	0.21	0.21	0.752	0.403
site	**1**	**42.79**	**42.79**	**153.099**	**<<0.001**
trt:site	1	0.04	0.04	0.155	0.7
Residuals	12	3.35	0.28		

Error: Within

	Df	Sum Sq.	Mean Sq.	F value	Pr(>F)
days	8	80.09	10.012	16.512	<<0.001
trt:days	**8**	**11.09**	**1.386**	**2.286**	**0.02763**
site:days	**8**	**16.44**	**2.055**	**3.389**	**0.00181**
trt:site:days	**8**	**11**	**1.375**	**2.268**	**0.02879**
Residuals	96	58.21	0.606		

Post-hoc tests by trt:days:

Trt	Days	WB-PB	df	Statistic	p	p.adj
A	10	0.625	108	-1.17	0.24	0.24
A	17	0.5	108	-0.94	0.35	0.35
A	24	0.375	108	-0.70	0.48	0.48
A	31	1.375	108	-2.58	0.01	**0.01**
A	40	0.625	108	-1.17	0.24	0.24
A	52	0.625	108	-1.17	0.24	0.24
A	66	0.625	108	-1.17	0.24	0.24
A	80	2.75	108	-5.15	0.00	**<0.01**
A	94	2	108	-3.75	0.00	**<0.01**
H	10	0.25	108	-0.47	0.64	0.64
H	17	0	108	0.00	1.00	1.00
H	24	0.875	108	-1.64	0.10	0.10
H	31	1.25	108	-2.34	0.02	0.02
H	40	0.75	108	-1.40	0.16	0.16
H	52	1.625	108	-3.04	0.00	**<0.01**
H	66	1.875	108	-3.51	0.00	**<0.01**
H	80	0.25	108	-0.47	0.64	0.64
H	94	3.25	108	-6.09	0.00	**<0.01**

Post-hoc test by site:days:

Site	Days	H-A	df	Statistic	p	p.adj
PB	10	0	108	0.00	1.00	1.00
PB	17	0.375	108	-0.70	0.48	0.48
PB	24	-0.25	108	0.47	0.64	0.64
PB	31	0	108	0.00	1.00	1.00
PB	40	0.125	108	-0.23	0.82	0.82
PB	52	0.125	108	-0.23	0.82	0.82

PB	66	0	108	0.00	1.00	1.00
PB	80	0	108	0.00	1.00	1.00
PB	94	0	108	0.00	1.00	1.00
WB	10	-0.375	108	0.70	0.48	0.48
WB	17	-0.125	108	0.23	0.82	0.82
WB	24	0.25	108	-0.47	0.64	0.64
WB	31	-0.125	108	0.23	0.82	0.82
WB	40	0.25	108	-0.47	0.64	0.64
WB	52	1.125	108	-2.11	0.04	**0.04**
WB	66	1.25	108	-2.34	0.02	**0.02**
WB	80	-2.5	108	4.68	0.00	**<0.01**
WB	94	1.25	108	-2.34	0.02	**0.02**

Initial number of internodes (Day 10)

	Df	Sum Sq.	Mean Sq.	F value	Pr(>F)
site	1	0.7656	0.7656	3.128	0.102
trt	1	0.1406	0.1406	0.574	0.463
site:trt	1	0.1406	0.1406	0.574	0.463
Residuals	12	2.9375	0.2448		

Final number of internodes (Day 94)

	Df	Sum Sq.	Mean Sq.	F value	Pr(>F)
site	**1**	**27.563**	**27.563**	**21.69**	**0.000554**
trt	1	1.562	1.562	1.23	0.289231
site:trt	1	1.562	1.562	1.23	0.289231
Residuals	12	15.25	1.271		

Post-hoc test by site (PB=Padilla, WB=Willapa)

PB-WB	df	statistic	p	p.adjusted
-2.6	14	-4.58	0.000426	0.000426

Table S5: Generalized additive model (GAM) results with gene expression values as response variable and temperature treatment (Ambient or +3°C Heated) and population (Willapa Bay, WB, and Padilla Bay, PB) as main effects. Estimate is shown for main effects with standard error in parentheses. Date was included as a global thin-plate regression spline (TP) smooth term. The interaction between date and treatment was included as a random factor smooth interactions term (FS). Tank number was included as a random effect smooth term (RE). Expression values were log10 transformed to fit assumptions of model.

	ZmaFT2	***ZmaFT4***	***ZmaFT9***	***ZmaTFL1a***
Intercept	-1.830 (0.090) t = -16.758 p = <2e-16	-3.180 (0.110) t = -28.922 p = <2e-16	-3.909 (0.196) t = -19.937 p = <2e-16	-5.755 (0.223) t = -28.838 p = <2e-16
Temperature (Ambient:Heated)	0.028 (0.136) t = 0.204 p = 0.838	0.169 (0.137) t = 1.230 p = 0.220	-0.484 (0.227) t = -2.134 p = 0.0337	0.0967 (0.283) t = 0.342 p =0.733
Population (WB:PB)	0.052 (0.105) t = 0.502 p = 0.616	0.056 (0.104) t = 0.536 p = 0.592	-1.691 (0.227) t = -7.445 p =1.32e-12	0.252 (0.197) t = 1.279 p = 0.202
Date (TP smoother term)	edf = 5.158 F = 11.624 p = <2e-16	edf = 5.158 F = 13.833 p =<2e-16	edf = 5.158 F = 4.090 p = 6.18e-04	edf = 5.158 F = 7.703 p = 2.48e-07
Date:Ambient (FS smooth term)	edf = 0.0002 F = 0.001 p = 1.0	edf = 1.000 F = 0.005 p = 0.944	edf = 3.767e-05 F = 0 p = 0.5	edf = 5.017e-05 F = 0.008 p = 0.999
Date:Heat (FS smooth term)	edf = 1.0002 F = 2.076 p =0.151	edf = 0.000 F = 0.011 p = 0.999	edf = 1.000 F = 7.435 p = 0.0068	edf = 1.001 F = 0.425 p = 0.5152
Tank (RE smooth term)	edf = 2.556 F = 0.747 p = 0.108	edf = 2.581 F = 0.763 p = 0.103	edf = 3.273e-04 F = 0 p = 0.914	edf = 3.111 F = 1.071 p = 0.0564

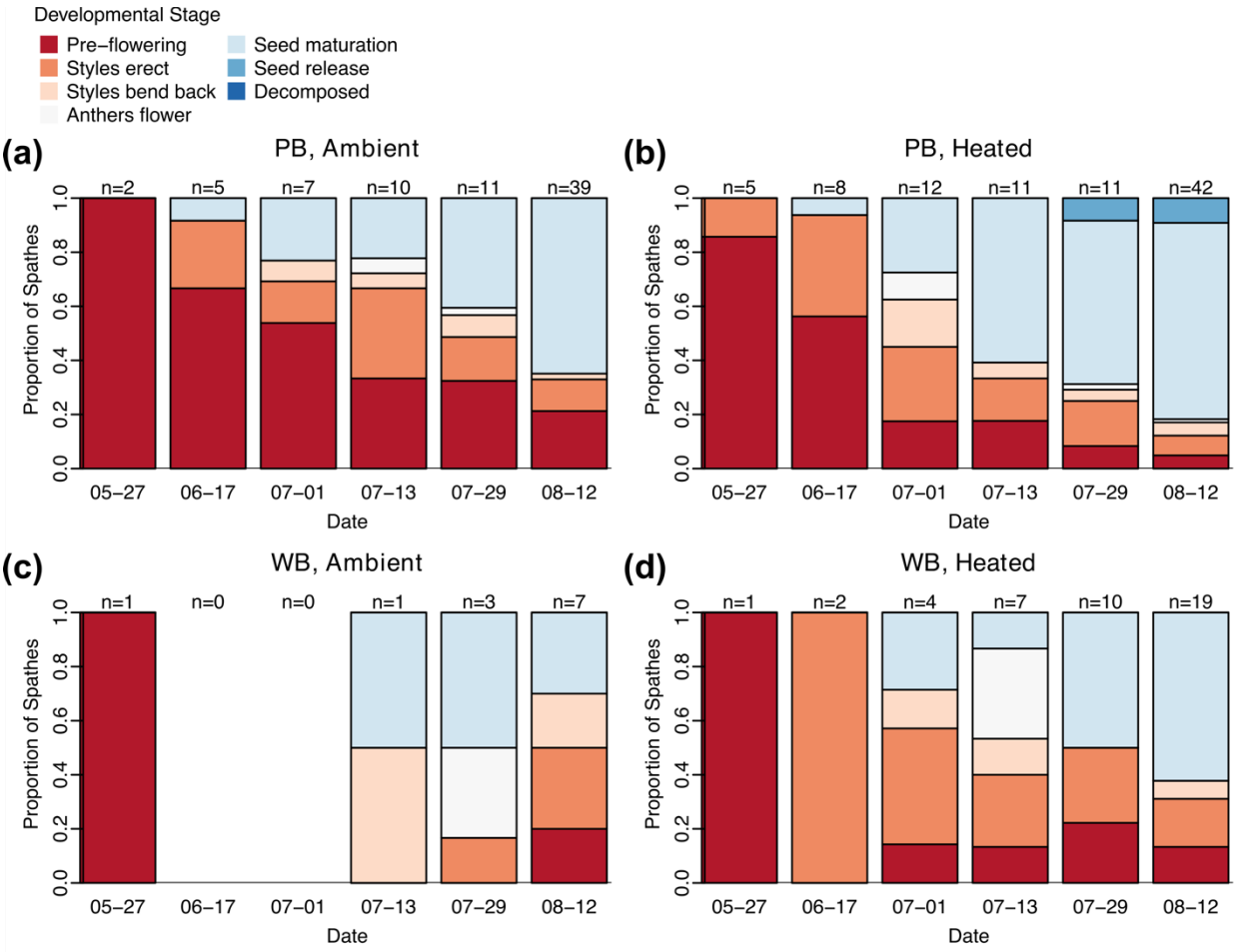

Figure S1: Developmental stage of spathes in each temperature treatment and population over the duration of the experiment (a-d). Abbreviations: PB = Padilla Bay; WB = Willapa Bay). Sample size shows the number of flowering shoots that were averaged for each census date (mm-dd). Developmental stages are based on De Cock (1980).

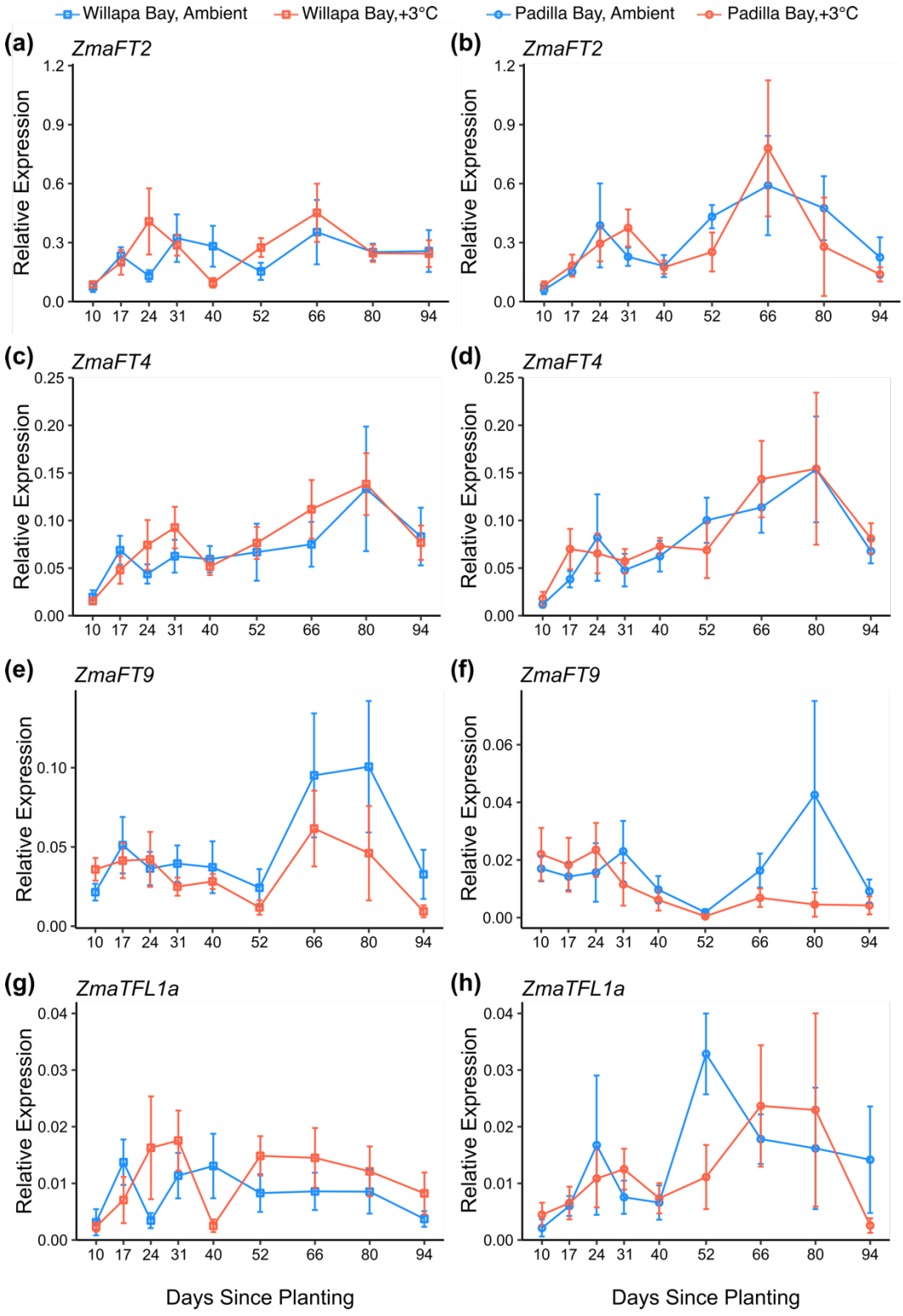

Figure S2: Relative expression of *ZmaFT2* (a, b), *ZmaFT4* (c, d), *ZmaFT9* (e, f), and *ZmaTFL1a* (g, h) genes in leaf tissue during annual growing season (May-July, shown as days since planting, which took place 2024-04-26) from both populations (Willapa, square, left; Padilla, circle right) within the mesocosm. Plot point represents mean, and error bars are standard error. Blue lines represent ambient treated

samples, and red lines indicate +3°C treated samples. All expression values are relative to 3 reference genes (*CYP2*, *ELF4A*, and *RPL28*). Plot point represents mean, and error bars are standard error.

Acknowledgements

I would like to express my gratitude to my advisor, Dr. Takato Imaizimi, for his unwavering support and guidance throughout this research journey, and for the willingness to take on such an interdisciplinary project that pushed everyone involved to challenge our assumptions about biological processes. I would like to thank Dr. Jennifer Ruesink, who was my guide and steward into the world of seagrass biology and marine ecology. Her support, enthusiasm, and insight not only inspired me throughout this project, but also invited others in and made the project the collaborative effort that was necessary for its success. I would like to thank Dr. Kerry Naish for her collaboration and insights into this project and associated publications, and Dr. Sylvia Yang for her support and partnership which made Chapter 3 possible. And I'd like to thank the other members of my committee, Dr. Jennifer Nemhauser and Dr. Soo-Hyung Kim, for their invaluable support and feedback.

I would like to acknowledge the hard-working faculty and staff in the Department of Biology at the University of Washington, who made it possible for any of our work to get done. I would like to thank all who collaborated on this project, including Dr. Cinde Donoghue, Dr. Jeffrey Gaeckle, Dr. Rachel Skubel, Dr. Cynthia Catton, Dr. Jim Kaldy, and others, as well as support from the Washington State Department of Natural Resources Aquatics Team and the Northwest Climate Adaptation Science Center.

Finally, I would like to express my sincere gratitude and appreciation for my family and friends who supported me throughout this process and encouraged me to keep going and believe in myself even when I felt I was no longer capable. To Steven, Orbit, and all others, this journey would not have been possible without you.